5 Contract NAS9-16055

2 THE SONIC SIMULATION OF THE SPS POWER BEAM

1 EE7 | Jack Seyl

NASA-CR-161049

FINAL REPORT

Prepared For:

National Aeronautics and Space Administration
Lyndon B. Johnson Space Center

Prepared by:
3 James H. Ott
James S. Rice

6 March 31, 1981

4 Novar Electronics Corporation
24 Brown Street
Barberton, Ohio 44203

NOVAR

35038

Contract NAS9-16055

THE SONIC SIMULATION OF THE SPS POWER BEAM

FINAL REPORT

Prepared For:

National Aeronautics and Space Administration
Lyndon B. Johnson Space Center

Prepared by:
James H. Ott
James S. Rice

March 31, 1981

Novar Electronics Corporation
24 Brown Street
Barberton, Ohio 44203

ACKNOWLEDGEMENTS

We give particular thanks to Mark Anglin, Stan DiDente, Jack Kato, Don Richards, and Steve Smith, all of Novar, for their contribution to the design, building, checkout, documentation, and utilization of the Sonic Simulator.

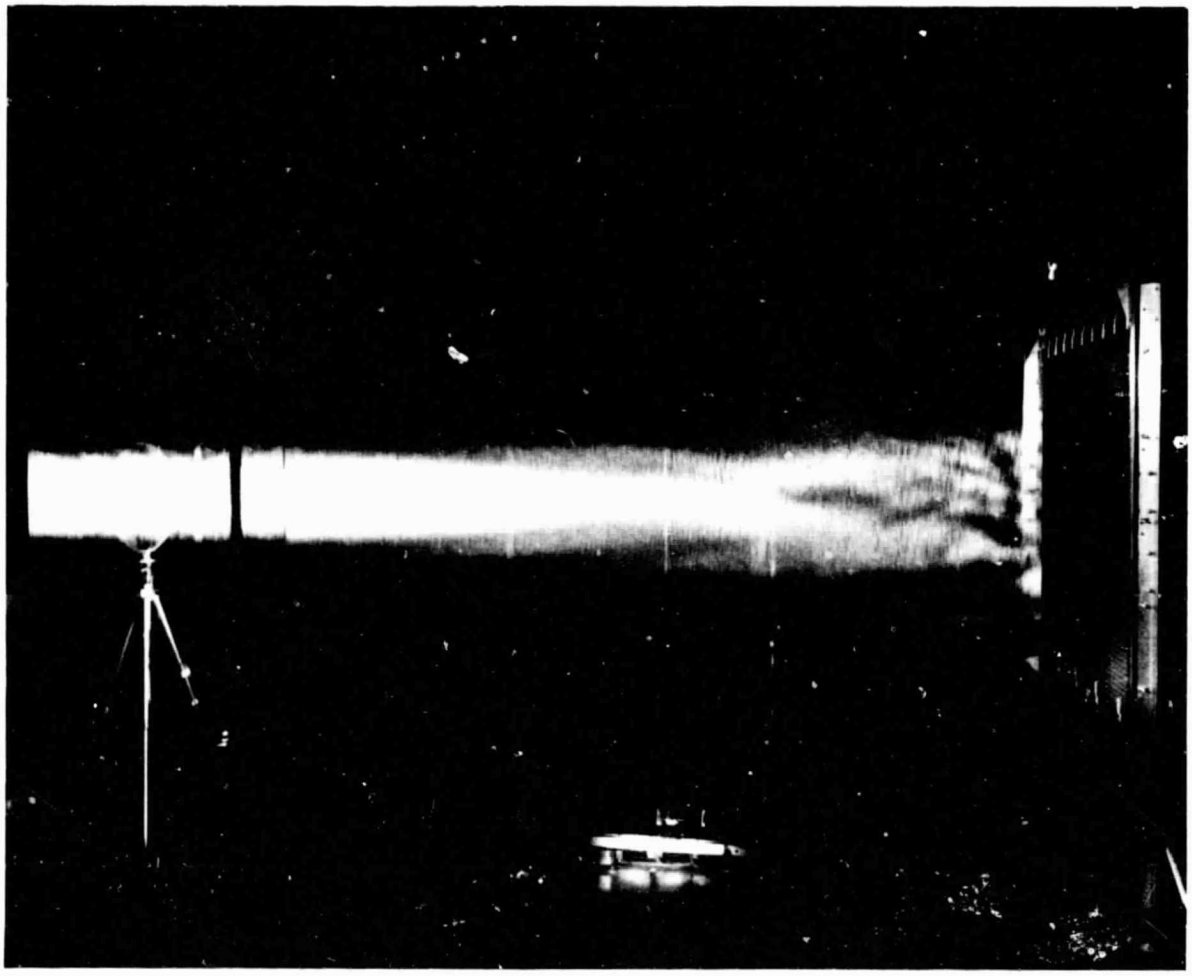

PHOTOGRAPH OF SIMULATED POWER BEAM

TABLE OF CONTENTS

APPENDIXES

FIGURES

TABLE

INTRODUCTION

BACKGROUND

Novar Electronics Corporation has built and extensively used a Satellite Power System Microwave Transmission Simulator. The simulator generates and transmits a beam of audible sound energy which is mathematically similar (see Appendix A) to the microwave beam which would transmit energy to earth from a Solar Power Satellite. This allows areas such as power beam formation to be studied in a laboratory environment.

SIMULATOR DESCRIPTION AND CAPABILITIES

The simulator, Figure 1, is shown in major functional block diagram form in Figure 2. The Sonic Transmitting Antenna (Figure 3) is a 1.2 meter-diameter phased array of 3348 acoustic transmitting elements which electronically focuses and steers a coherent sonic beam. The transmitting elements are connected in a 64 row by 64 column matrix. Each column is driven by circuitry which multiplexes each of the rows. This enables the simulator's computer to independently control the amplitude, phase, and frequency of each of the 3348 transmitting elements. The simulator is designed to transmit the sonic power beam at one of three selectable frequencies, 8.24 kHz, 8.73 kHz, or 11.64 kHz. Any illumination

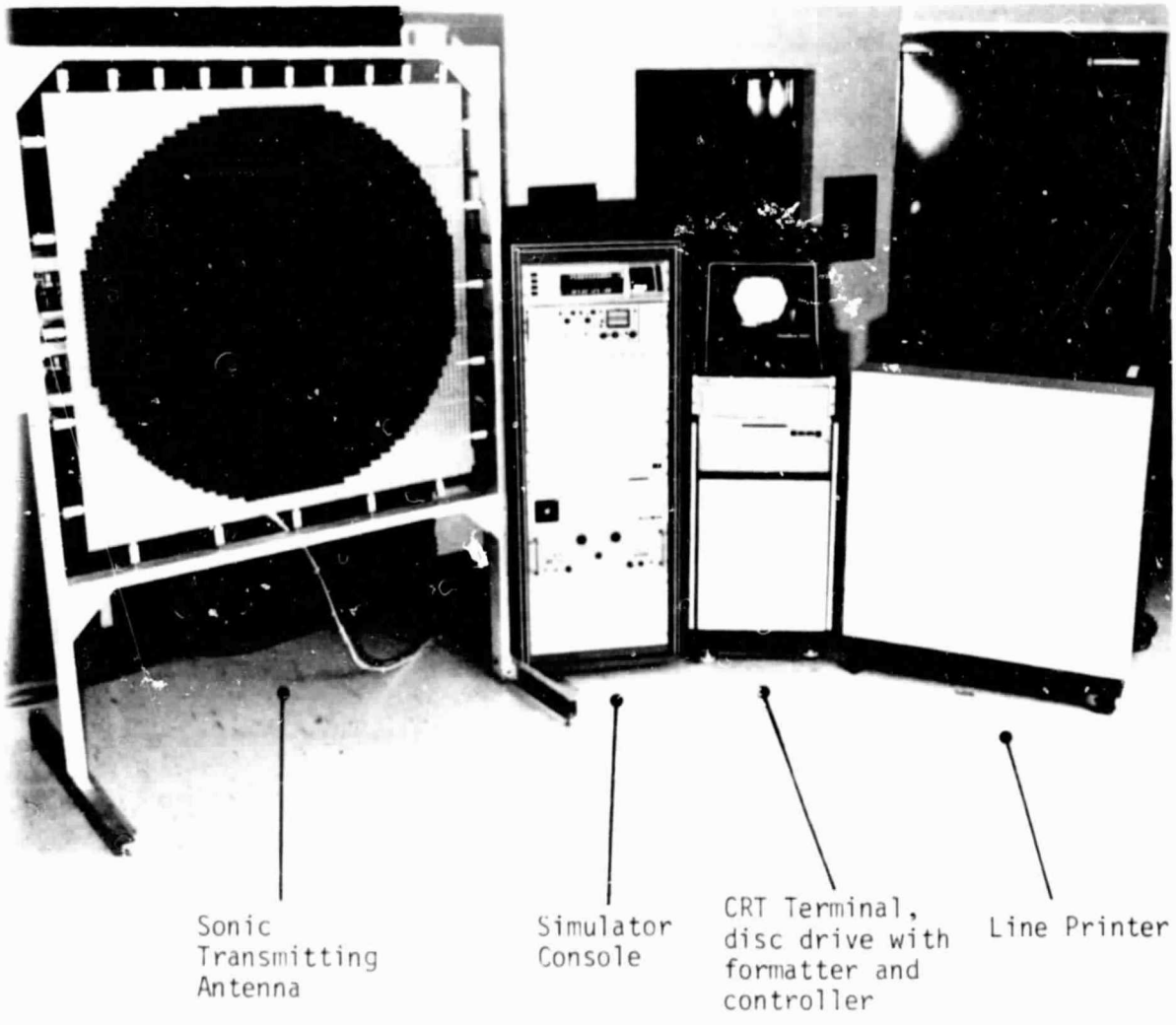

FIGURE 1

SATELLITE POWER SYSTEM SONIC SIMULATOR

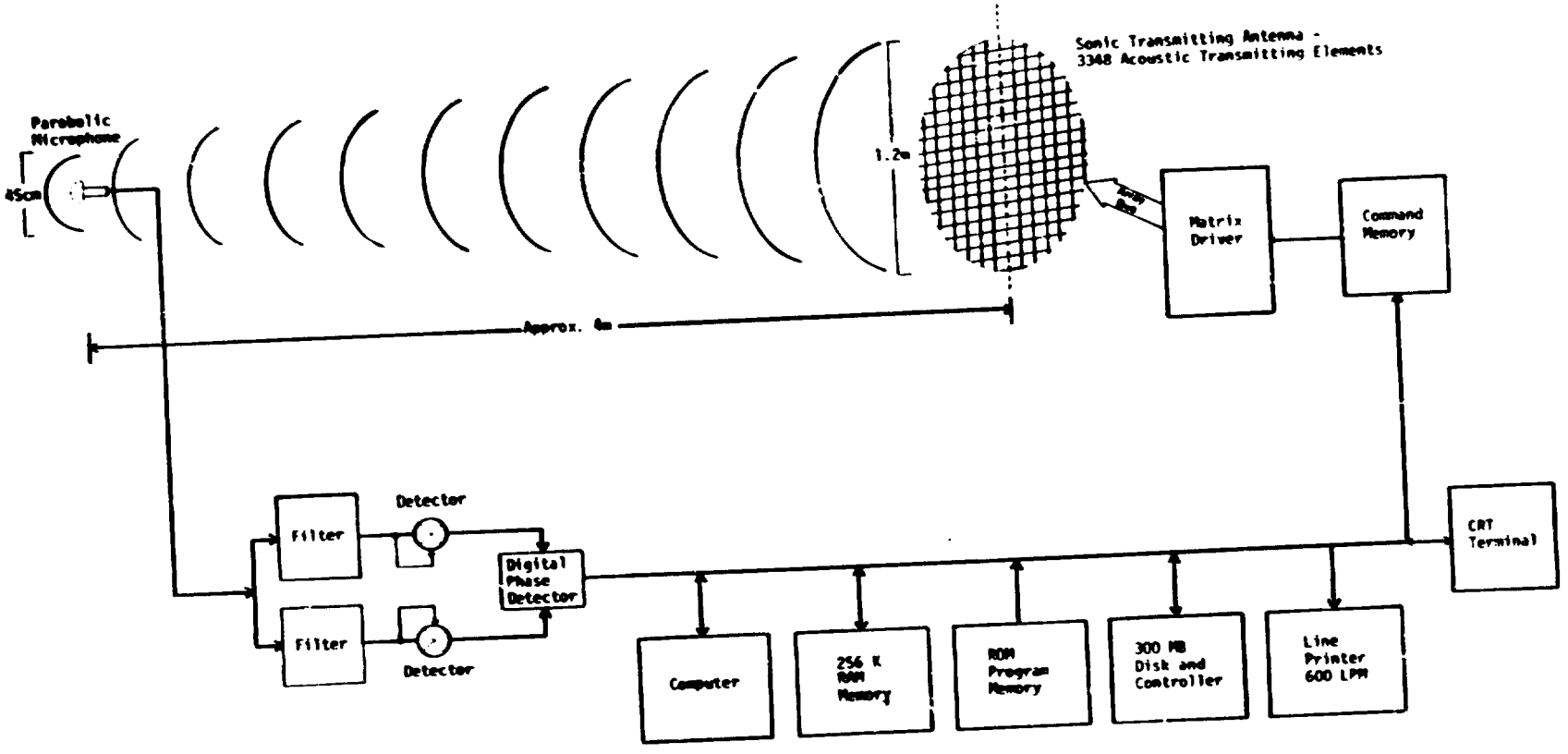

FIGURE 2

SPS SONIC SIMULATOR MAJOR FUNCTIONAL BLOCKS

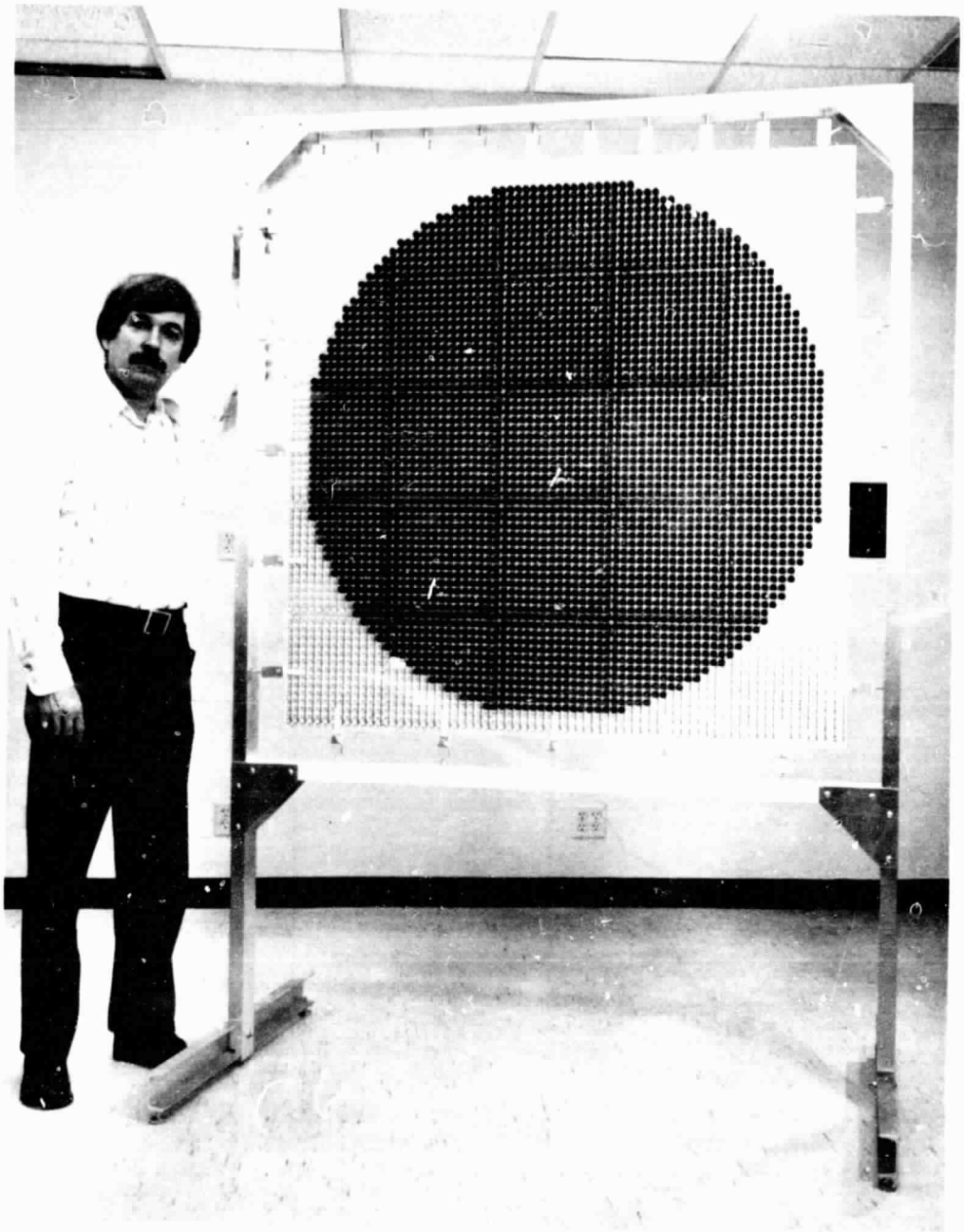

FIGURE 3

SONIC TRANSMITTING ANTENNA -- 3348
Sound Emitting Elements

taper, e.g., Gaussian, can be programmed and the resultant far field and near field antenna patterns studied. A computer, RAM memory, 300 MB disc drive, line printer, and CRT terminal are incorporated to provide a very high degree of experimental flexibility.

The beam is formed using Novar's closed loop phase control technique - Interferometer-Based Phase Control (IPC)[1,2]. (A detailed discussion of IPC is given in Appendix B.) At the digital phase detector (Figure 1), IPC sequentially determines the phase of each transmitting element signal as received at the parabolic microphone relative to the phase of a signal received at the microphone from a reference transmitting element located near the center of the Sonic Transmitting Antenna. The system then adjusts the phase of each transmitting element signal to be the same at the microphone as that from the reference transmitting element. Since all transmitting element signals will then be received at the same phase at the microphone, the beam will be focused and pointed at that point. The far field antenna pattern of the Sonic Transmitting Antenna will then exist in the region of the microphone. This antenna pattern is the acoustic analog of the microwave power beam ground pattern.

The transmitting element spacing (0.6 wavelengths at 11.16 kHz) was selected so that no grating lobes would be created. However they can be created if desired by having

the computer turn off every other row and column of transmitting elements therby effectively doubling the spacing to greater than a wavelength. The Sonic Transmitting Antenna is designed to permit mechanical flexure and shape distortion. Phase Control in the face of such factors can then be studied.

An SPS phase control system can be simulated in real time, with appropriate time scaling, to study such time related factors as the control system's frequency response, step response, and control resolution. Phase can be controlled to a resolution of approximately 6^{o}. This is quite adequate for beam formation and to demonstrate the system's capability to electronically steer the beam.

A unique feature of the Sonic Simulator is its ability to provide actual photographs or the transmitted power beam. Figure 4 shows a scanning system which provides a light intensity modulated raster of the sonic beam sound intensity pattern. By adding a coherent phase signal to the intensity modulator, phase information is produced which enables the phase pattern of the beam to be photographed.

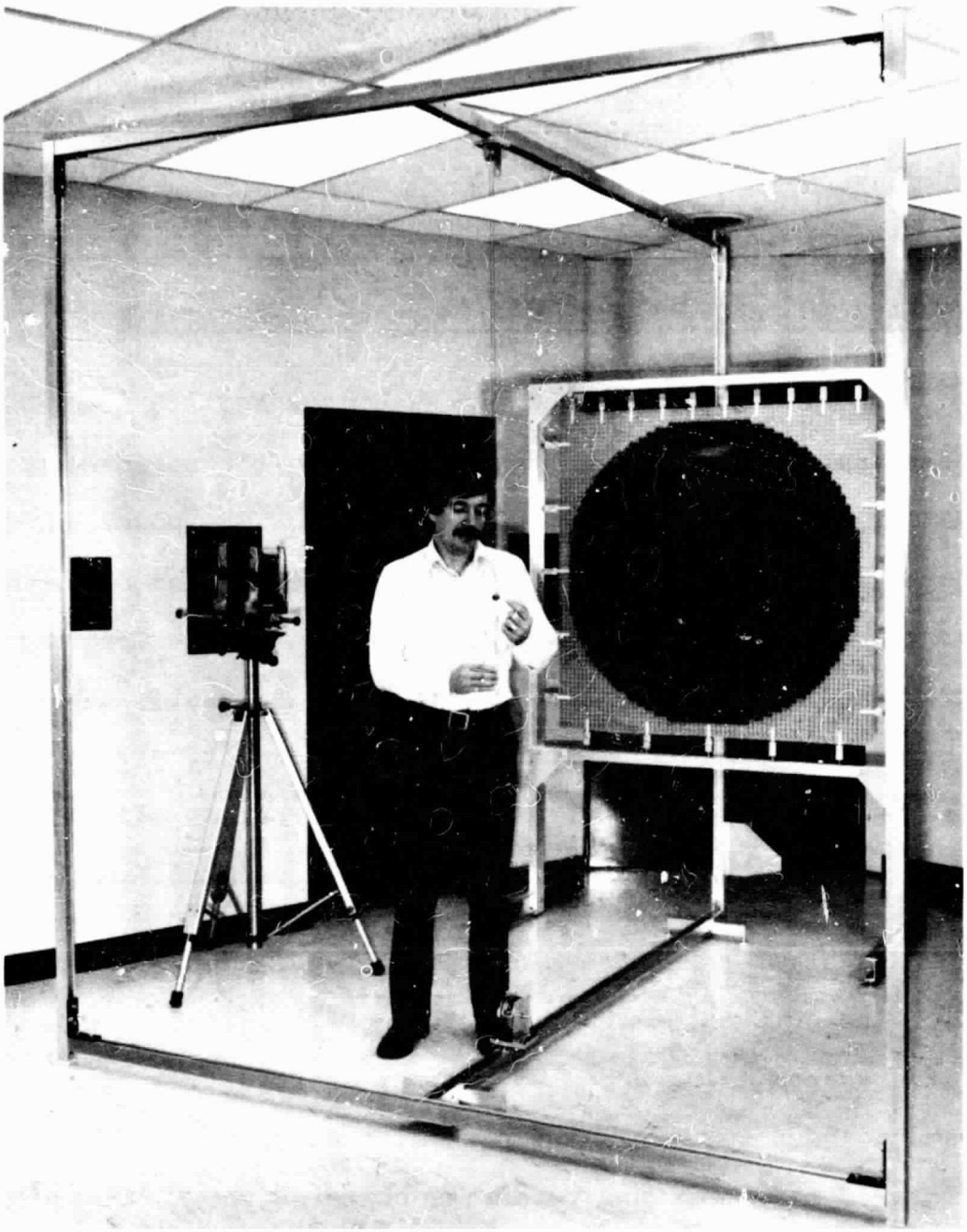

FIGURE 4

SONIC BEAM PHOTOGRAPHING SYSTEM

-A precision mechanical scanning system provides an actual photograph of the sonic beam. The camera lens remains open in a darkened room while the sound-to-light modulator (device being pointed at) provides a light output proportional to the intensity of the sonic beam. The modulator is scanning up and down and forward and backward to provide a photograph of a cross section of the beam.

RESULTS

SIMULATIONS DEMONSTRATING BASIC SYSTEM CAPABILITIES

The viability of the Sonic Simulator and its attendant photographic technique is demonstrated by the sonic beam photographs shown in Figures 5 through 8. The power distribution at the transmitting antenna for Figures 5 through 8 was uniform. When the power distribution of the transmitting array is changed to approximately a 10 dB Gaussian taper, Figures 9 through 12, which correspond respectively to Figures 5 through 8 are the result. Figure 13 provides additional far field detail in the main lobe of the beam of Figure 9.

A test of the phase measurement system was performed in which the outputs of the transmitting elements on one-half of the transmitting array were phase shifted 180° after a beam had been formed at the parabolic microphone. This generated the phase and intensity patterns shown in Figures 14 through 17.

Reflecting surfaces can be used to purposely alter the sonic beam. An example of this is shown in Figure 18 where the sonic beam was "bounced" off a hard flat surface.

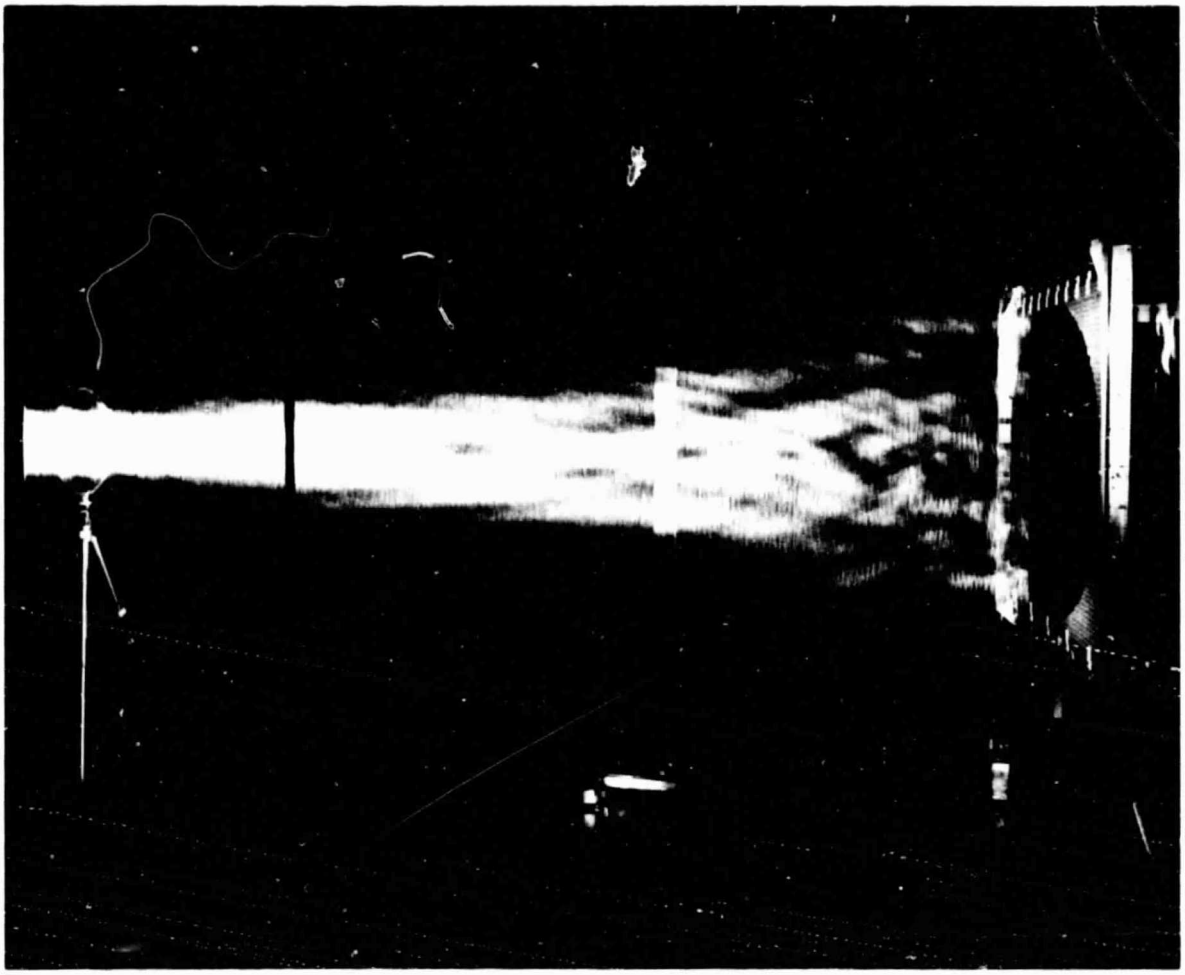

FIGURE 5

SONIC BEAM INTENSITY PATTERN - UNIFORM
POWER DISTRIBUTION AT TRANSMITTING ARRAY

-Cross section along axis of beam. The frequency is 8.24 kHz. Beam focused at a point in vicinity of parabolic microphone on left. Distance between microphone and array requires photographing the beam in three segments. The region in the segment nearest the array, the near field, is characterized by the near field modes resulting from differences in the relative phases of the signals from the transmitting elements. This causes the interference pattern seen.

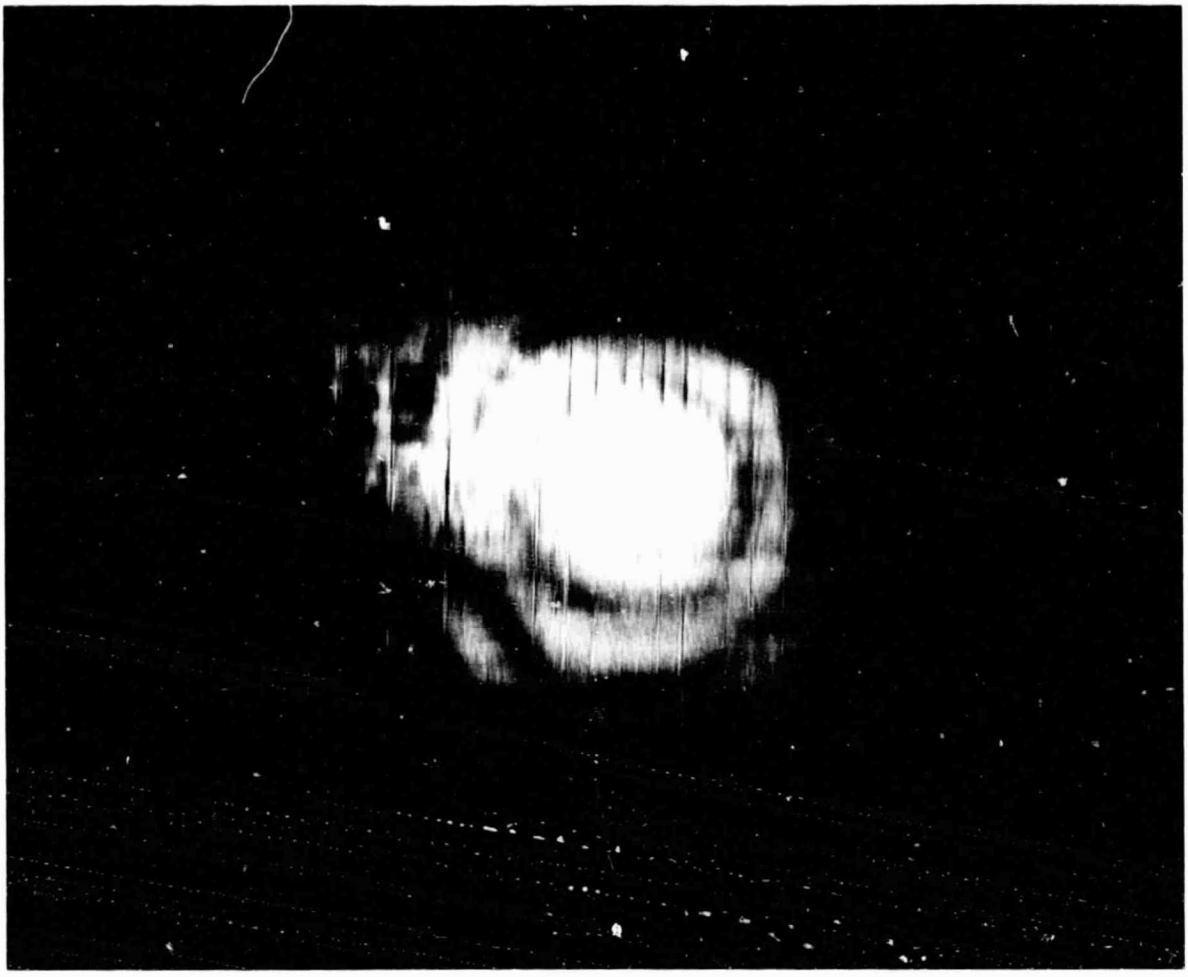

FIGURE 6

SONIC BEAM FAR FIELD INTENSITY PATTERN - UNIFORM
POWER DISTRIBUTION AT TRANSMITTING ARRAY

-Cross section of the beam of Figure 5 perpendicular to beam axis at the parabolic microphone. The sound-to-light modulator gain was greatly increased to show sidelobe detail. (Sidelobes appear as rings of light.) (The blurring was caused primarily by two factors. Room reflections were not totally attenuated by the room's sound absorbant material. Secondly, there were small variations in the transmitting antenna's amplitude distribution resulting from variations between transmitting elements in their input/output characteristics. The simulator's computer can be programmed to correct for the effects of the latter.)

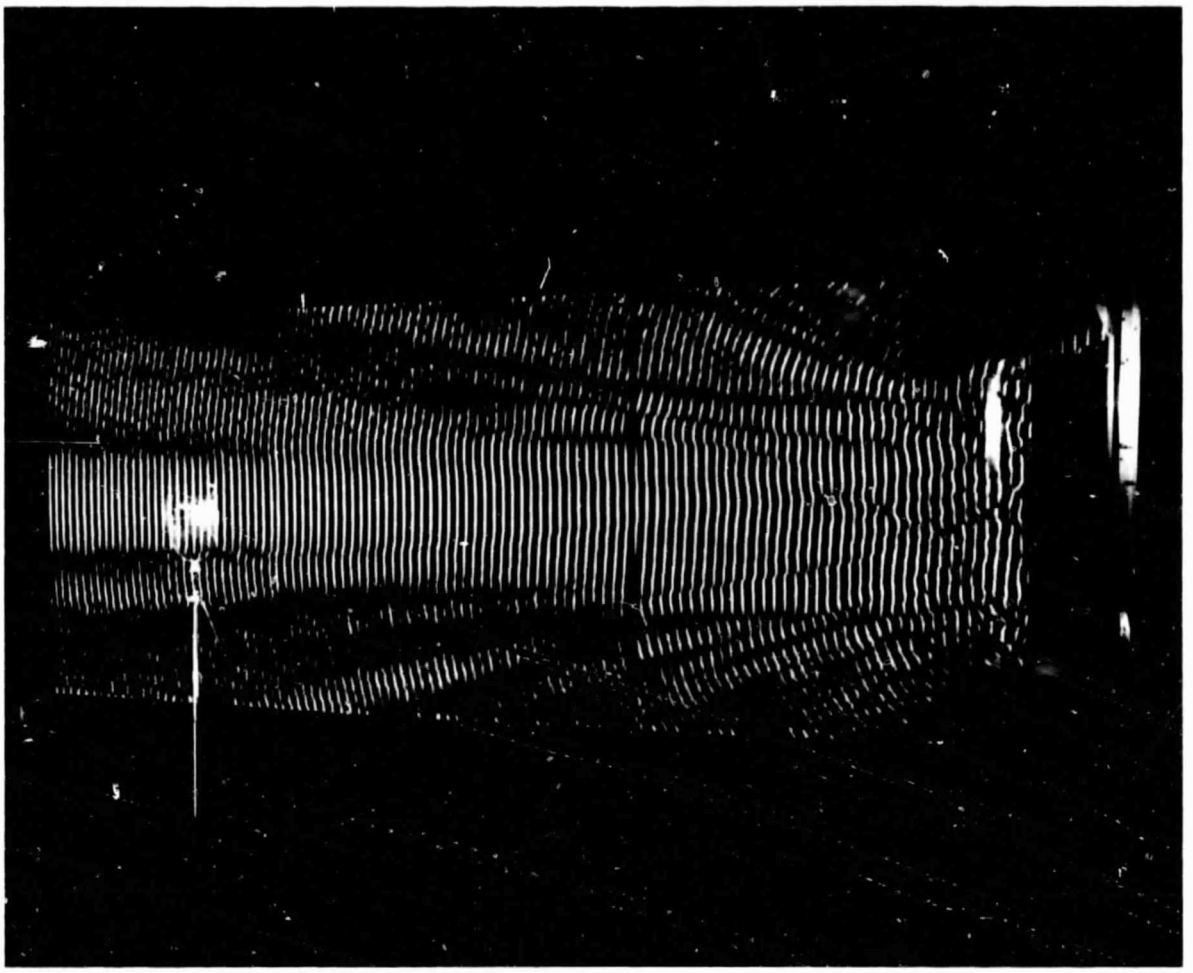

FIGURE 7

SONIC BEAM PHASE PATTERN - UNIFORM POWER
DISTRIBUTION AT TRANSMITTING ARRAY

-Phase information scan was made along axis of beam of Figure 5. The centers of the light or dark bands are one wavelength apart. White bands are the locations where the beam is in phase with the phase reference signal; dark bands are where the two are 180^{o} out of phase. Note the expected 180^{o} phase between the main beam and the first sidelobes in the far field (the region of the parabolic microphone.) Due to the phase processing technique of the sound-to-light modulator, phase patterns, including the above, do not provide scaled representations of beam amplitude. The sidelobe features are greatly exagerated.

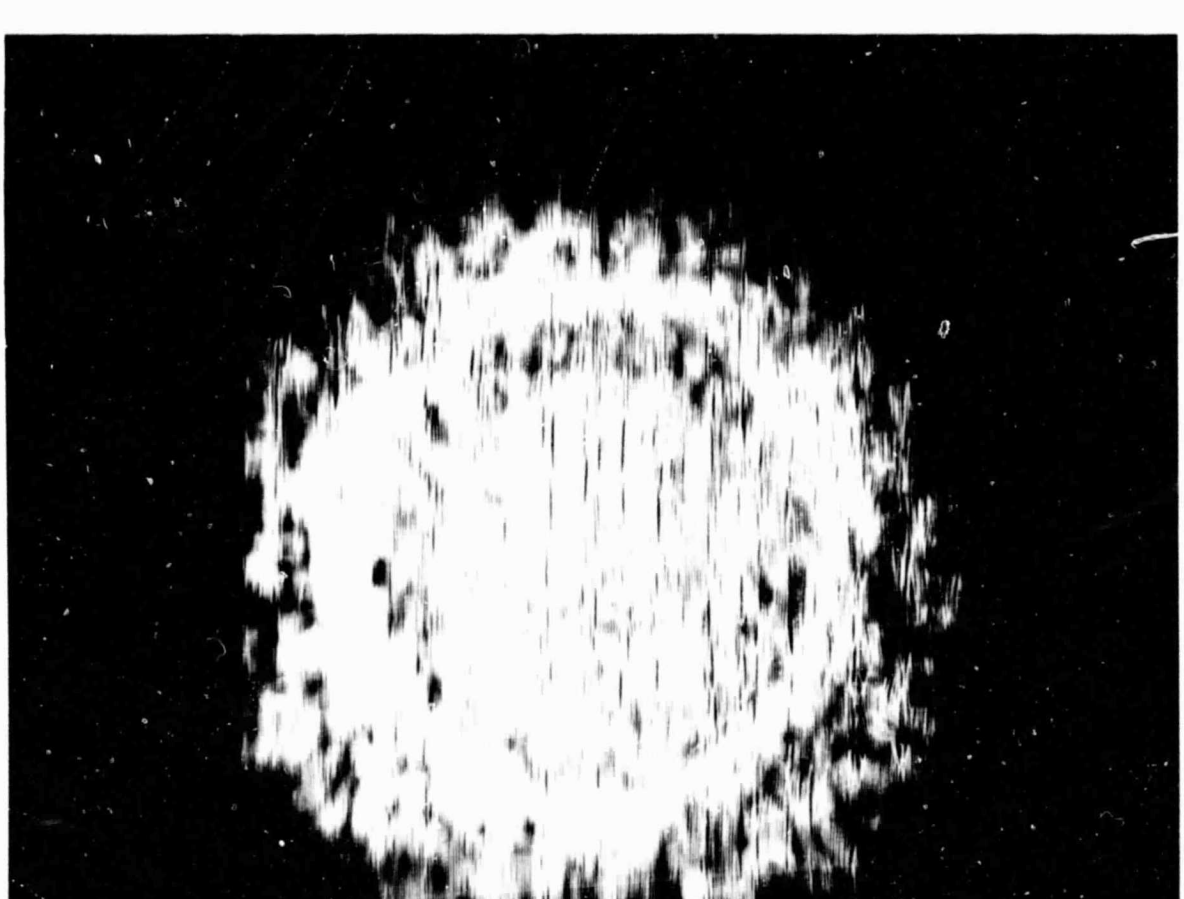

FIGURE 8

SONIC BEAM NEAR FIELD INTENSITY PATTERN - UNIFORM POWER DISTRIBUTION AT TRANSMITTING ARRAY

-Cross section of the beam of Figure 5 parallel to and 5 cm from the transmitting array. Ring shaped pattern is result of spherical phase taper required for the beam to be focused at a point other than infinity (4 meters here). (The blurring is caused by the extreme sensitivity of a pattern this distance from the array (1.2 λ at 8.24 kHz) to any variations in the distance during a photographic scan, to acoustic standing waves between the array and the sound-to-light modulator, and to the transmitting element output characteristic differences discussed with Figure 6.)

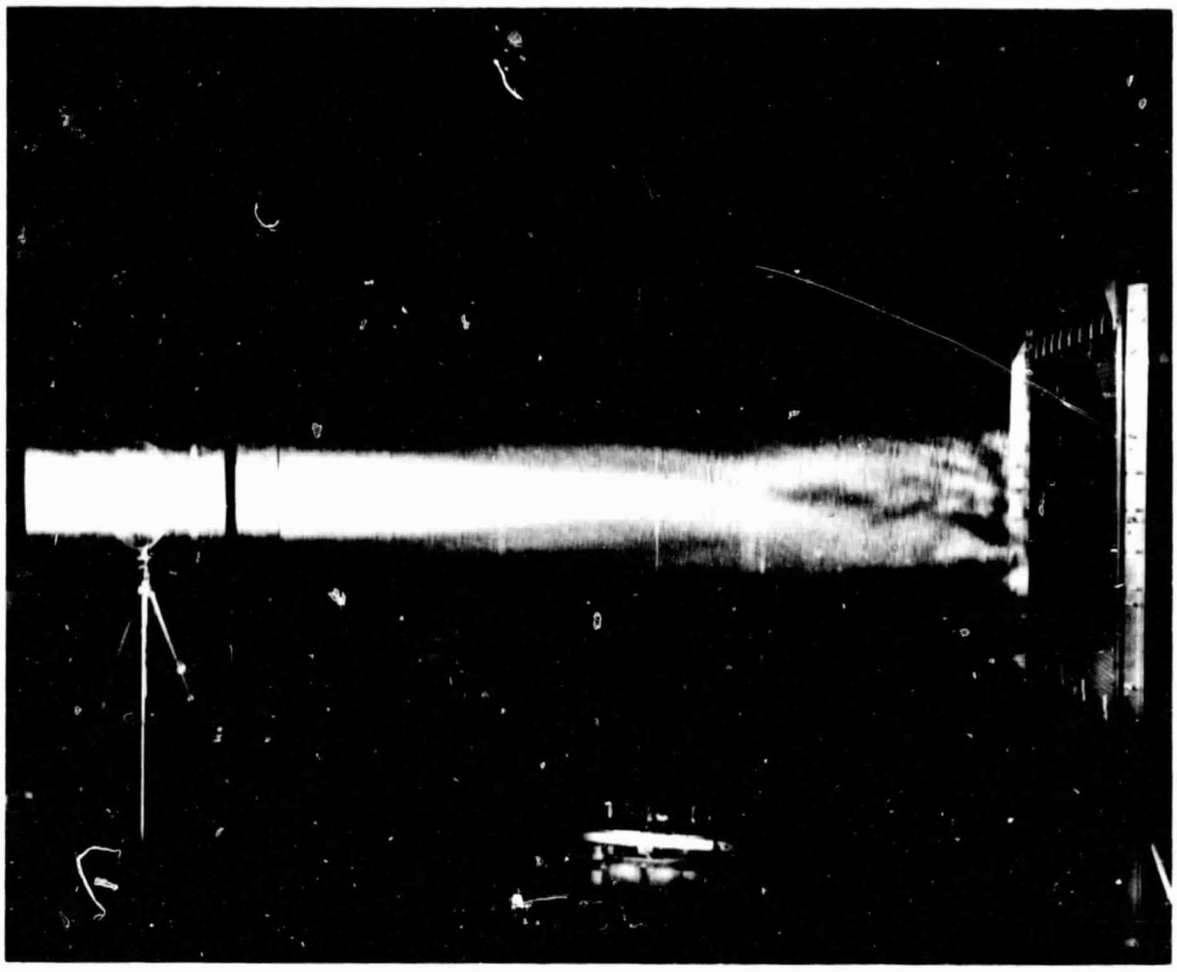

FIGURE 9

SONIC BEAM INTENSITY PATTERN - GAUSSIAN
POWER DISTRIBUTION

-Cross section along axis of beam formed by a 10 dB gaussian taper approximation for the power distribution at the transmitting array. The frequency is 8.24 kHz. Beam focused at a point in vicinity of parabolic microphone. Note that beam width is wider than that for the uniform power distribution in Figure 5, as expected from antenna theory.

FIGURE 10

SONIC BEAM FAR FIELD INTENSITY
PATTERN - GAUSSIAN POWER DISTRIBUTION

-Cross section of the beam of Figure 9 perpendicular to the beam at the parabolic microphone. (Beam width is wider than that in Figure 6 although it appears narrower because sound-to-light modulator gain and photographic reduction factor are different.)

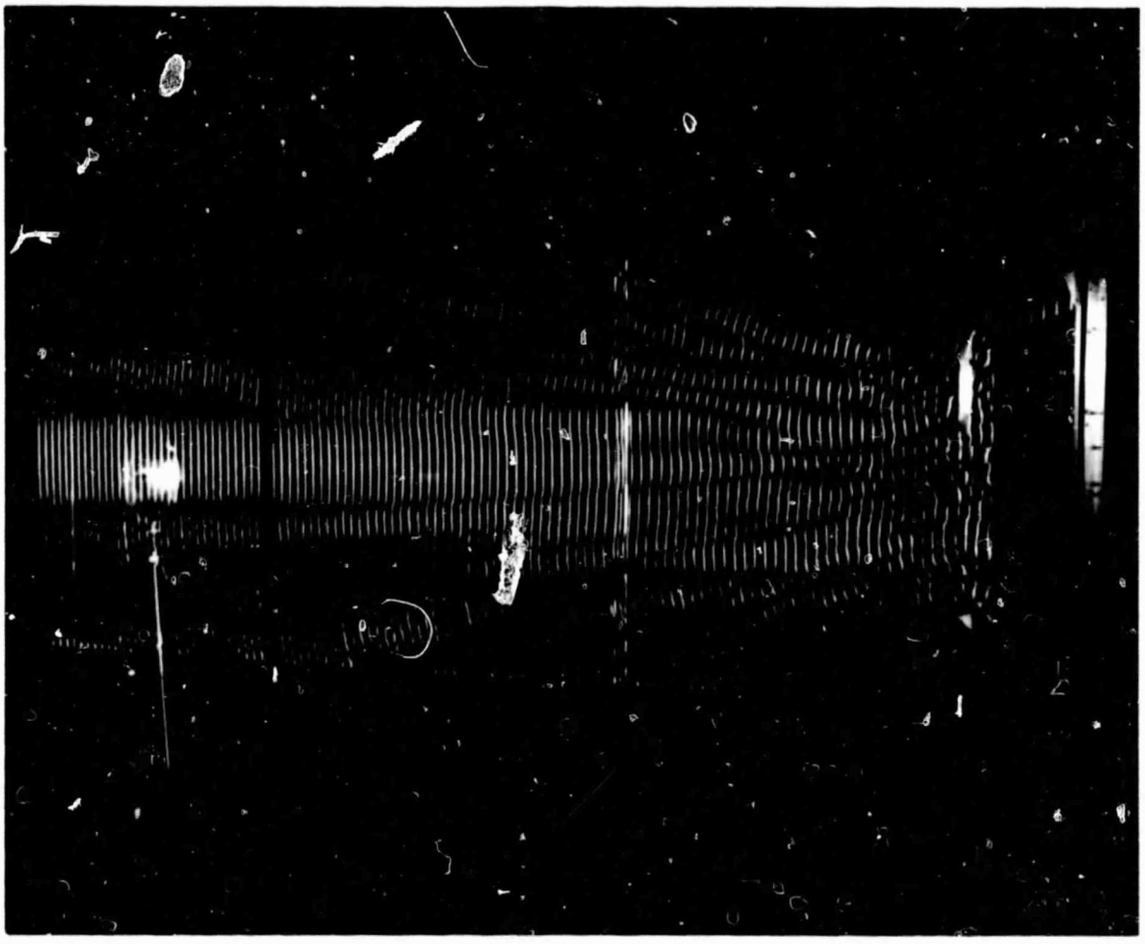

FIGURE 11

SONIC BEAM PHASE PATTERN - GAUSSIAN
POWER DISTRIBUTION

-Phase information scan along axis of beam of Figure 9. (See comment associated with Figure 7 concerning the phase processing technique of the sound-to-light modulator.)

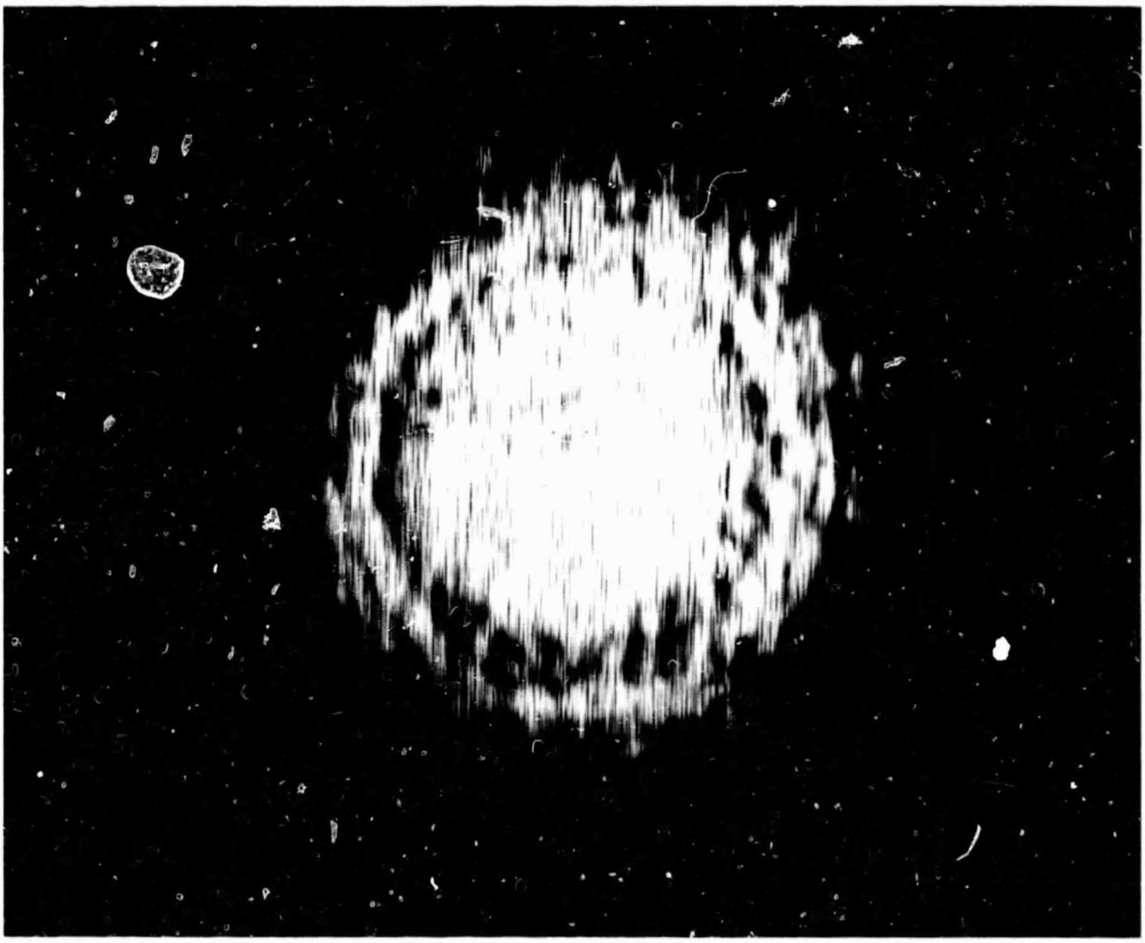

FIGURE 12

SONIC BEAM NEAR FIELD INTENSITY
PATTERN - GAUSSIAN POWER DISTRIBUTION

-Cross section of the beam of Figure 9 at a distance 5 cm from transmitting array.

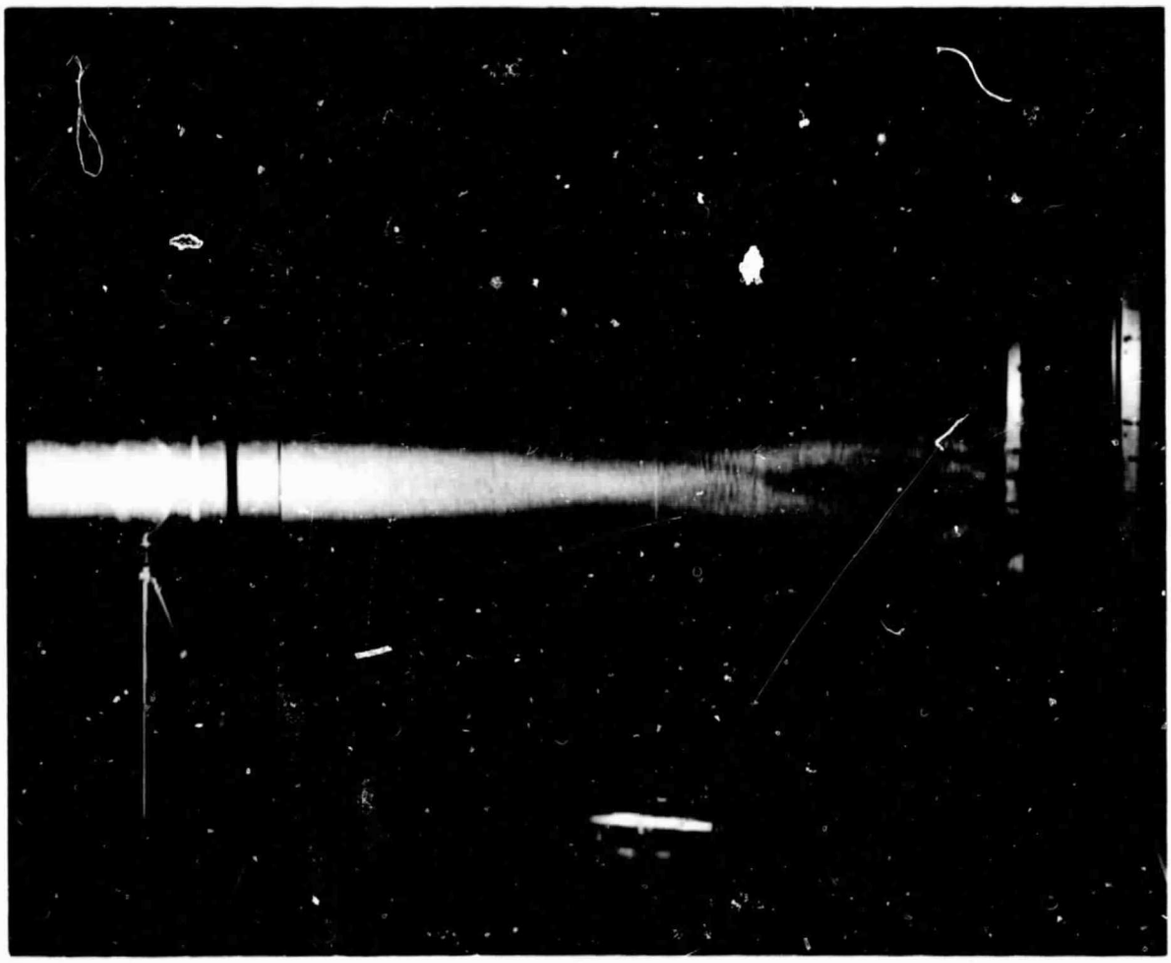

FIGURE 13

SONIC BEAM INTENSITY PATTERN - GAUSSIAN
POWER DISTRIBUTION

-Same as Figure 9 except photographed with reduced sound-to-light modulator gain to better show variation in main beam intensity in far field (region of parabolic microphone).

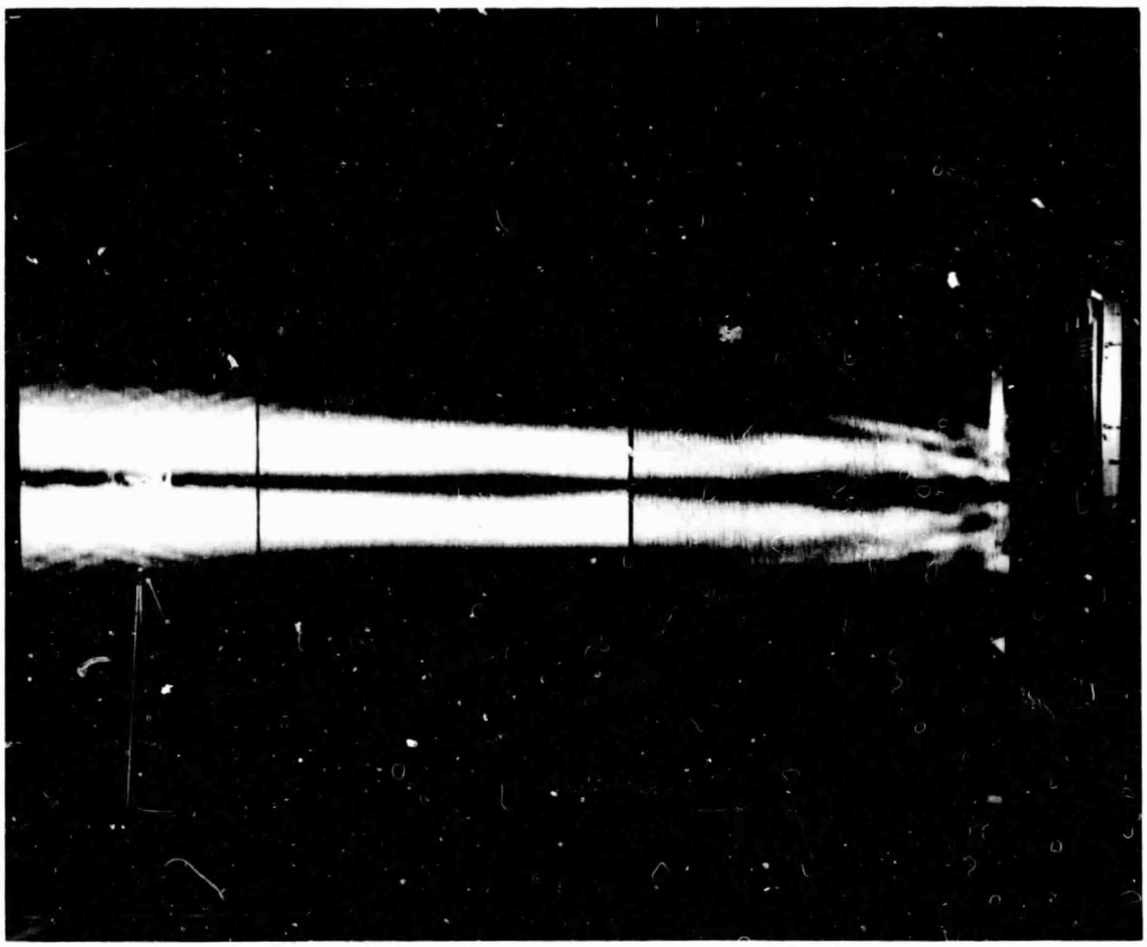

FIGURE 14

DUAL BEAM INTENSITY PATTERN

-Beam was generated by phase shifting the outputs of the transmitting elements on the top half of the transmitting array 180^{o} from those on the bottom. Power distribution at the transmitting array was a gaussian taper. Photographic scan is through beam center.

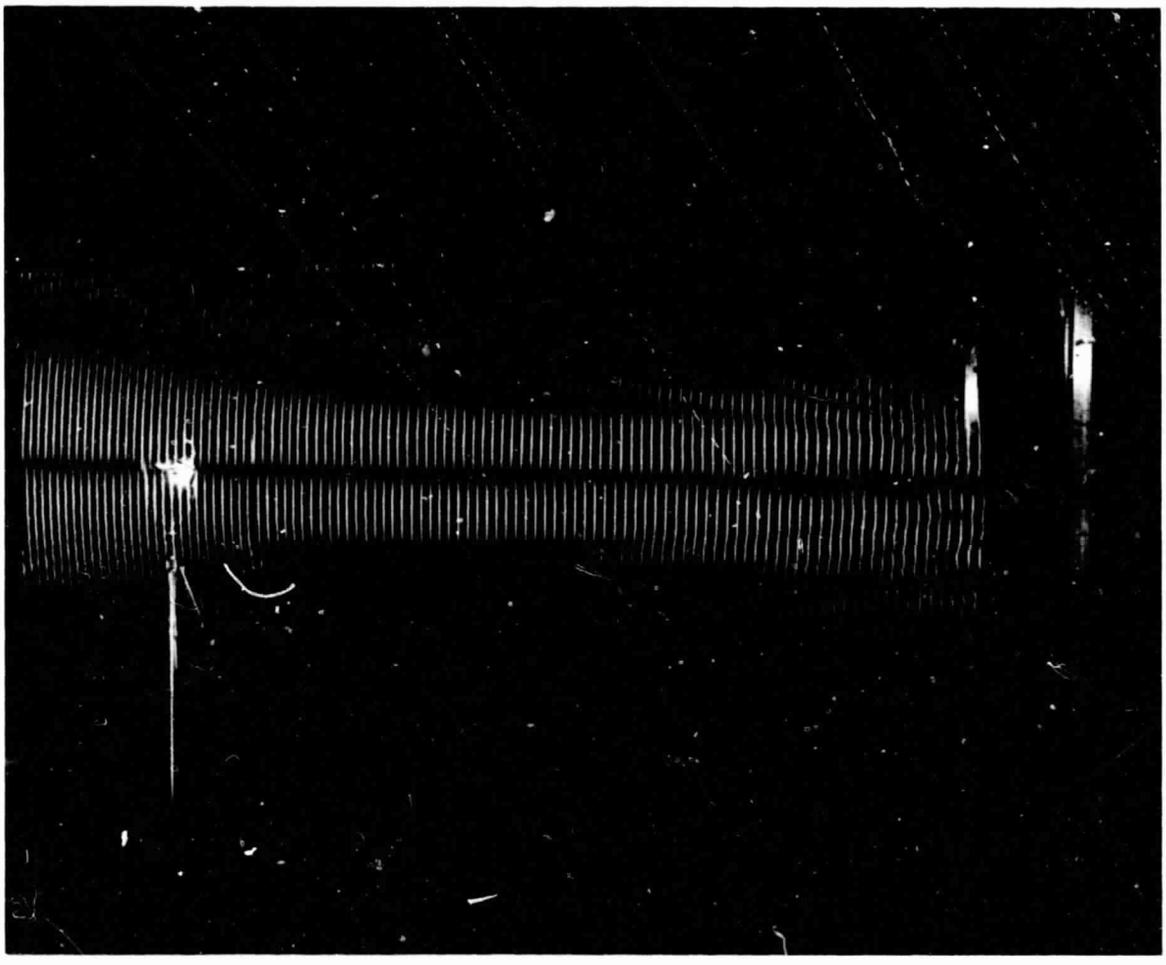

FIGURE 15

DUAL BEAM PHASE PATTERN

-Cross section phase scan through center of beam of Figure 14. Note the 180^{o} phase between the two main lobes of the beam.

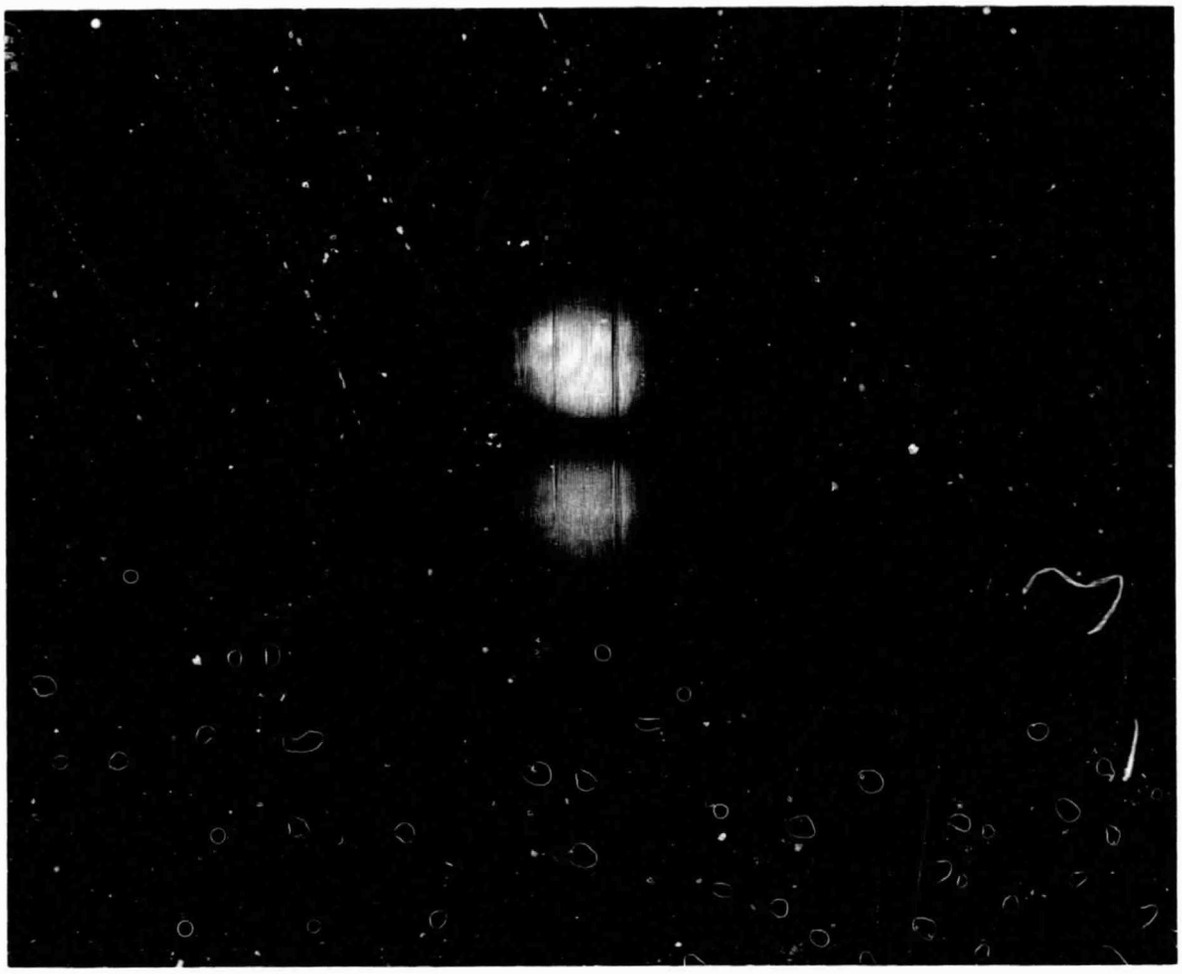

FIGURE 16

DUAL BEAM FAR FIELD INTENSITY PATTERN

-Cross section of the beam of Figures 14 and 15 at the parabolic microphone.

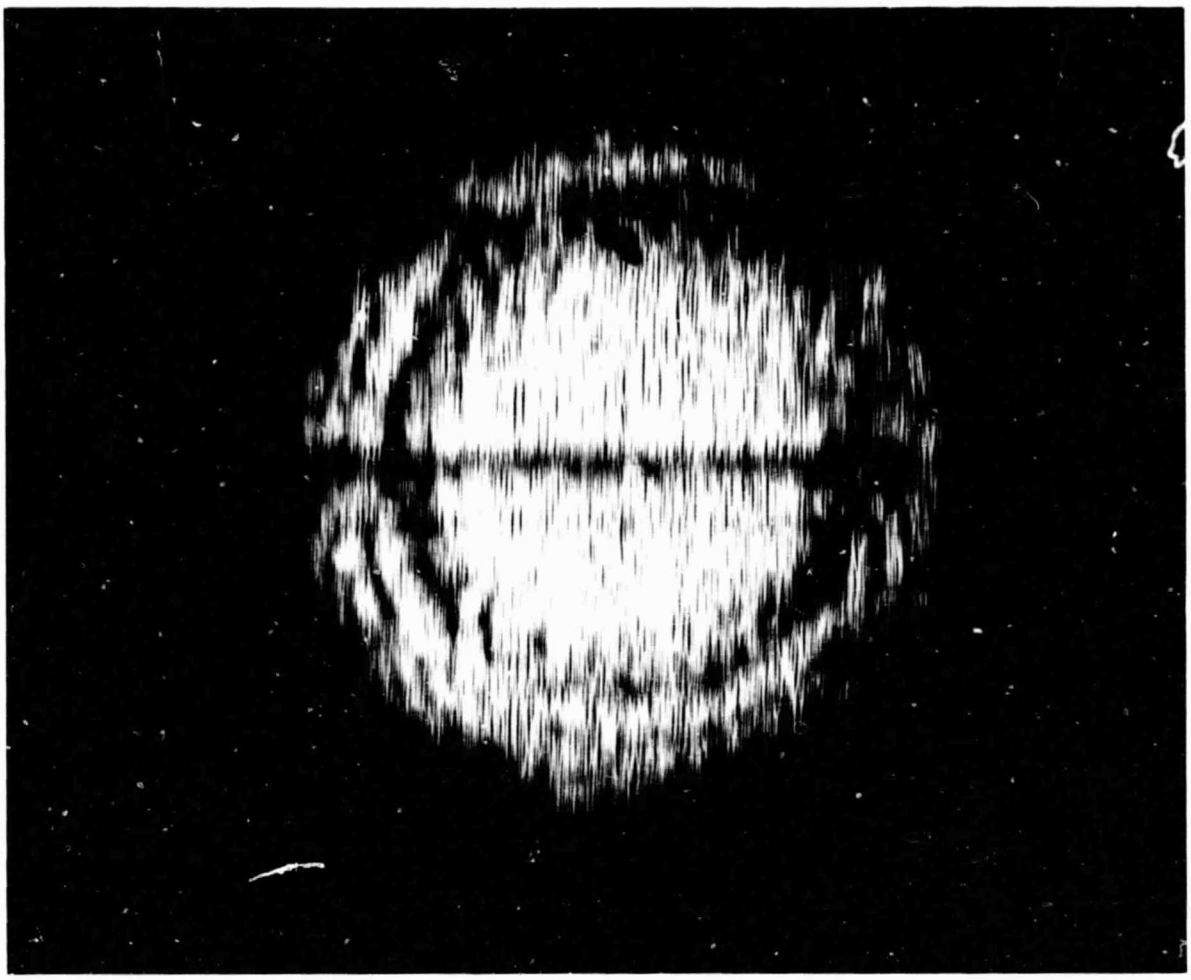

FIGURE 17

DUAL BEAM NEAR FIELD INTENSITY PATTERN

-Cross section of the beam of Figures 14 and 15 5 cm from transmitting array. Note the horizontal null through the center of the pattern due to the 180^{o} phase between the top and bottom of the transmitting array.

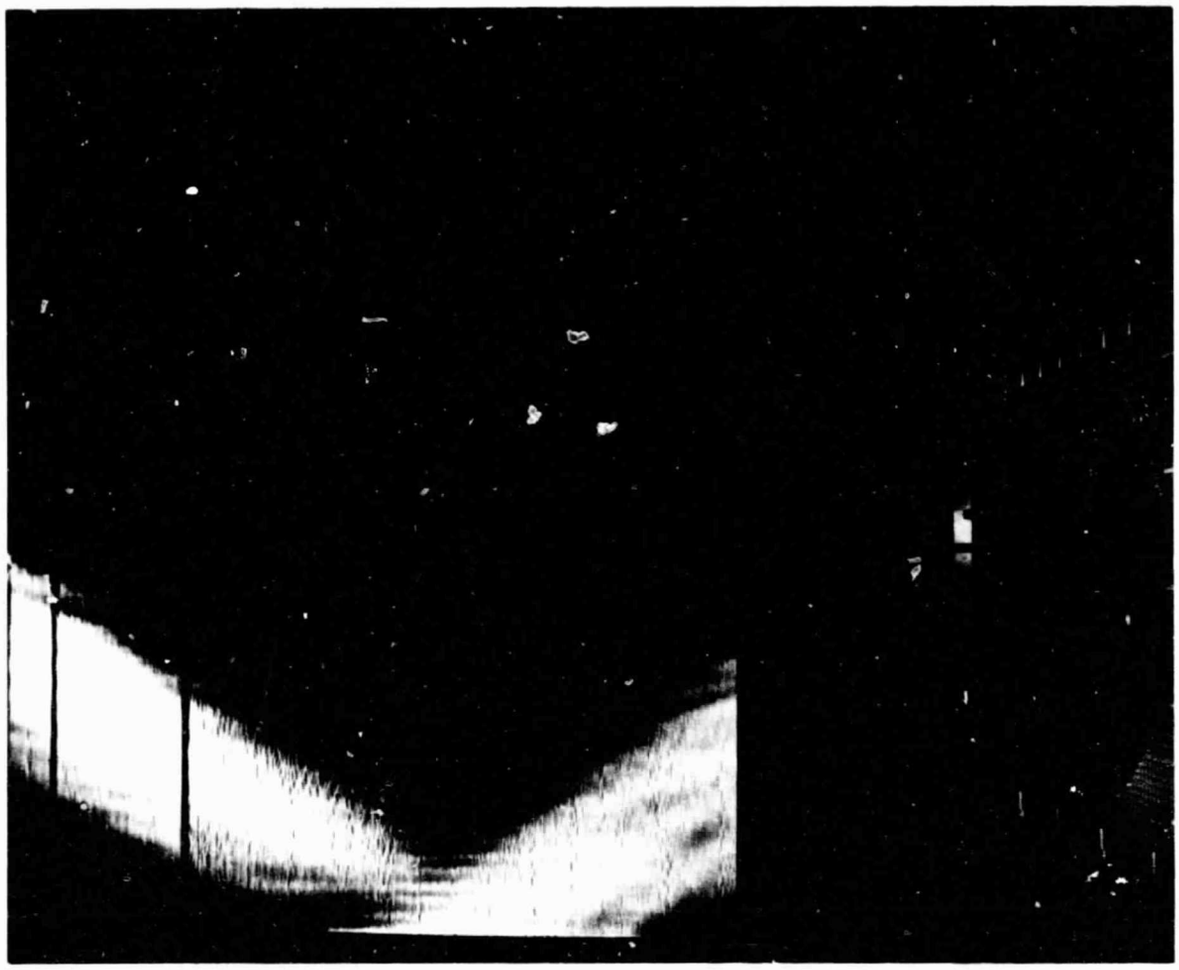

FIGURE 18

SONIC BEAM FORMED BY REFLECTION

-A hard flat surface parallel to the floor was used to form and focus the beam at the parabolic microphone beyond the left edge of the photograph. The lower photograph scan limit is a few centimeters above the surface. (Transmitting array power distribution was uniform.) Sound waves reflect from stiff acoustically-flat surfaces as electromagnetic waves reflect from conductive electromagnetically flat surfaces.

PHASE ERROR SIMULATIONS

The applicability of the Sonic Simulator to evaluation of ionospheric disturbances on the SPS phase control process is demonstrated by the simulator's capability to have phase errors programmed across its transmitting array. The simulator's phase error programming capability is shown by the sonic beams photographed in Figures 19 through 24. For comparison, Figure 13, which was photographed with the same light intensity as the gaussian beams in Figures 22, 23, and 24, can be though of as a gaussian beam with 0^{o} phase error. For phase errors uniformly distributed in probability from - 180^{o} to + 180^{o}, the transmitted energy is essentially totally diffused and there is no beam.

When the signals transmitted by the radiating elements of an array contain random phase errors, a fraction of the array's transmitted power that would have been in the main beam and sidelobes is scattered. The larger the phase errors, the greater the scattered power and the less the power in the main beam. The net effect on the far field pattern is that the main beam and the near sidelobes decrease in level, and the scattered power shows up as a filling up of the nulls between the sidelobes near the main beam and an increase in the overall power level in the region of the far sidelobes. However, as Figures 19 through 24 show, the main beam does not broaden. The simulator therefore demonstrates that the power level does

not increase in the geographical area surrounding the Rectenna due to random phase errors at the Space Antenna. The main beam power reduction measured for the beams shown in Figures 19 through 24 are in close agreement with theory[3] for the "rectangular phase error probability density function" that characterizes the phase errors programmed into the simulator.

As a part of the study of the applicability of the simulator to evaluation of ionospheric disturbances on the SPS phase control process, the use of controlled air turbulence to alter the propagation of the sonic beam was investigated. Air currents induced in the lab (through the use of blowers) did not noticeably affect the sonic beam. It was determined that to do so would require such large air velocities that the increased background noise would interfere with beam measurement.

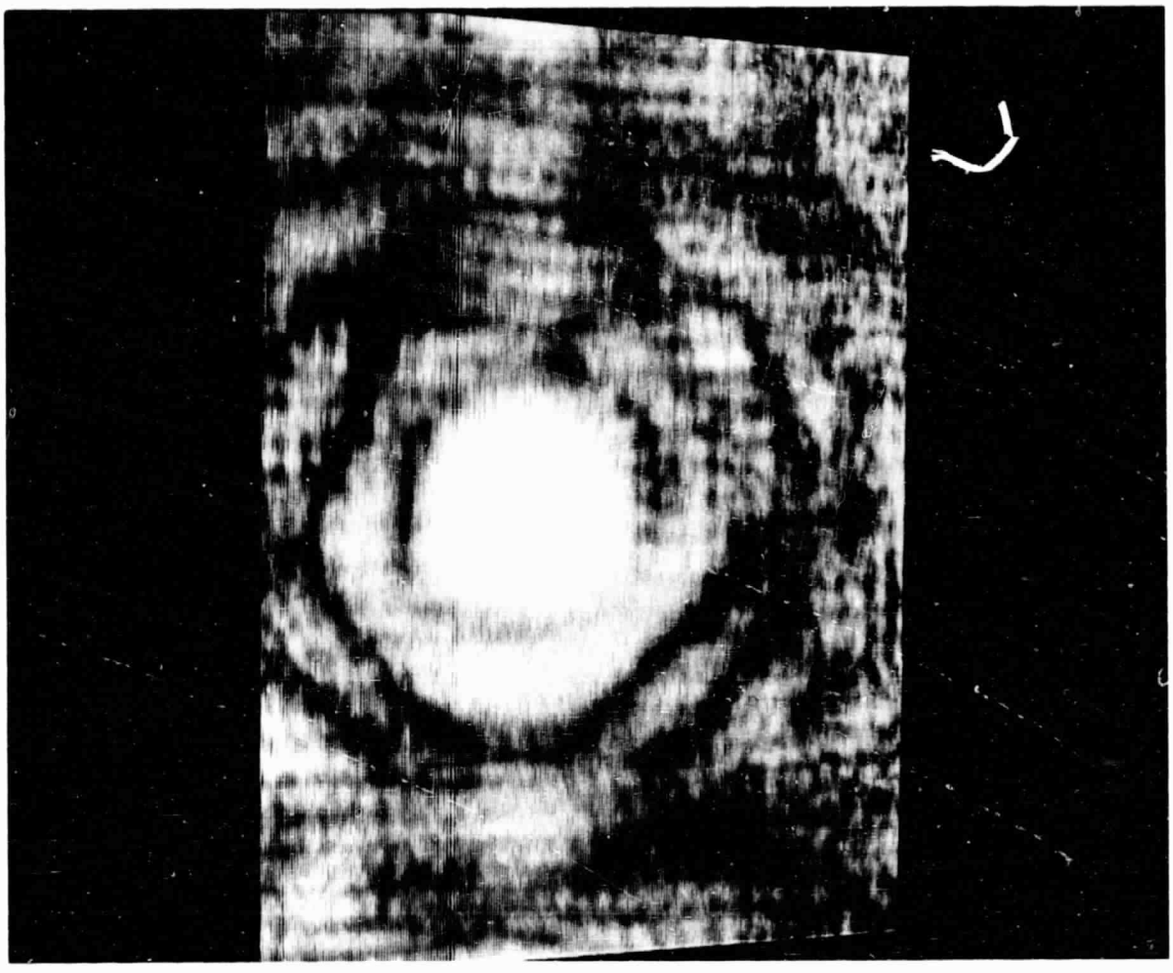

FIGURE 19

SONIC BEAM FAR FIELD INTENSITY PATTERN - 90^{o}
PHASE ERROR PROGRAMMED INTO TRANSMITTING ARRAY

-Gaussian beam identical to that in Figure 10 except for phase errors consisting of random phases between the acoustic signals emitted by the transmitting elements on the transmitting array. Phase errors are uniformly distributed in probability from -90^{o} to $+ 90^{o}$ (37^{o} RMS). Main beam power reduction for this phase error compared to 0^{o} phase error was measured to be 4 dB. The sound-to-light modulator gain was greatly increased to show sidelobe detail.

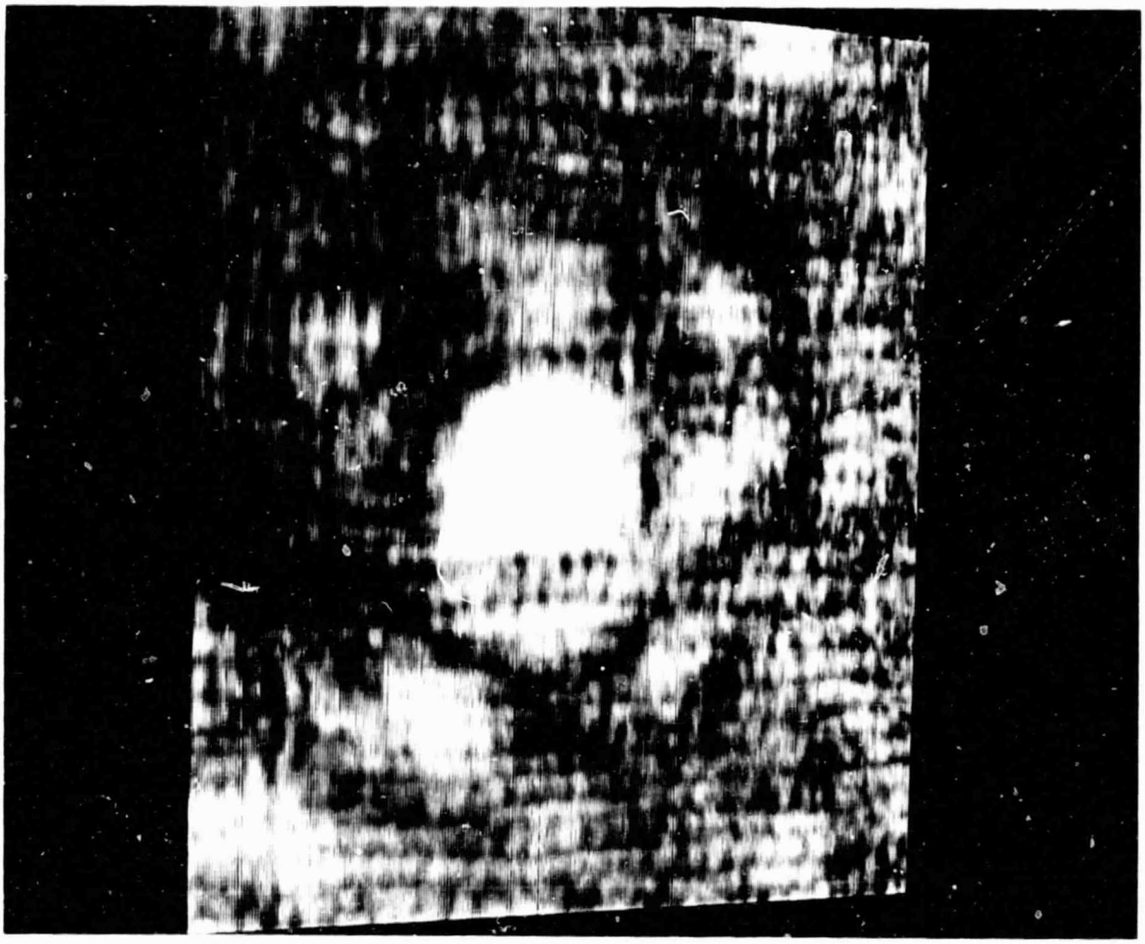

FIGURE 20

SONIC BEAM FAR FIELD INTENSITY PATTERN - 120^{0}
PROGRAMMED PHASE ERROR

-Gaussian beam identical to Figure 19 except that phase error is uniformly distributed in probability from -120^{0} to $+120^{0}$ (57^{0} RMS). Main beam power reduction is 7 dB compared with 0^{0} phase error (Figure 10). (Sound-to-light modulator gain is increased 3 dB over that in Figure 19.)

FIGURE 21

SONIC BEAM FAR FIELD INTENSITY PATTERN - 150^{o}
PROGRAMMED PHASE ERROR

-Gaussian beam identical to Figure 19 except that phase error is uniformly distributed in probability from -150^{o} to $+150^{o}$ (79^{o} RMS). Main beam power reduction is 14 dB compared with 0^{o} phase error (Figure 10). (Sound-to-light modulator gain increased to 10 dB over that in Figure 19.)

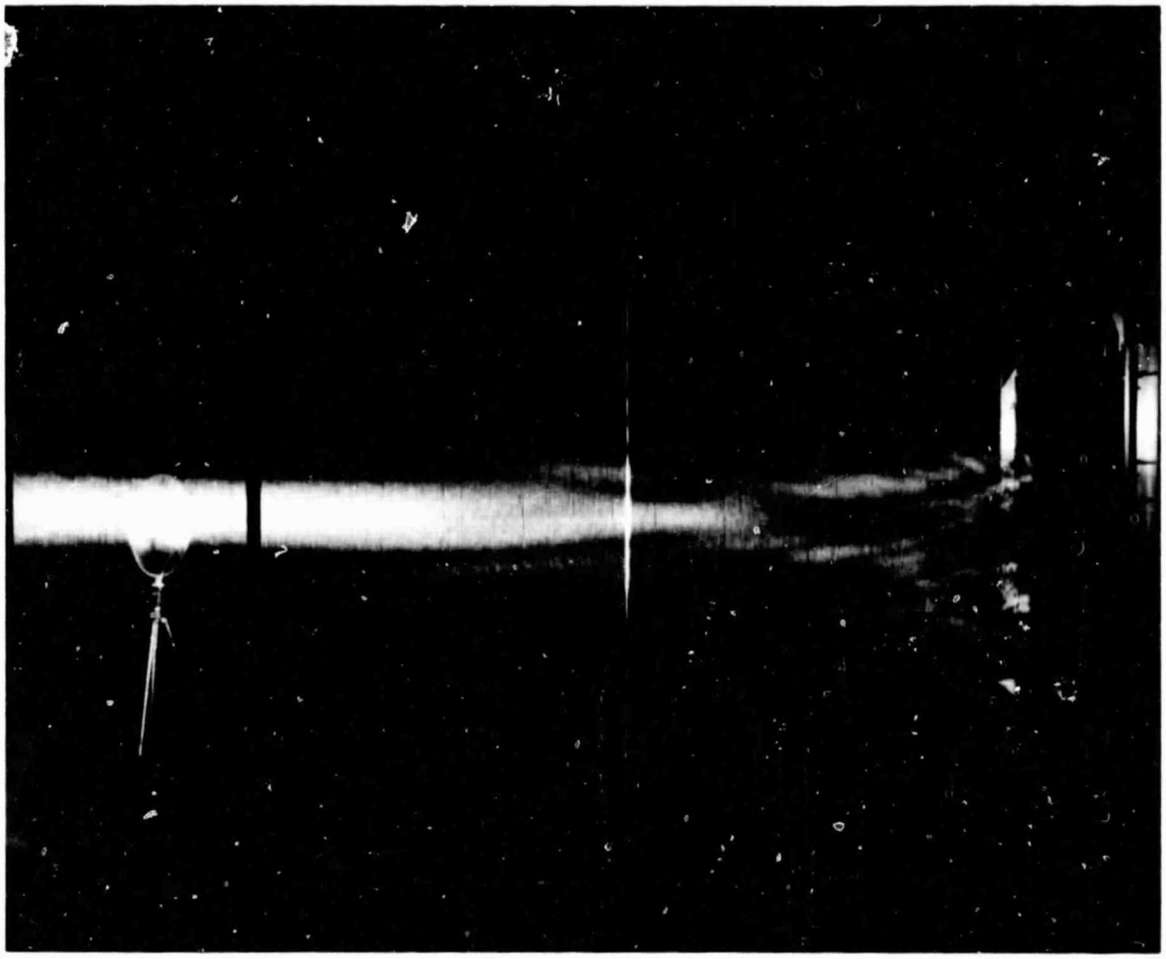

FIGURE 22

SONIC BEAM INTENSITY PATTERN - 90^{o}
PROGRAMMED PHASE ERROR

-Cross section along axis of gaussian beam of Figure 19.
Same as Figure 13 except for phase error.

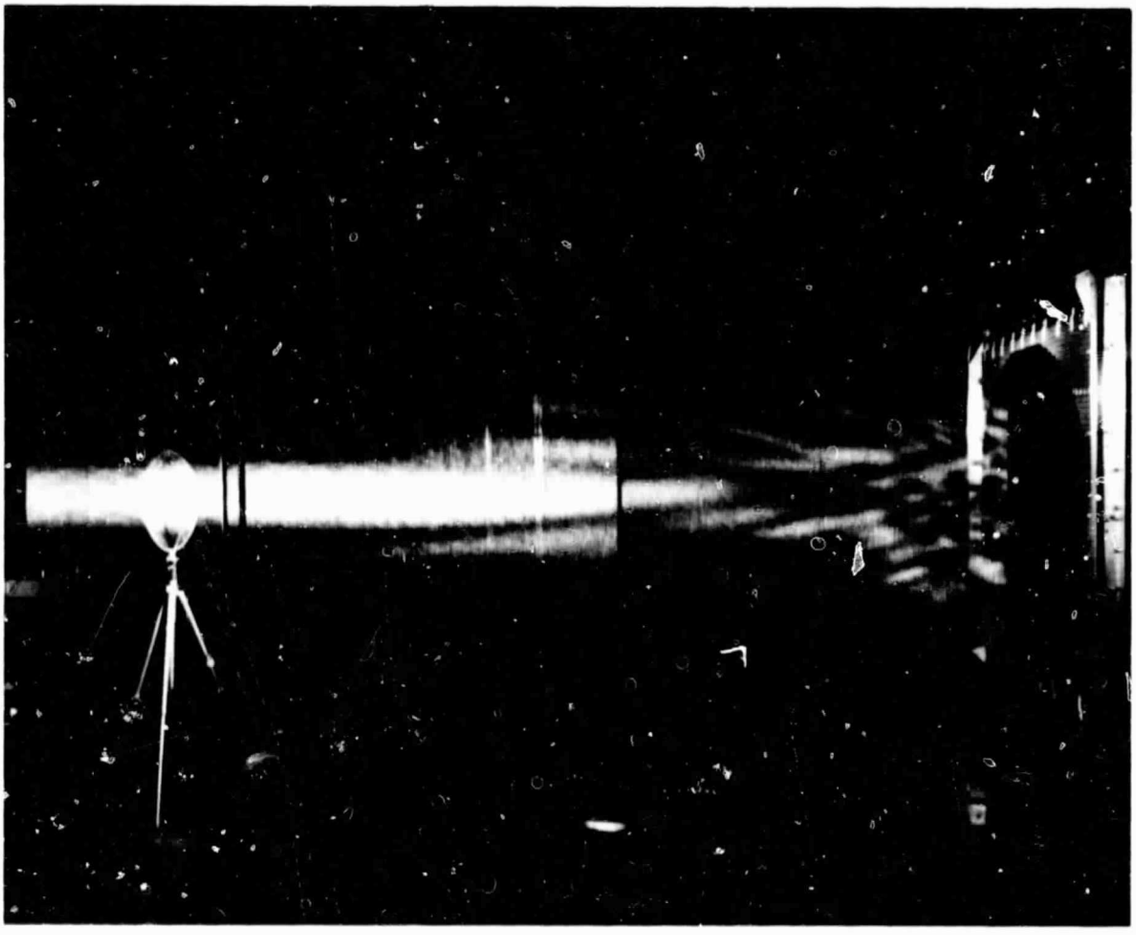

FIGURE 23

SONIC BEAM INTENSITY PATTERN - 120°
PROGRAMMED PHASE ERROR

-Cross section along axis of gaussian beam of Figure 20. Same as Figure 13 except for phase error. (Sound-to-light modulator gain same as Figure 22.)

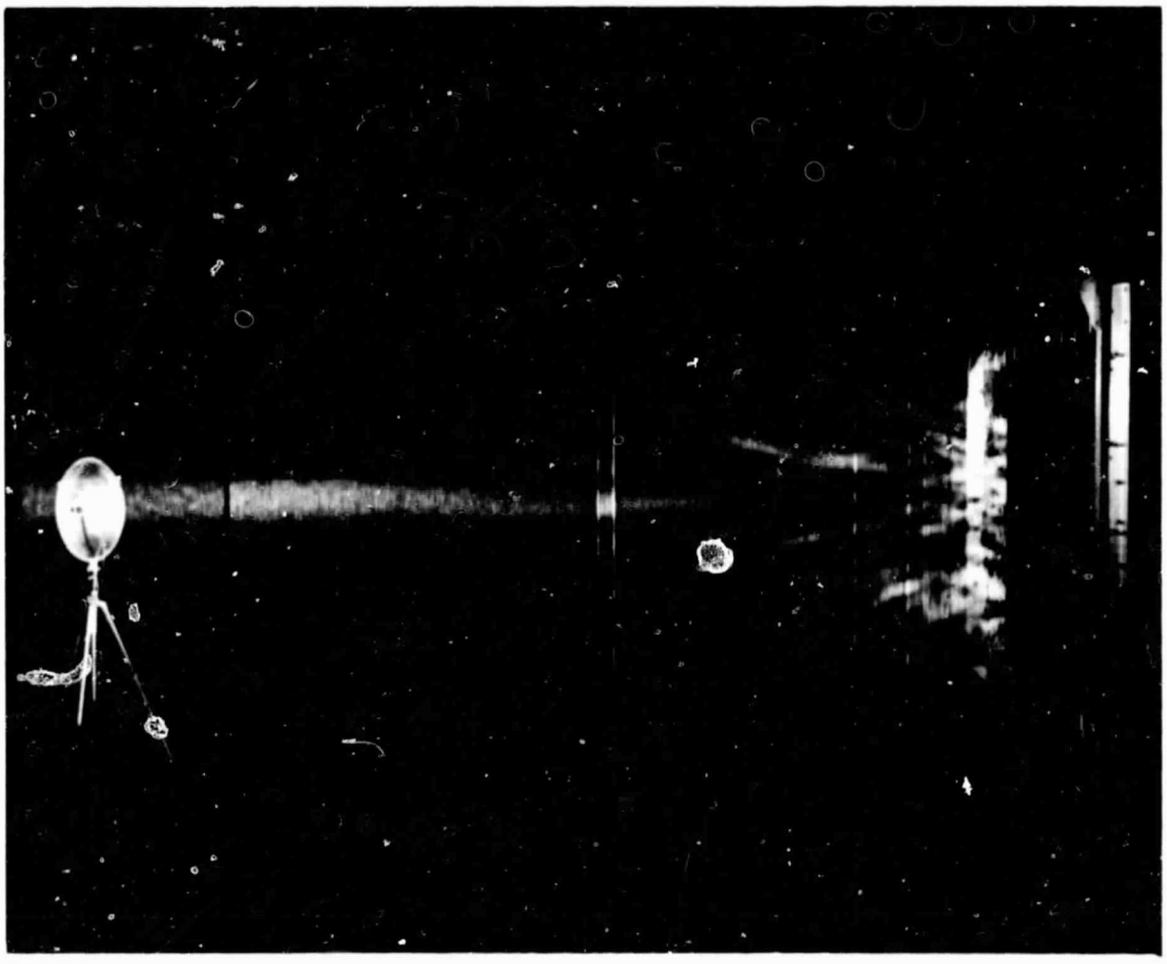

FIGURE 24

SONIC BEAM INTENSITY PATTERN - 150°
PROGRAMMED PHASE ERROR

-Cross section along axis of gaussian beam of Figure 21. Same as Figure 13 except for phase error. (Sound-to-light modulator gain same as Figure 22.)

MULTIPLE BEAM SIMULATIONS

Because any amplitude and phase distribution (sound illumination taper) can be programmed into the transmitting array, a successful effort was undertaken to generate multiple beams with the Sonic Simulator. A multiple beam forming Space Antenna has appeal because it would give a Solar Power Satellite the capability to simultaneously transmit to a number of independently located Rectennas with a single Space Antenna. The area required for a Rectenna site can be decreased by increasing the area of the Space Antenna. In a multiple beam system, the beamwidth of each power beam benefits from the entire aperture of the Space Antenna. A larger multiple beam Space Antenna with correspondingly smaller Rectennas may be economically advantageous.

Figure 25 depicts a multiple beam system transmitting 4 GW to four Rectennas in 1 GW power beams. Since the Space Antenna is twice the area (1.41 times the diameter) of that of the Reference System, each Rectenna only has to be one-half the area (0.707 times the diameter) of the Reference System Rectenna.

An experiment performed with the Sonic Simulator formed two independent beams by mixing alternate rows of transmitting

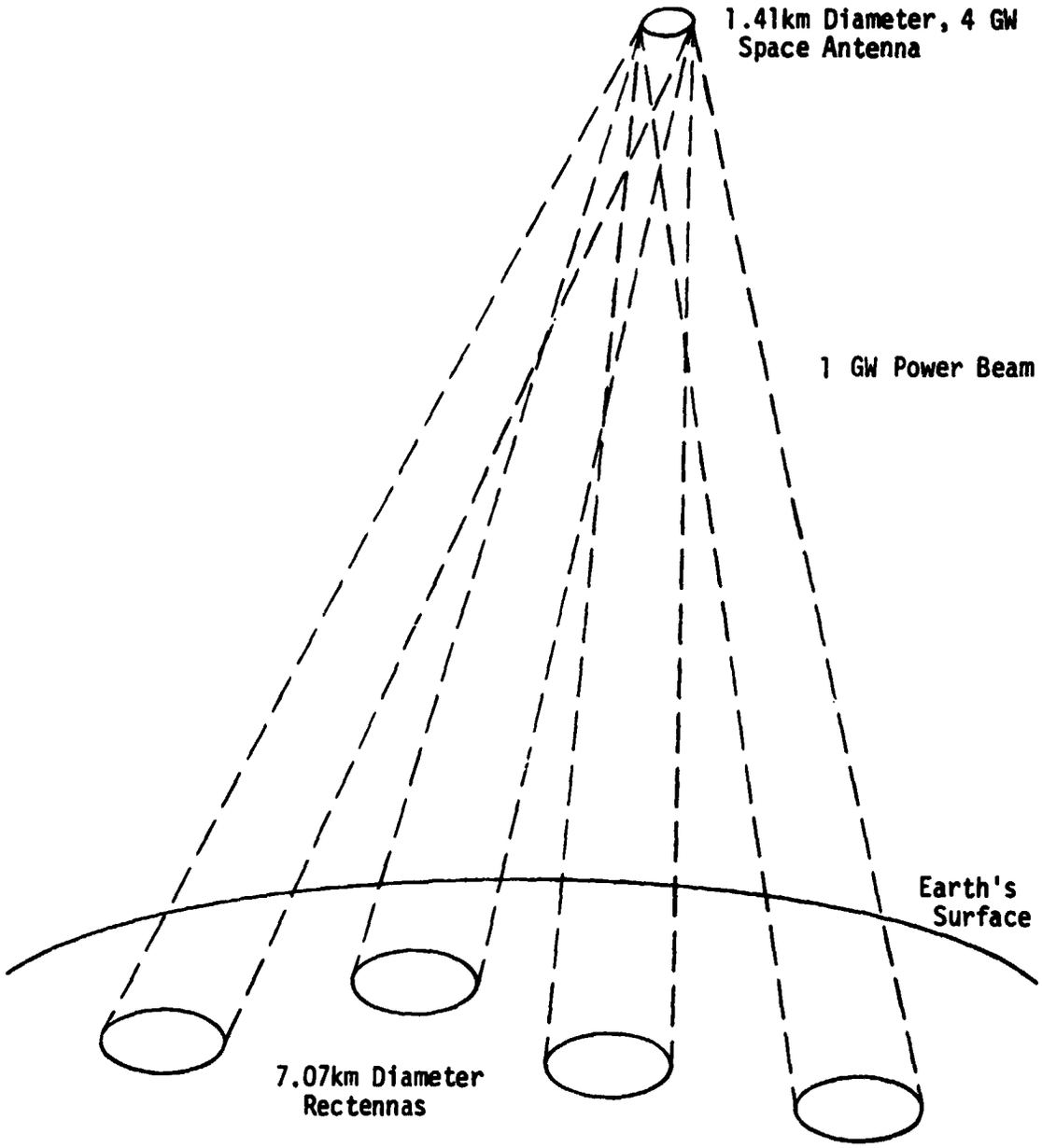

FIGURE 25

MULTIPLE BEAM FORMING SPACE ANTENNA

-Depicted is a Solar Power Satellite Space Antenna transmitting 4 GW in four equal-power beams to indepently located Rectennas. The power density variation in each beam is gaussian. Note that the beamwidths are narrower that the Reference System power beam because each power beam benefits from the entire Space Antenna aperture which is larger here.

elements on the transmitting array with the two sets of phase distributions required to form and point the two beams. This was equivalent to forming the beams with two independent interleaved arrays. Figures 26 and 27 show the results. This technique is not a candidate for practical SPS application.

A multiple beam forming method was developed that enables all transmitting elements to contribute to all beams. It provides a high degree of flexibility in chosing the number of beams to be formed and the power to be transmitted in each beam. The method involves, first, choosing the amplitude distribution and determining the phase distribution at the transmitting array that would be required to form each desired beam separately. Then the resulting amplitude distribution and phase distribution required to transmit all beams simulteneously are obtained by superposition - the phasor (vector) sum at each transmitting element of the amplitude and phase of the signal required to form each beam separately. (The resulting amplitude distribution and phase distribution required to transmit all beams simultaneously can vary dramatically from transmitting element to transmitting element.) Examples of the flexibility of this method are shown in Figures 28 through 31.

The beams in Figures 28 through 31 were "mathematically synthesized", that is, the phase distribution that would be required to form each beam separately was determined by computer. (The beam widths are the same in these figures; the beam spacings and photographic reduction factors are different.)

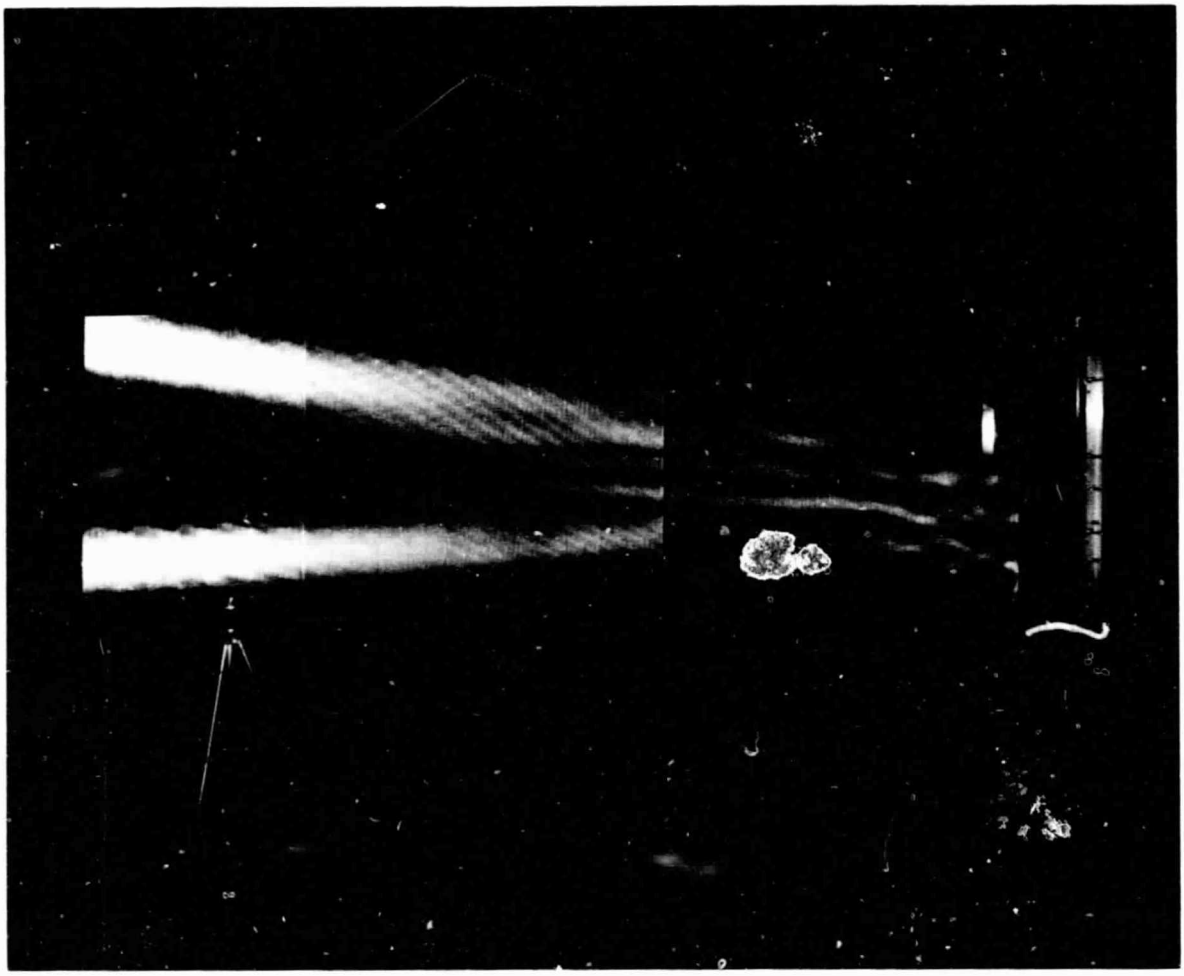

FIGURE 26

INTENSITY PATTERN OF TWO INDEPENDENTLY FORMED
AND SIMULTANEOUSLY TRANSMITTED BEAMS

-Cross section through centers of beams formed by phase tuning every other row of transmitting elements to one location of the parabolic microphone and the alternate rows of transmitting elements to a second location. The power distribution is gaussian.

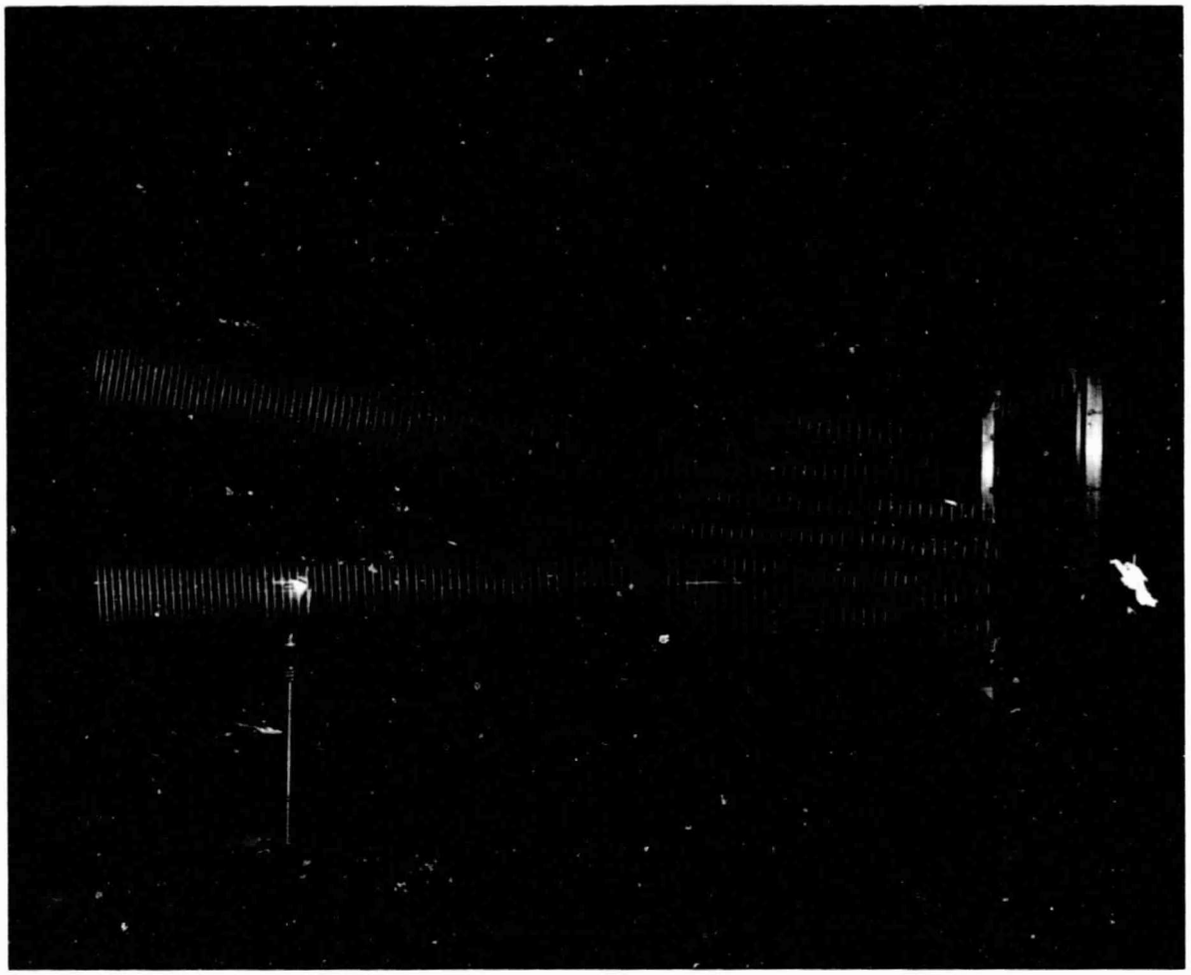

FIGURE 27

PHASE PATTERN OF TWO INDEPENDENTLY FORMED
AND SIMULTANEOUSLY TRANSMITTED BEAMS

-Cross section phase scan through the centers of the beams of Figure 26.

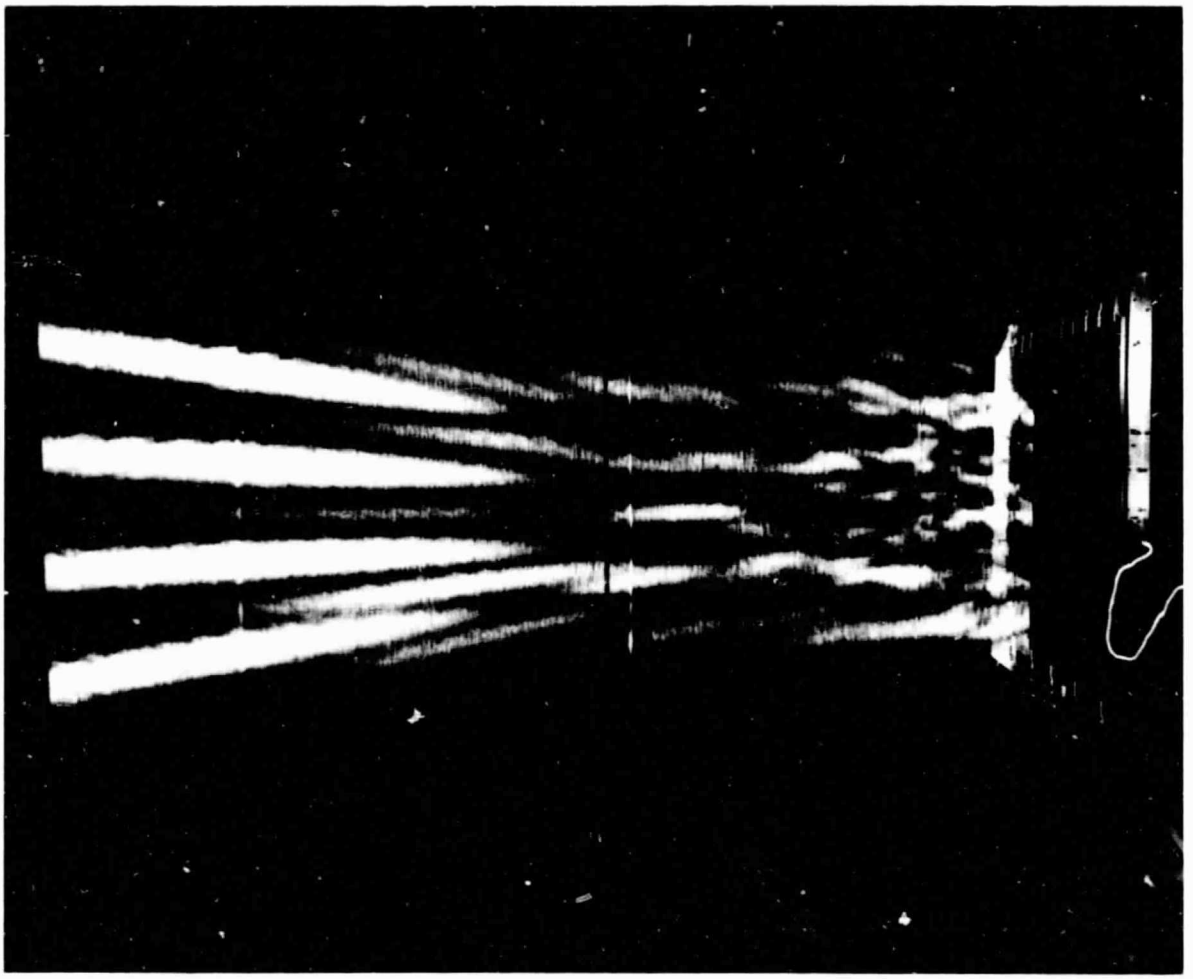

FIGURE 28

INTENSITY PATTERN OF FOUR SIMULTANEOUS BEAMS

-Each transmitting element contributes simultaneously to all four beams. The transmitting array phase taper was synthesized by mathematically determining the phase tapers to form each beam separately.

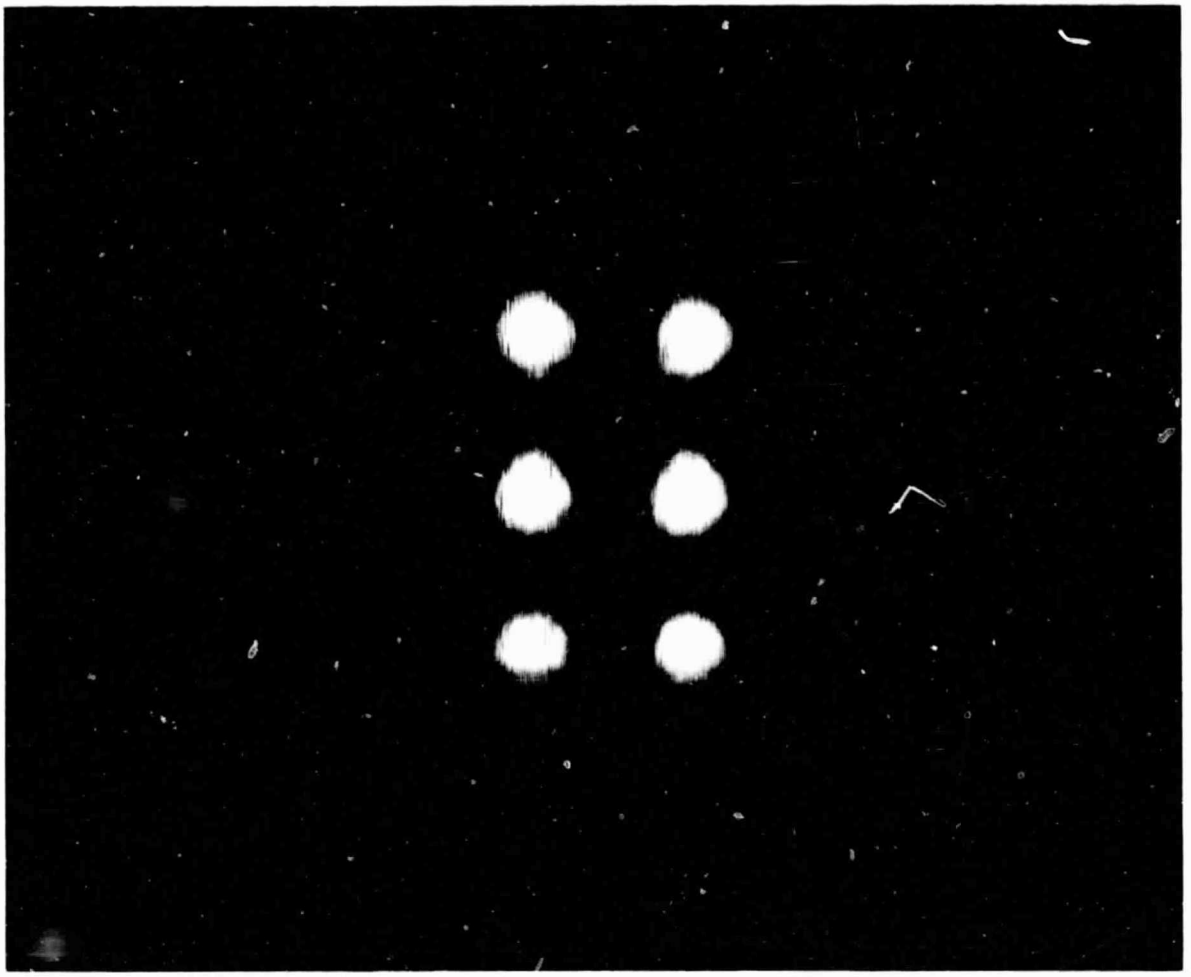

FIGURE 29

FAR FIELD INTENSITY PATTERN OF
SIX SIMULTANEOUS BEAMS

-The beams are shown focused in a plane 2.5 meters from the transmitting array. Horizontal and vertical spacing of beam centers is approximately 40 cm.

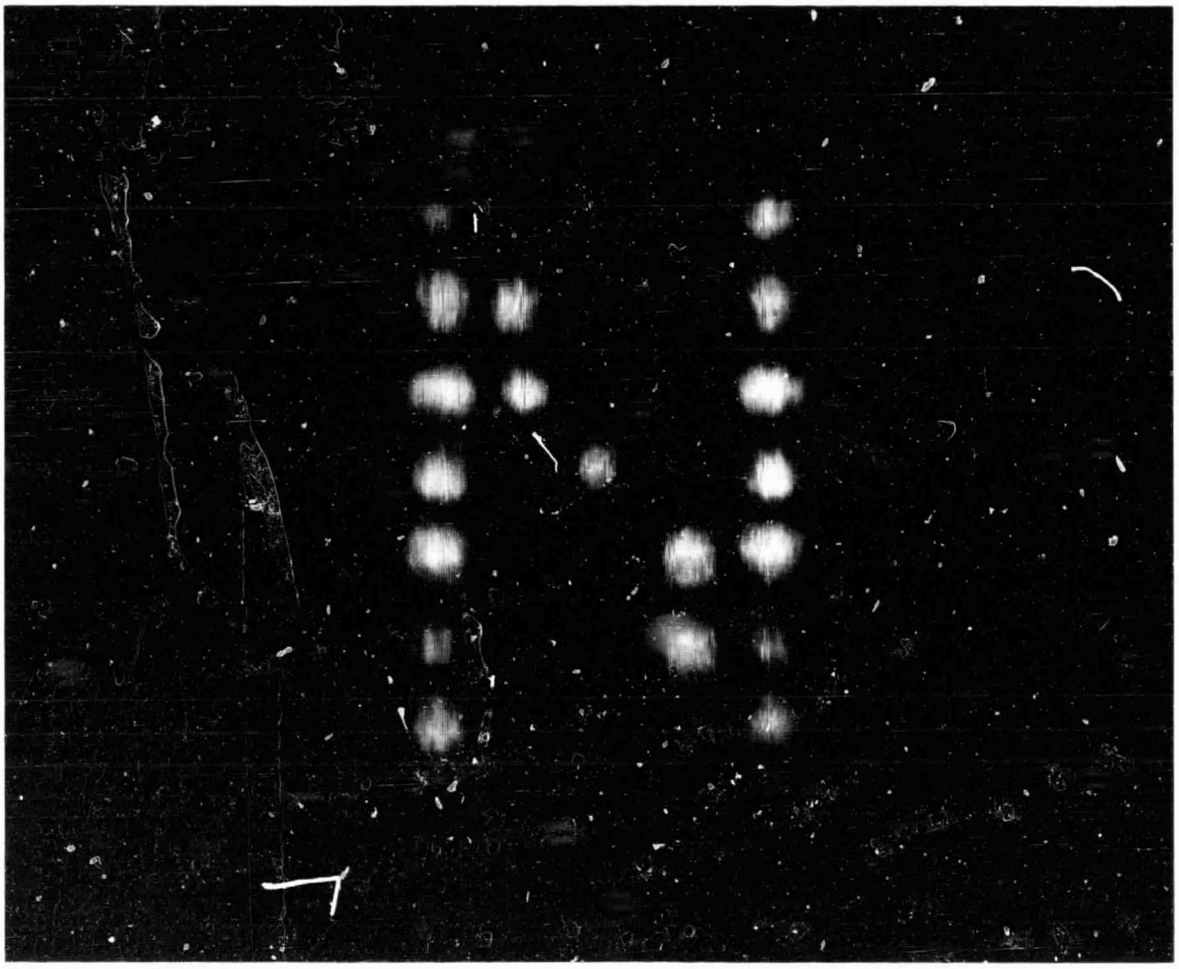

FIGURE 30

NINETEEN SIMULTANEOUS BEAMS
FORMING THE LETTER "N"

-Beams are focused in a 1 x 1.5 meter area 2.5 meters from the transmitting array.

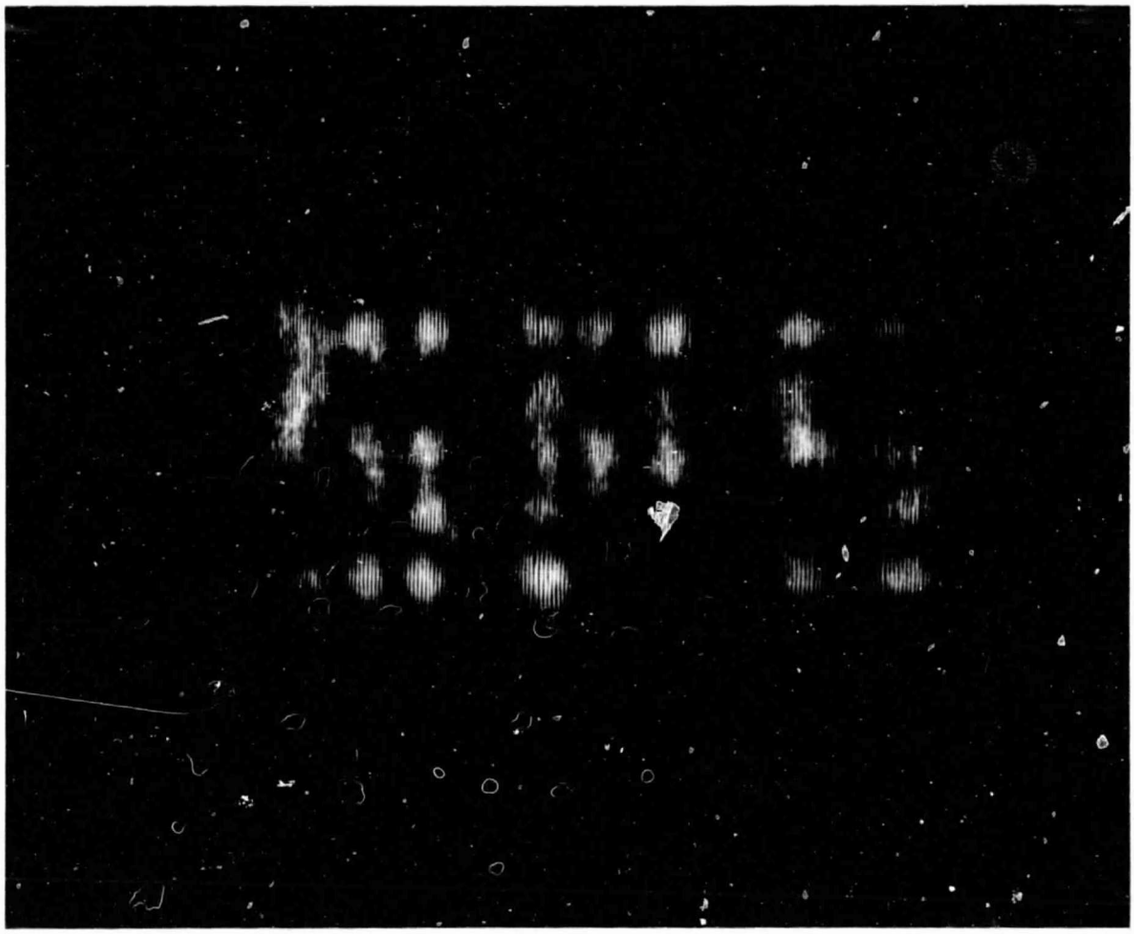

FIGURE 31

THIRTY-TWO SIMULTANEOUS BEAMS
FORMING THE LETTERS "SPS"

-The letters are formed 2.5 meters from the transmitting array in an area approximately 1.75 x 0.8 meters.

CONCLUSIONS

-- Sonic simulation is a viable technique for studying beam formation by a solar power satellite space antenna.

-- Interferometric Phase Control (IPC) is a feasible ground based phase control technique.

-- Sonic simulation should be able to provide a means for experimentally studying various aspects of retrodirective phase control.

-- Sonic simulation is highly applicable to the study of multiple power beams.

-- Ionospheric effects can be simulated by programming the simulator with the phase errors induced by the ionosphere or by physically disrupting the sonic beam with sculptured reflecting surfaces.

RECOMMENDATIONS

Based on the demonstrated capabilities of the sonic simulation technique we recommend that the following studies be conducted:

Sonic Simulation Study of Multiple Beam Formation by a Satellite Power System Space Antenna.

The specific areas that can be studied include, but are not limited to the following:

-- Determine factors affecting the formation of a multiple number of power beams, including limits on the number of beams and the requirements for the space antenna amplitude and phase tapers.

-- A cursory investigation has shown that the resultant amplitude and phase taper required at the space antenna to generate a multiple number of independent power beams can vary dramatically from power module to power module in a somewhat oscillatory manner. Amplitude taper appears to be less critical for multiple power beam formation than phase taper, at least for the main lobes. For this reason, it may be desireable to impose some sort of limits on the amplitude taper to minimize the magnitude of the dramatic excursions. Therefore, amplitude taper limiting and its effects on main beam formation, the maximum sidelobe level, and average power that can be transmitted, will be determined.

-- Determine the sensitivity of the ground patterns and amplitude and phase tapers to phase control corrections in one of the beams.

Retrodirective Sonic Simulation Study

Fabricate and test a sonic simulator version of a retrodirective phase control system. (See page 68.) Conduct simulations to study system operation.

Sonic Simulation Study of Power Beam Startup

Perform sonic simulations to display the ground patterns and power density levels resulting from the various power beam startup procedures analyzed by NASA. Using the sonic simulator, attempt to identify other viable startup procedures.

DETAILED HARDWARE DESCRIPTION

SONIC BEAM GENERATION AND CONTROL

The major components of the Sonic Simulator for sonic beam generation and control are the Sonic Transmitting Antenna, Simulator Console, and Parabolic Microphone.

A close-up view of the Simulator Console is given in Figure 32. Two 12 digit numbers can be displayed on the LED display unit. The phase detection monitor consists of two differential amplifiers and a dual trace oscilloscope to monitor the input and internal signals of the Phase Detector located near the rear of the console behind the Interface Panel. The computer, designed and built by Novar, is a special purpose ultra high speed machine with 270 K bytes of memory. The power supply at the bottom of the console provides all Sonic Transmitting Antenna and computer power.

Some key details of the construction of the Sonic Transmitting Antenna are shown in Figures 33 and 34. The transmitting elements are mounted on circuit cards. Figure 34 shows the rear-mounted Sonic Transmitting Antenna control/drive electronics and a close up view of the rear of the circuit cards showing the diode matrix which isolates the transmitting elements from each other.

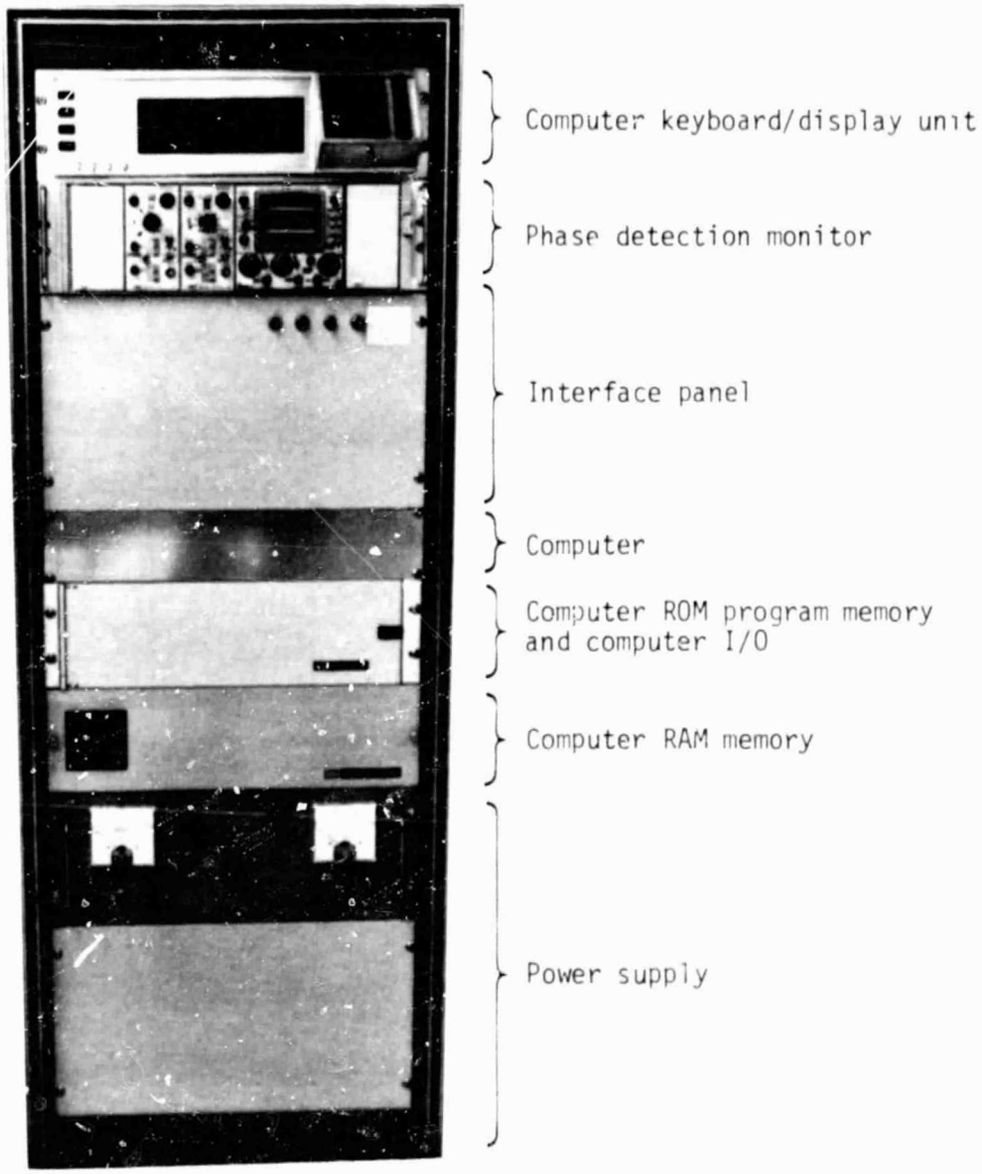

FIGURE 32

SIMULATOR CONSOLE

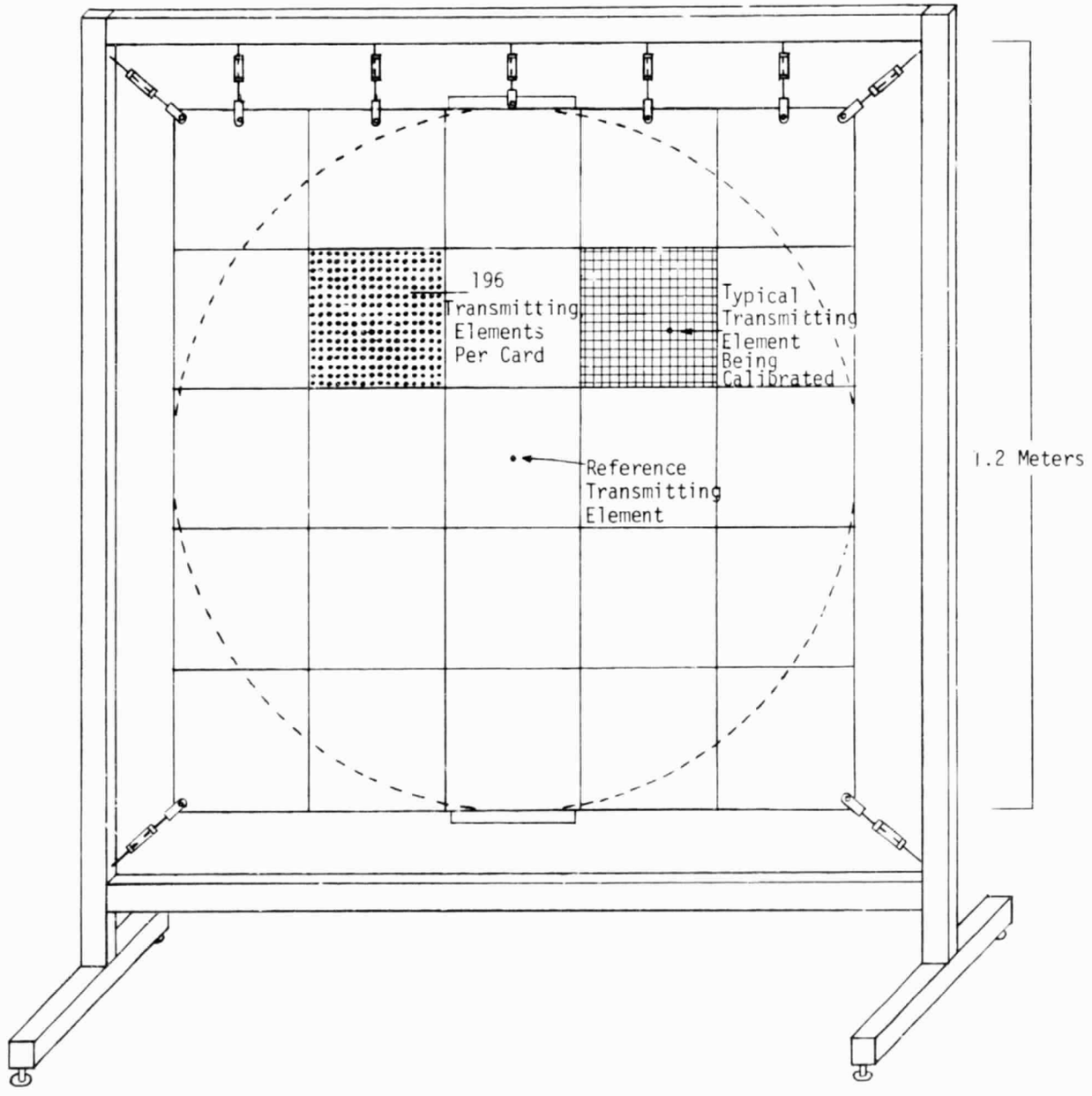

FIGURE 33

TRANSMITTING ELEMENT CONFIGURATION DETAILS -
SONIC TRANSMITTING ANTENNA

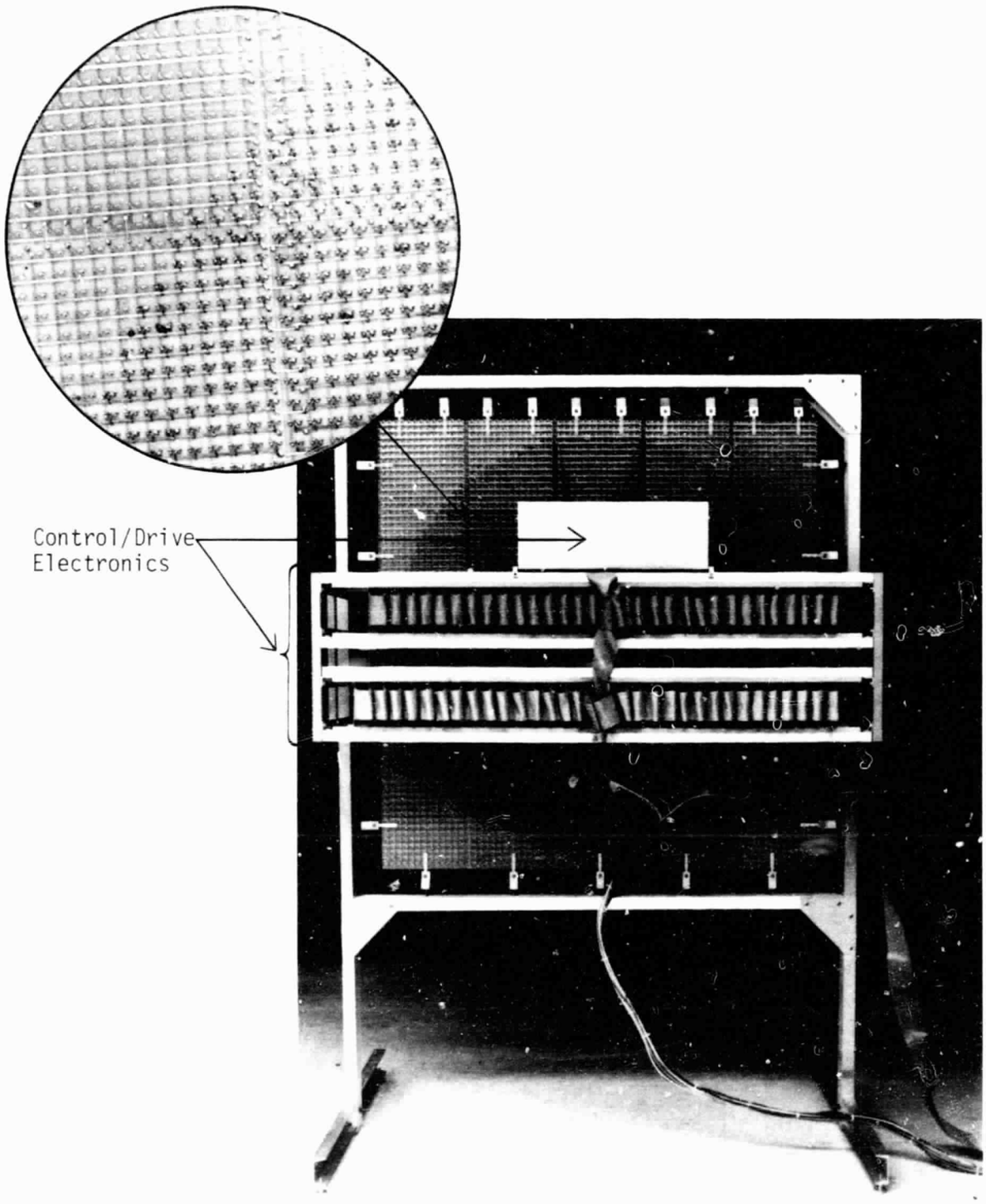

FIGURE 34

REAR VIEW - SONIC TRANSMITTING ANTENNA

The reference transmitting element, shown near the center of the array in Figure 33, is driven by a signal from the Frequency Synthesizer (Figure 35) located on the rear of the Sonic Transmitting Antenna. The synthesizer coherently generates this and other signals described below from a 7.45 MHz crystal-controlled master oscillator/clock. The closed loop phase control system is designed to make phase comparisons during normal operation of the power beam. As discussed in Appendix B, the phase comparisons are made sequentially at two different phase reference frequencies. Accordingly, the synthesizer generates three frequencies (9.7 kHz, 10.67 kHz, and 11.16 kHz) for transmission by the reference transmitting element. Each transmitting element on the sonic antenna can transmit a sonic signal at one of three frequencies--11.64 kHz, the sonic beam frequency, or 8.73 kHz or 8.24 kHz for phase tuning. When a transmitting element transmits at 8.73 kHz, the reference transmitting element transmits simultaneously at 9.7 kHz and 10.67 kHz. The frequency difference between 9.7 kHz and 10.67 kHz and between 9.7 kHz and 8.73 kHz is 0.97 kHz, one of the two phase reference frequencies. When a transmitting element transmits at 8.24 kHz, the reference transmitting element transmits simultaneously at 9.7 kHz and 11.16 kHz. The frequency difference between 9.7 kHz and 8.24 kHz and between 9.7 kHz and 11.16 kHz is 1.46 kHz, the other phase reference frequency. The appropriate frequency for a transmitting element is derived by frequency division of one of the three synthesizer signals generated at frequencies

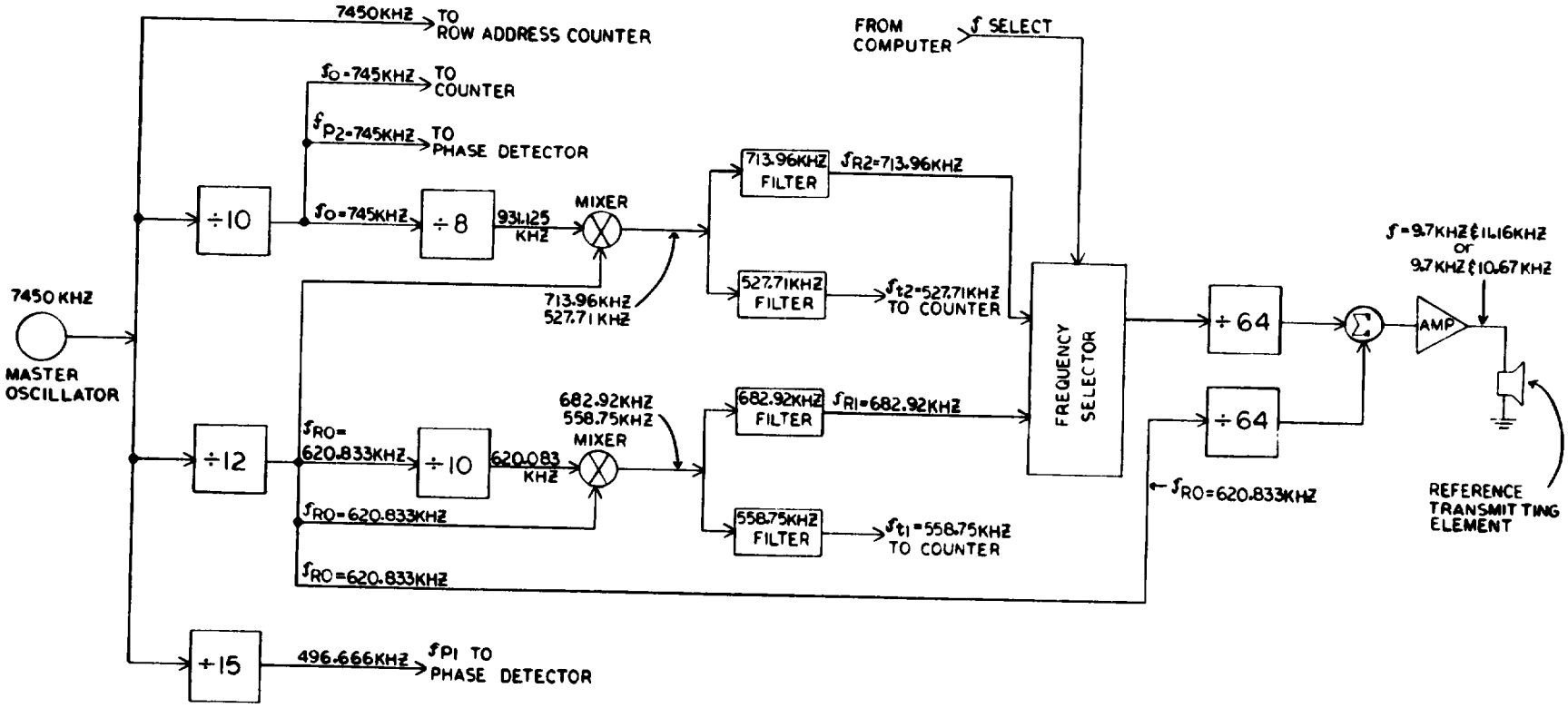

FIGURE 35

SIMULATOR'S FREQUENCY SYNTHESIZER

f_o = 745 kHz, f_{t1} = 558.75 kHz, and f_{t2} = 527.71 kHz. (If a particular sonic simulation study does not require phase tuning to take place during normal transmission of the sonic beam, the phase tuning operation can be somewhat simplified. With the sonic beam off, each transmitting element is phase tuned at only one phase reference frequency. Then the sonic beam is transmitted at the frequency used for phase tuning.) The Frequency Synthesizer also generates two signals for phase detector clocking. One is at frequency f_{p1} = 496.666 kHz, and the other is at f_{p2} = 745 kHz.

The parabolic microphone (Figure 36), which receives the phase tuning signals transmitted from the transmitting antenna, consists of a 45 cm. diameter parabolic dish and seven electrostatic microphones. The microphones are arrayed in a mounting assembly as shown and have their signal outputs in parallel. The mounting assembly is manually adjustable along the axis of the dish so that only the transmitting antenna is "seen" by the parabolic microphone.

To phase tune the transmitting antenna, the Phase Detector (Figure 37) generates a 6-bit digital phase data word which is processed by the computer. The signals received by the microphone are up-converted by mixing with a 5.6353 MHz oscillator signal and split into two groups by means of the two 2.6 kHz bandwidth crystal filters in the signal splitter shown in Figure 37. The upper signal path of the signal splitter detects a signal whose frequency is the difference

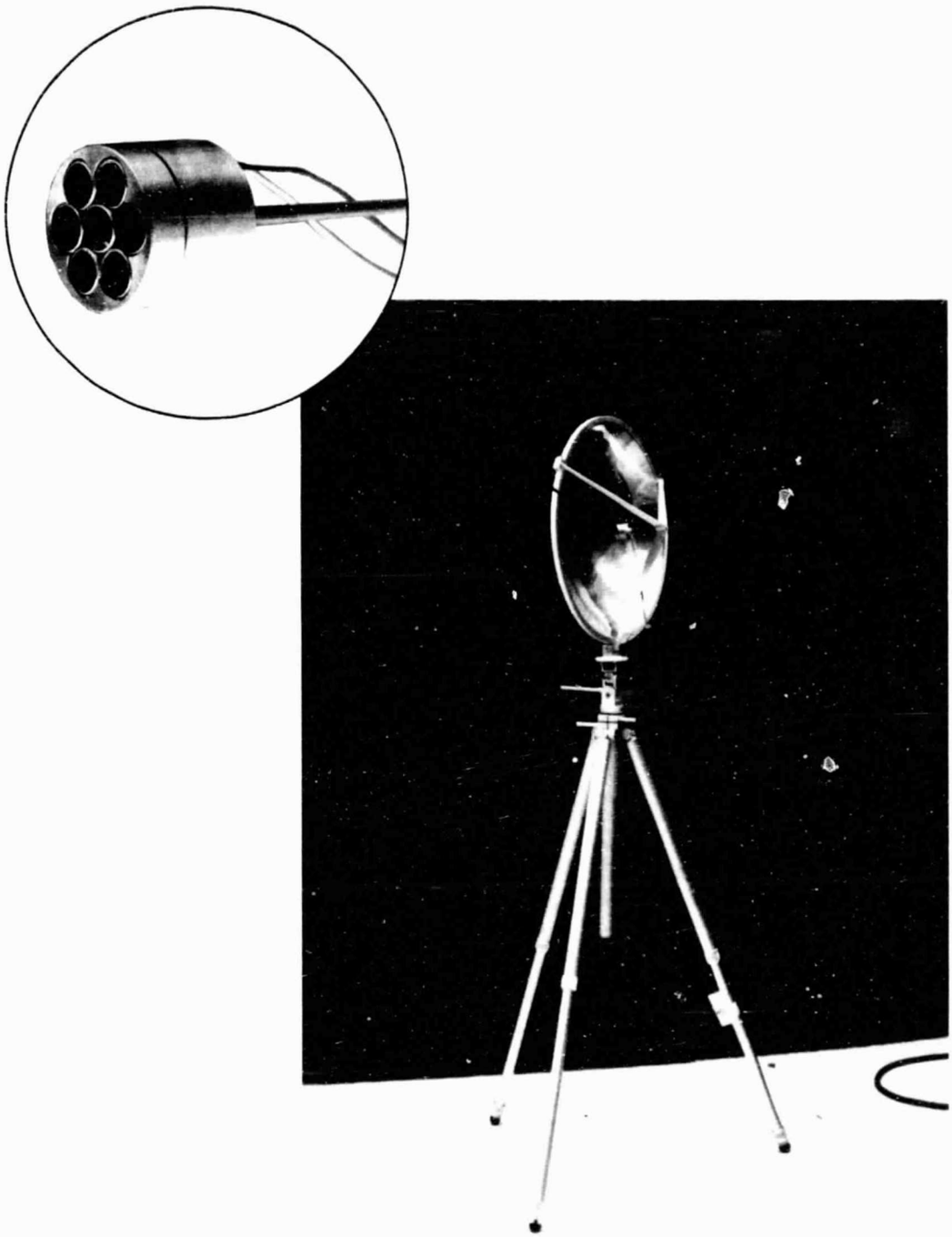

FIGURE 36

PARABOLIC MICROPHONE

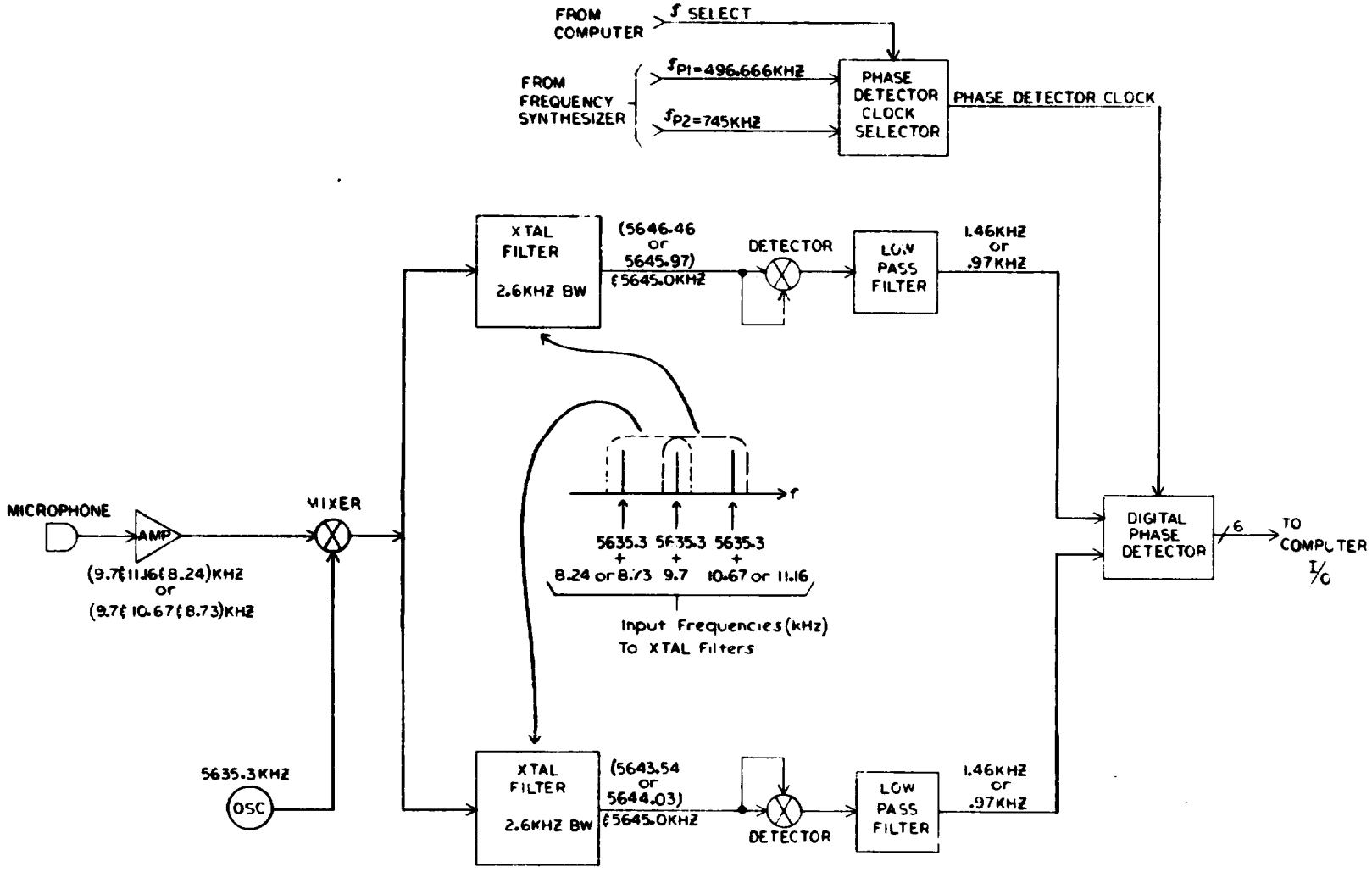

FIGURE 37

PHASE DETECTOR

between that of the up-converted 9.7 kHz signal from the reference transmitting element and the up-converted signal from the transmitting element being phase tuned. This detected signal is input to the digital phase detector which determines its phase relative to a phase reference signal generated in the lower signal path of the splitter. The phase reference signal is a detected signal whose frequency is the difference between the up-converted 9.7 kHz and 10.67 kHz or 11.16 kHz signal from the reference transducer. When the phase reference frequency is changed from 0.97 kHz to 1.46 kHz, the computer also changes the phase detector clock rate to be approximately 2^9 times the frequency of the two signals being phase detected. The digital phase data word generated by the digital phase detector is input to the computer for calculation of the phase correction to be output to the transmitting element.

The computer sends the column and row address coordinates, frequency and phase data for each transmitting element to the appropriate column Driver/Memory Board (Figures 38 and 39). Stored in the ROM on the Column Driver/Memory Board (Figure 39) are 15 different amplitude sinewaves plus one zero amplitude one. The 15 sinewaves range in 2 dB amplitude steps from 0 dB, which corresponds to maximum amplitude, down to 28 dB below maximum amplitude. This allows a range of power levels and/or amplitude tapers to be programmed. The particular amplitude level desired for a transmitting element is selected by the amplitude address input to the ROM. Each sinewave

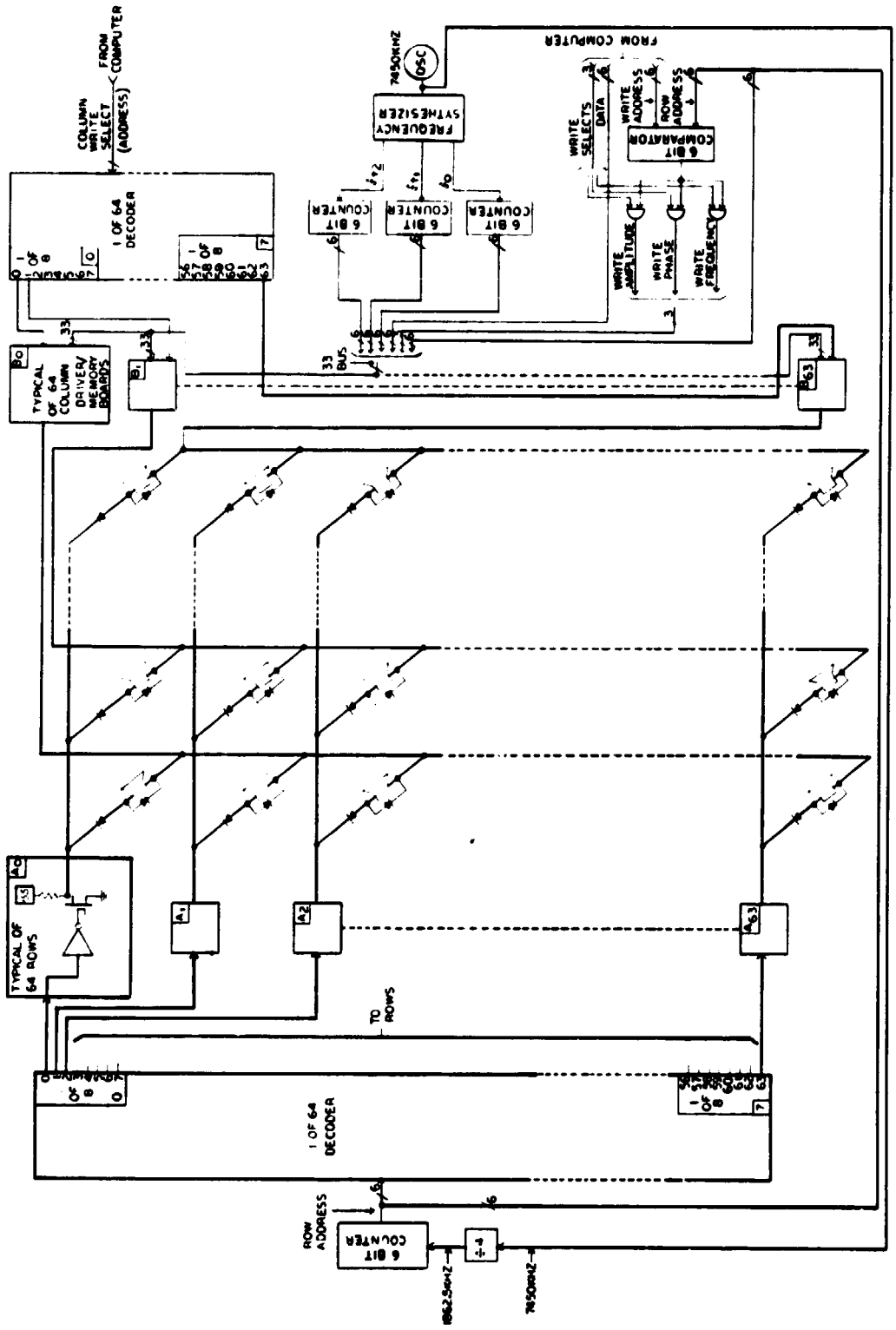

FIGURE 38

SONIC TRANSMITTING ANTENNA CIRCUITRY

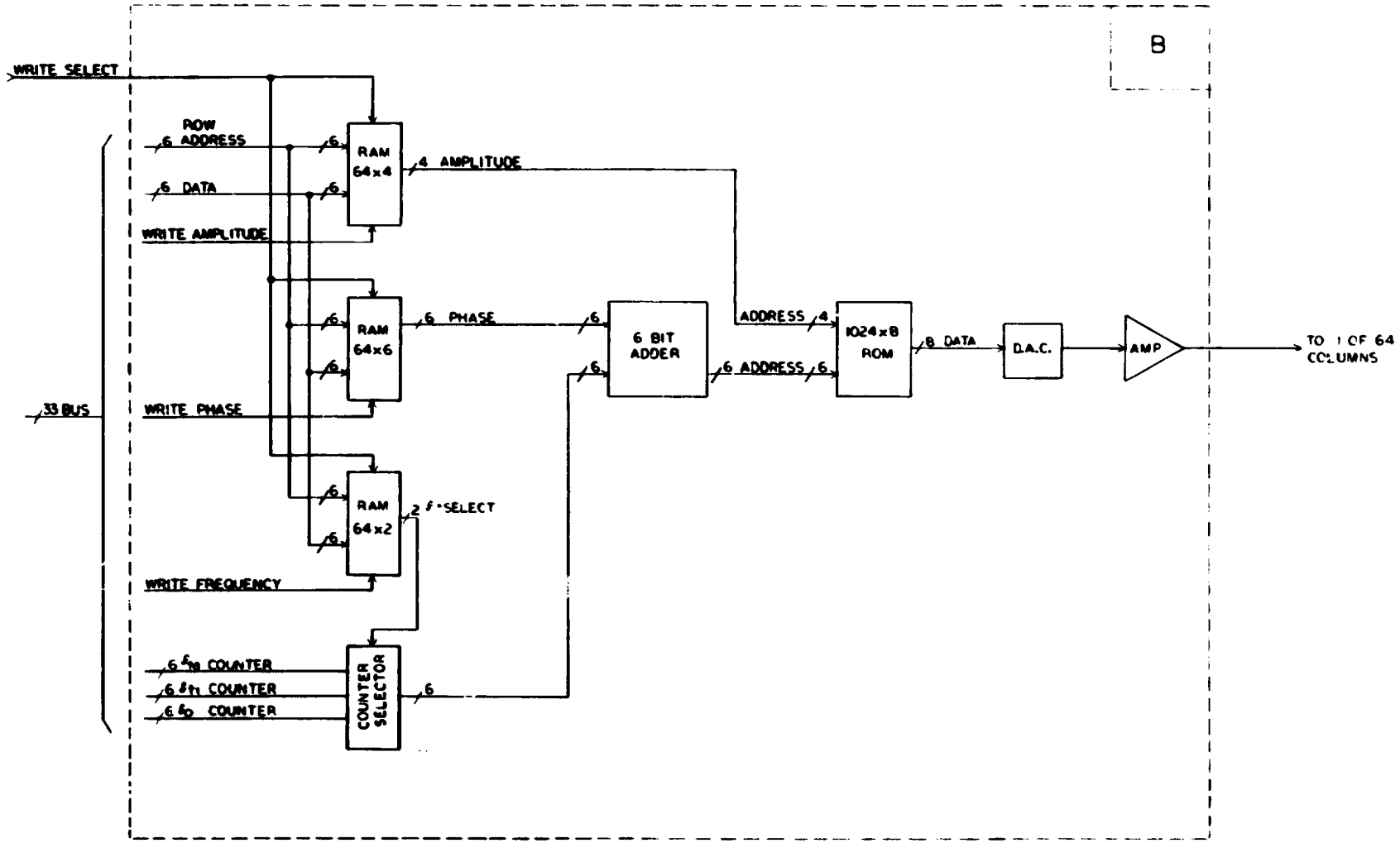

FIGURE 39

COLUMN DRIVER AND MEMORY

consists of 64 8-bit binary data words. The data words respectively correspond to the values of the instantaneous amplitude of the sinewave as its phase varies from 0^{o} to 360^{o} in increments of 360 : 64 = 5.625^{o}. Each data word address is a phase address corresponding appropriately to one of the 64 increments in phase of the sinewave. If the amplitude address input to the ROM were constant, then clocking through the 64 phase addresses at one of the three selectable counter rates would generate a step-approximated sinewave out of the DAC whose frequency was 1/64th that of the counter. The amplitude and phase addresses acutally input to the ROM are those of the sinewaves associated with the 64 transmitting elements in the column being driven by the column driver. Each sinewave is amplitude and phase addressed at 1/64th of the 1862.5 kHz row address counter rate. This produces multiplexed information for 64 sinewaves which are output from the DAC as a composite signal (Figure 40) of 64 uniformly interleaved pulse trains, one per sinewave. Each pulse train is, in effect, the result of pulse amplitude modulating a 29,101.5625 pulses/sec. continuous pulse train with a sinewave. To output the composite signal, which has step amplitude changes occurring up to 1.8625×10^{6} times/sec, the Column Driver/Memory Board has an output slew rate greater than 1000V/μsec. After being output in pulse amplitude modulated and multiplexed form by the Column Driver/Memory Board, each sinewave is extracted by demultiplexing and by the intrinsic analog filtering that

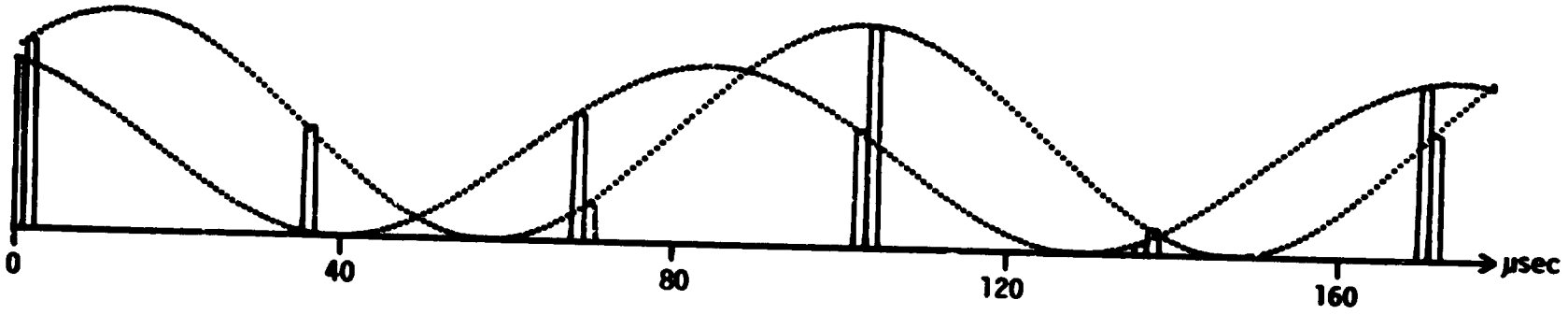

FIGURE 40

GENERATION OF A COMPOSITE SIGNAL AT DAC
OF COLUMN DRIVER/MEMORY BOARD

-Two of the 64 sinewaves making up a composite signal are shown. Space between pulses is filled by remaining pulse generated sinewaves.

takes place at its respective row transmitting element to become the drive signal for that element.

The relative phase of each of the sinewaves output by the column driver is determined by adding counts from 0 to 63 by means of the 6 bit adder (Figure 41) to the phase address being clocked into the ROM at the time that the amplitude and phase addresses for an individual sinewave are being input to the ROM. The counts from 0 to 63 correspond to phase shifts from 0° to 354.375°. Therefore any phase shift in that range, in 5.625° increments, can be obtained.

Demultiplexing of the row signals input to the 64 columns of transmitting elements from the 64 column drivers is accomplished in the Sonic Transmitting Antenna Circuitry (Figure 38) by sequentially strobing each row of transmitting elements in the 64 column by 64 row matrix. The strobes are generated at a 29,101.5625 times/sec. rate by the row address decoder and are input to the matrix from 64 row drivers which operate in synchronism with the row pulses being output for a particular row by the column drivers. Therefore 64 transmitting elements in a row are simultaneously driven by the column and row drivers at one time.

Analog filtering of the demultiplexed pulses at the transmitting elements is accomplished by the element's natural low-pass filter characteristic which filters out frequencies

above the audio range in the pulse amplitude modulated pulse train.

Construction and physical configuration details of the Sonic Transmitting Antenna circuitry given in Figures 35, 38, and 39 are shown in Figure 41. Signal connections to the simulator's computer is via the 60 conductor ribbon cable shown in the bottom center of the photograph in Figure 41.

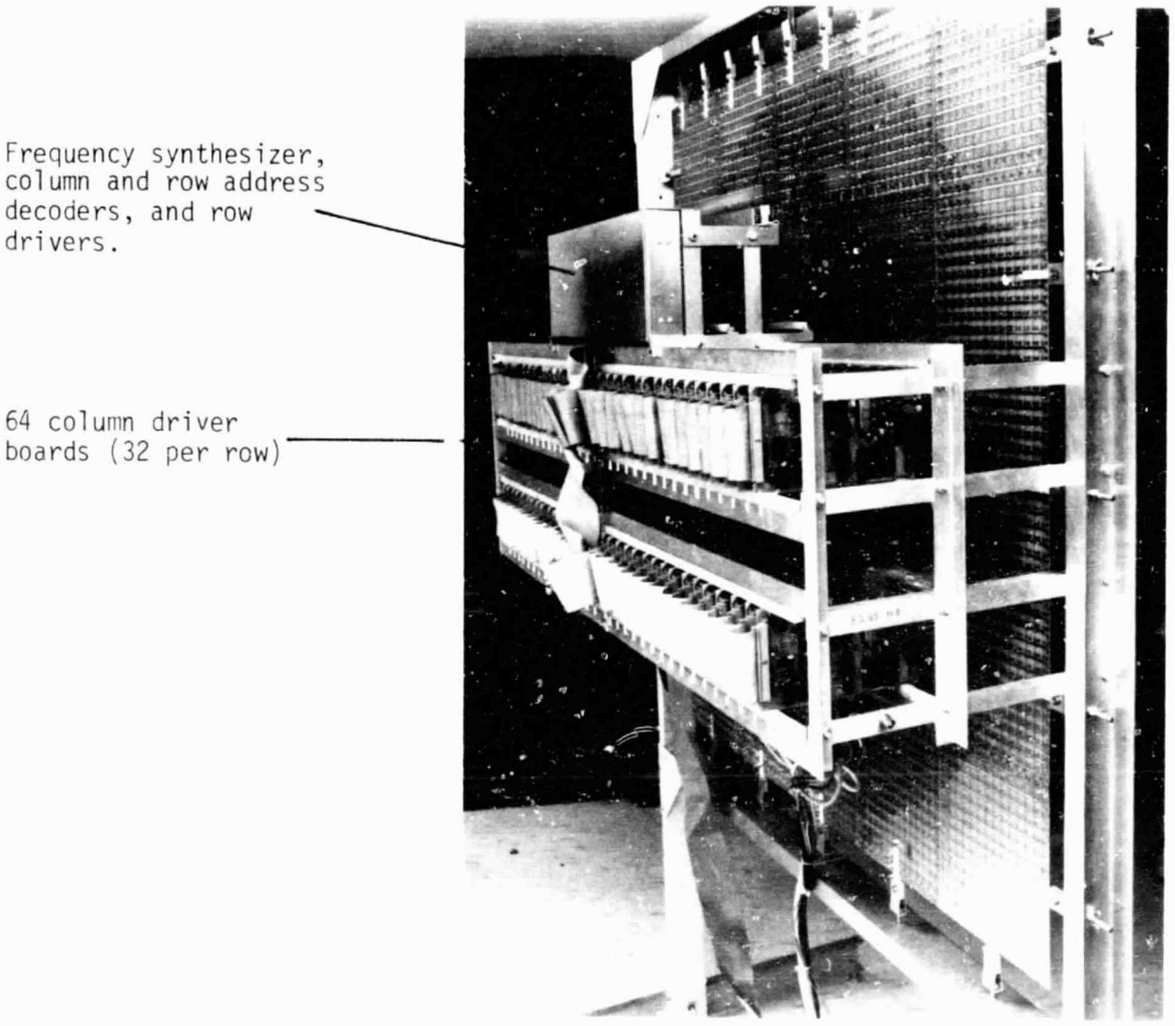

FIGURE 41

SONIC TRANSMITTING ANTENNA
CIRCUITRY CONSTRUCTION DETAILS

SONIC BEAM PHOTOGRAPHING

Pertinent details of the photographic measurement system, which is patterned after a concept developed at Bell Laboratories in the early 1950's[4], are shown in Figure 42. The sound-to-light modulator converts the sound energy received at its microphone to a drive signal that powers a miniature incadescent bulb. The signal is logarithmically amplified to better show the range in sound intensity in the sonic beam photographs. (In effect the decibel sound level is photographed.) A bandpass filter at the power beam frequency prevents extraneous acoustic noises from affecting the sound-to-light modulator output. For phase pattern photographs a phase reference signal at the sonic beam frequency and coherent with the sonic frequency source is summed with the signal input from the microphone. This generates a signal at the output of the summer whose amplitude varies as a function of the phase between the reference signal and the sonic beam. As the sound-to-light modulator is scanned through the beam, the summer output signal amplitude ranges from a maximum when a point in the sonic beam is in phase with the reference to a minimum at a point 180° out of phase (Figure 43).

The sound-to-light modulator is vertically scanned by attachment to a cord driven by the vertical drive motor. Modulator vertical scan limits are sensed by photo detectors at the top and bottom of the scanning system frame. One side of the drive cord passes through the detectors and has

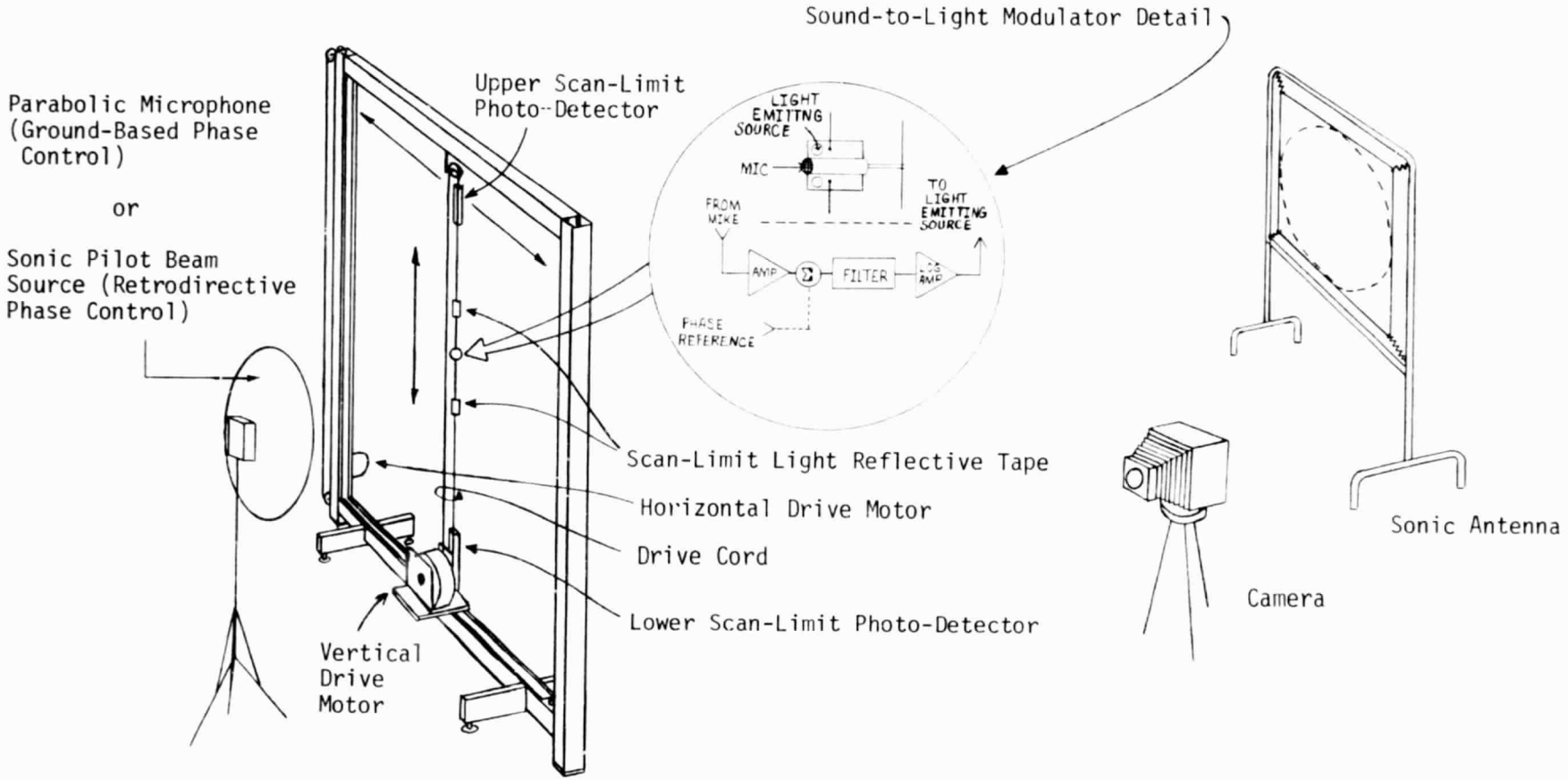

FIGURE 42

SONIC BEAM PHOTOGRAPHING SYSTEMS DETAILS

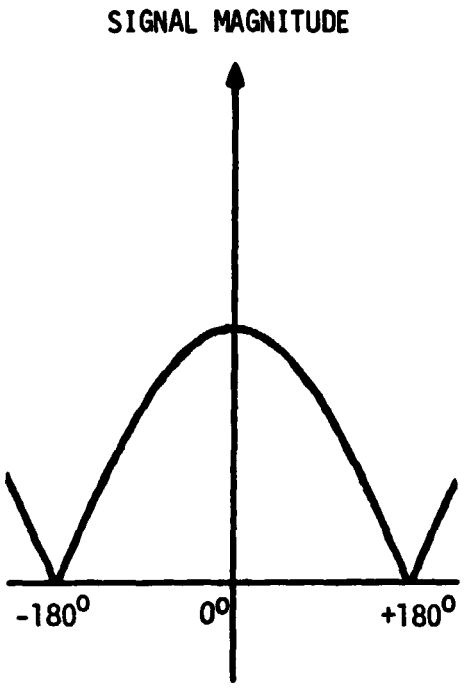

FIGURE 43

SOUND-TO-LIGHT MODULATOR RESPONSE
CHARACTERISTIC -- PHASE PATTERN PHOTOGRAPHS

light reflective tape attached to it on either side of the modulator. When the tape enters the detector, light from an internal source is reflected onto a photocell which causes the direction of rotation of the vertical drive motor to reverse.

The vertical scanning apparatus is slowly scanned horizonally by the horizontal drive motor to generate the photographic raster. An optimum raster is produced when the vertical and horizonal scan speeds, both manually adjustable, are in a ratio of about 2700 : 1. The scan speeds used for this report, which were in this ratio, produced a complete photographic scan in about 45 minutes. A much faster scan would be possible by modifying the scanning mechanism.

The scanning system frame in Figure 42 is shown positioned to photograph a far field cross section of the sonic beam. Figure 44 shows the frame positioned to photograph the near field. Figure 45 shows the frame supporting members reconfigured to photograph a cross section of the beam through the beam axis ("z" dimension). The relative position of the dish during beam forming prior to photographing is shown as a dotted outline. Figure 46 shows the scanning frame positioned to photograph the z - dimension near field of the beam.

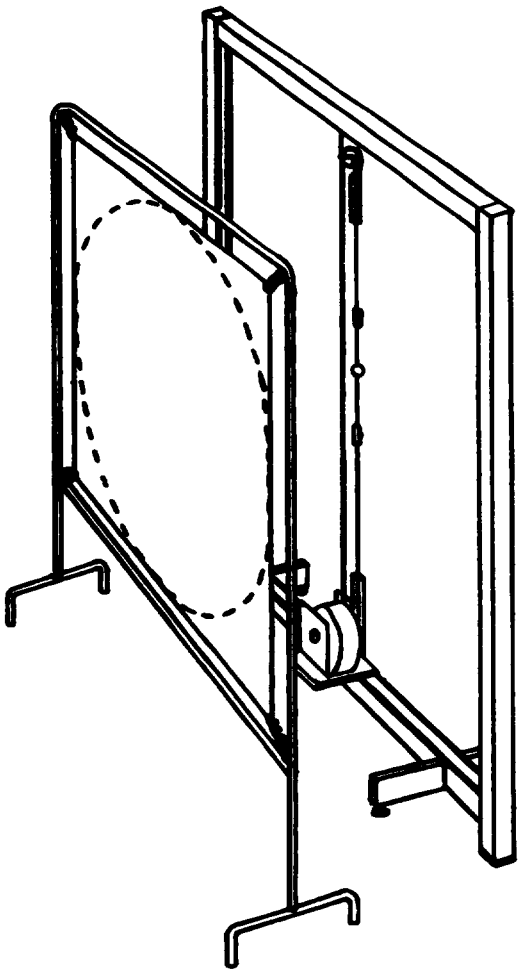

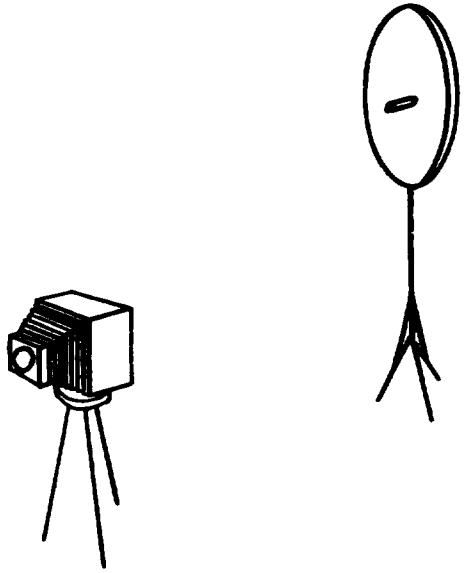

FIGURE 44

PHOTOGRAPHING NEAR FIELD CROSS SECTION OF SONIC BEAM

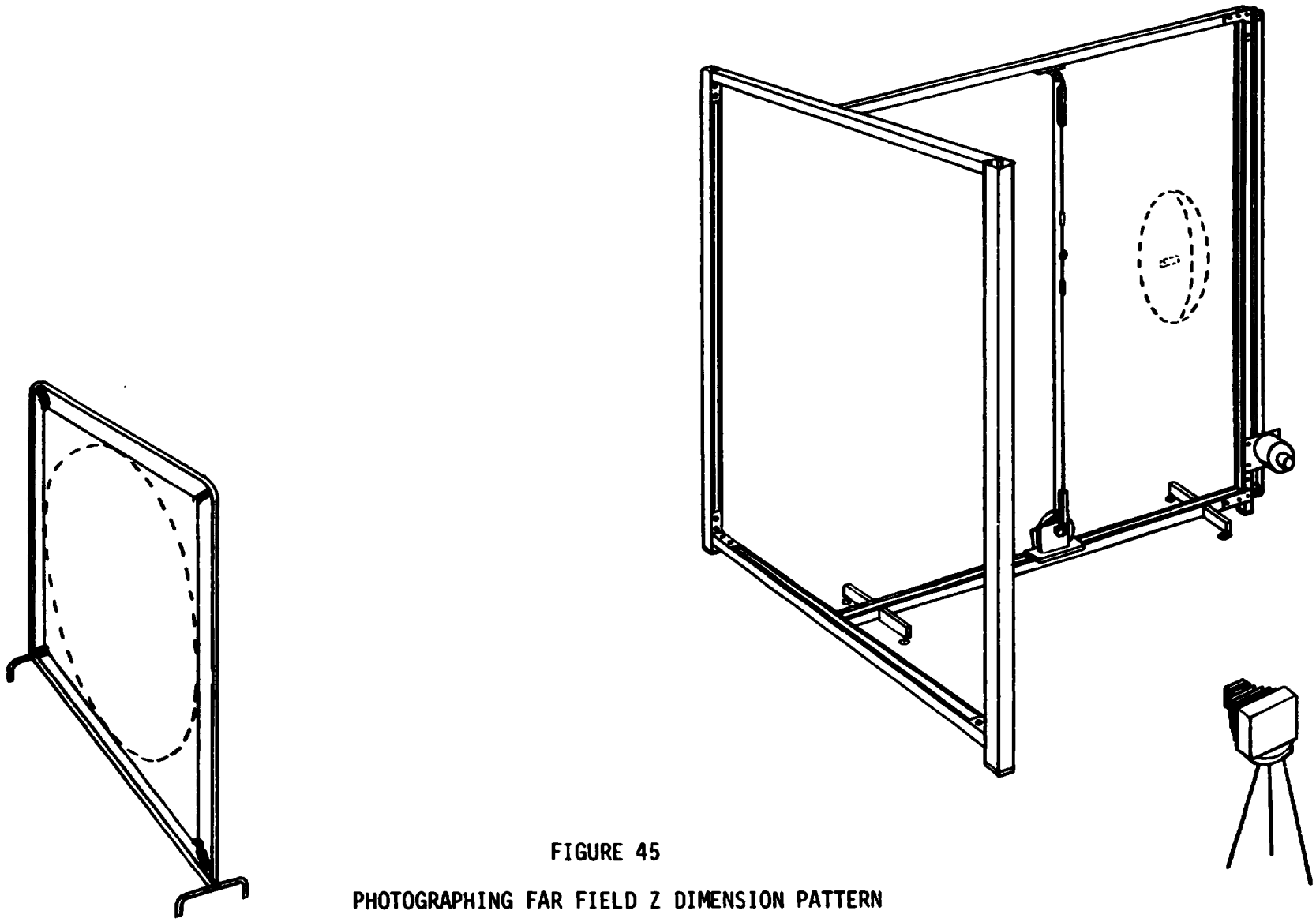

FIGURE 45

PHOTOGRAPHING FAR FIELD Z DIMENSION PATTERN

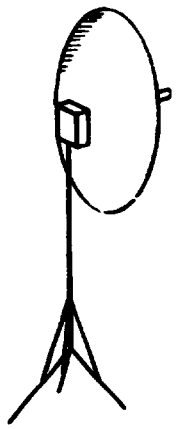

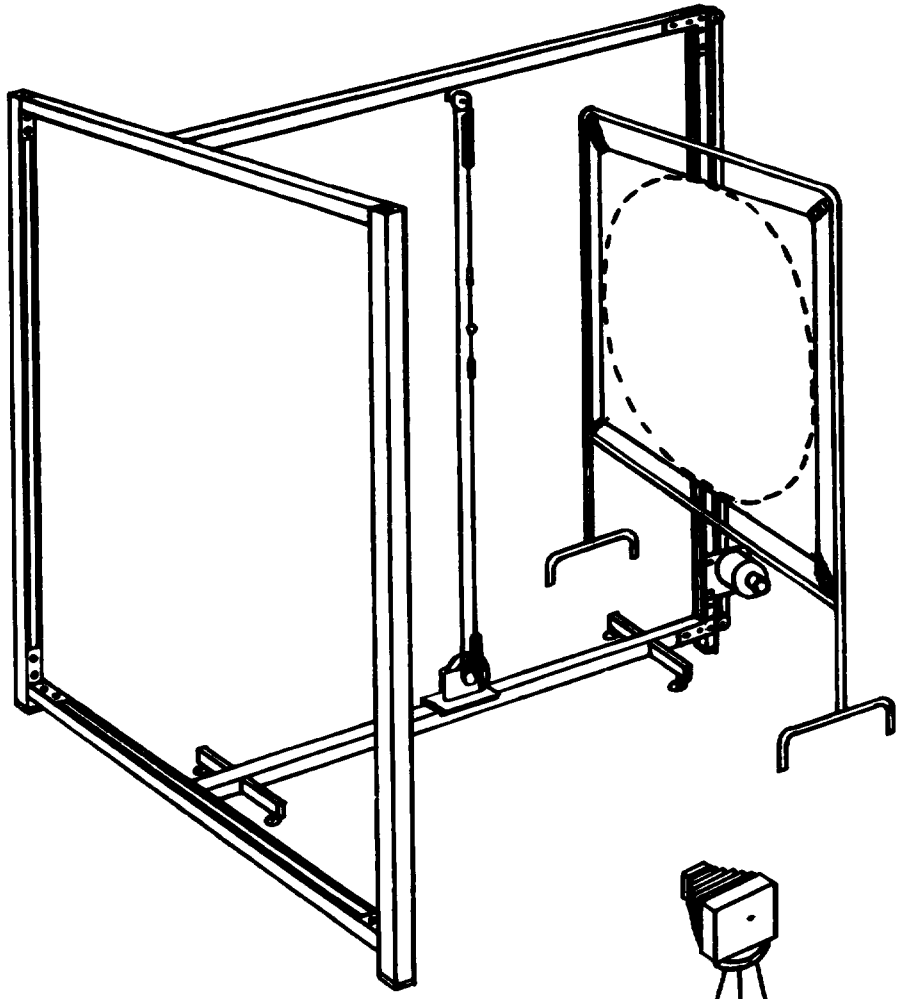

FIGURE 46

PHOTOGRAPHING NEAR FIELD Z DIMENSION PATTERN

PROPOSED RETRODIRECTIVE PHASE CONTROL SONIC SIMULATOR

GENERAL DESCRIPTION AND CAPABILITIES

Figure 47 shows the major functional blocks of the proposed retrodirective phase control sonic simulator. The retrodirective sonic antenna is a circular array, 1.2 meters in diameter, of 216 pairs of acoustic elements, each pair consisting of one transmitting and one receiving element. The transmitting elements form a phased array that electronically focuses and steers a coherent sonic beam. The pairs of acoustic elements are configured in a 16 row by 16 column matrix. Each column of transmitting elements is driven by drivers which multiplex each of the 16 rows of transmitting elements 32,000 times per second. This enables the simulator's computer to control the amplitude and phase of each of the 216 transmitting elements. The simulator is designed to ransmit the sonic power beam in the 2 kHz to 4 kHz range. As in the ground based control sonic simulator, any illumination taper can be programmed.

Contrasted to ground based phase control, phase control information for each transmitting element is obtained through reception of an acoustic pilot beam signal by the receiving element associated with each transmitting element and by a reference receiving element. The reference receiving element is an arbitrarily selected one near the center of the array.

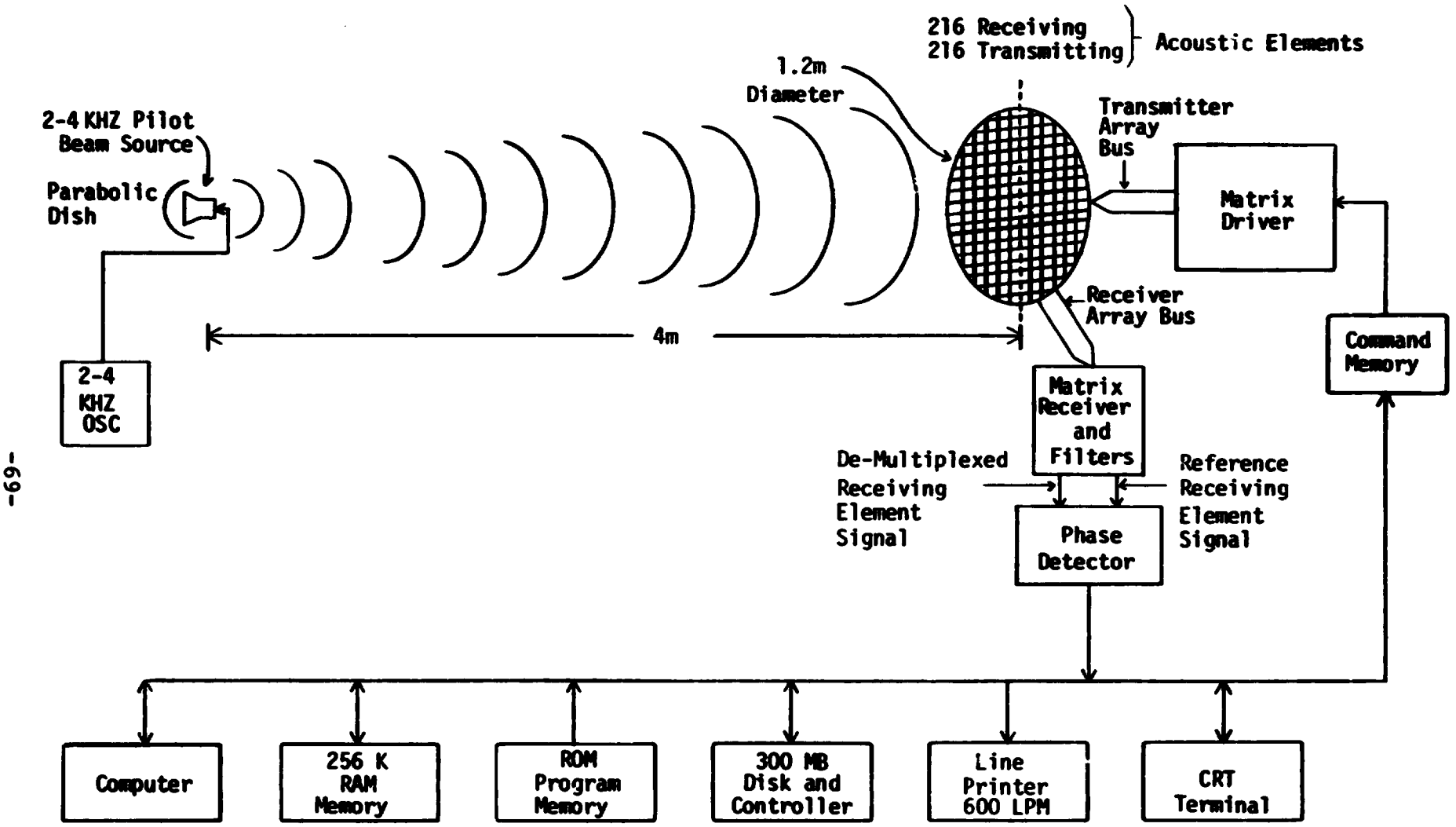

FIGURE 47

SONIC SPS RETRODIRECTIVE PHASE CONTROL SIMULATOR
MAJOR FUNCTIONAL BLOCKS

As in the ground based control sonic simulator, a computer, RAM memory, 300 MB disc drive, line printer, and CRT terminal are incorporated (Figure 47) to provide a very high degree of experimental flexibility.

DETAILED HARDWARE DESCRIPTION

Details of the retrodirective sonic antenna showing the configuration of the transmitting and receiving elements are given in Figures 48 and 49. The system is clocked by a 1024 kHz crystal-controlled master oscillator/clock (Figure 50) which is divided down to a 512 kHz row driver and phase clock signal, a 128 kHz column clock, and the pilot beam signal at, for purposes of this detailed description, 2 kHz.

Under computer control, each receiving element is accessed and connected to the digital phase detector (Figure 50). The phase detector determines the phase of the pilot beam received at the selected receiving element relative to the phase of the pilot beam received at the reference receiving element. The phase detector generates a 6-bit digital phase data word for inputting to the computer. The computer conjugates this phase by taking its complement with respect to 360°, and outputs the resulting phase information to the associated transmitting element. The signal from this transmitting element then arrives back at the location of the pilot beam source at a phase which is the sum of the conjugated phase plus the propagation phase delay. This phase sum is equal to

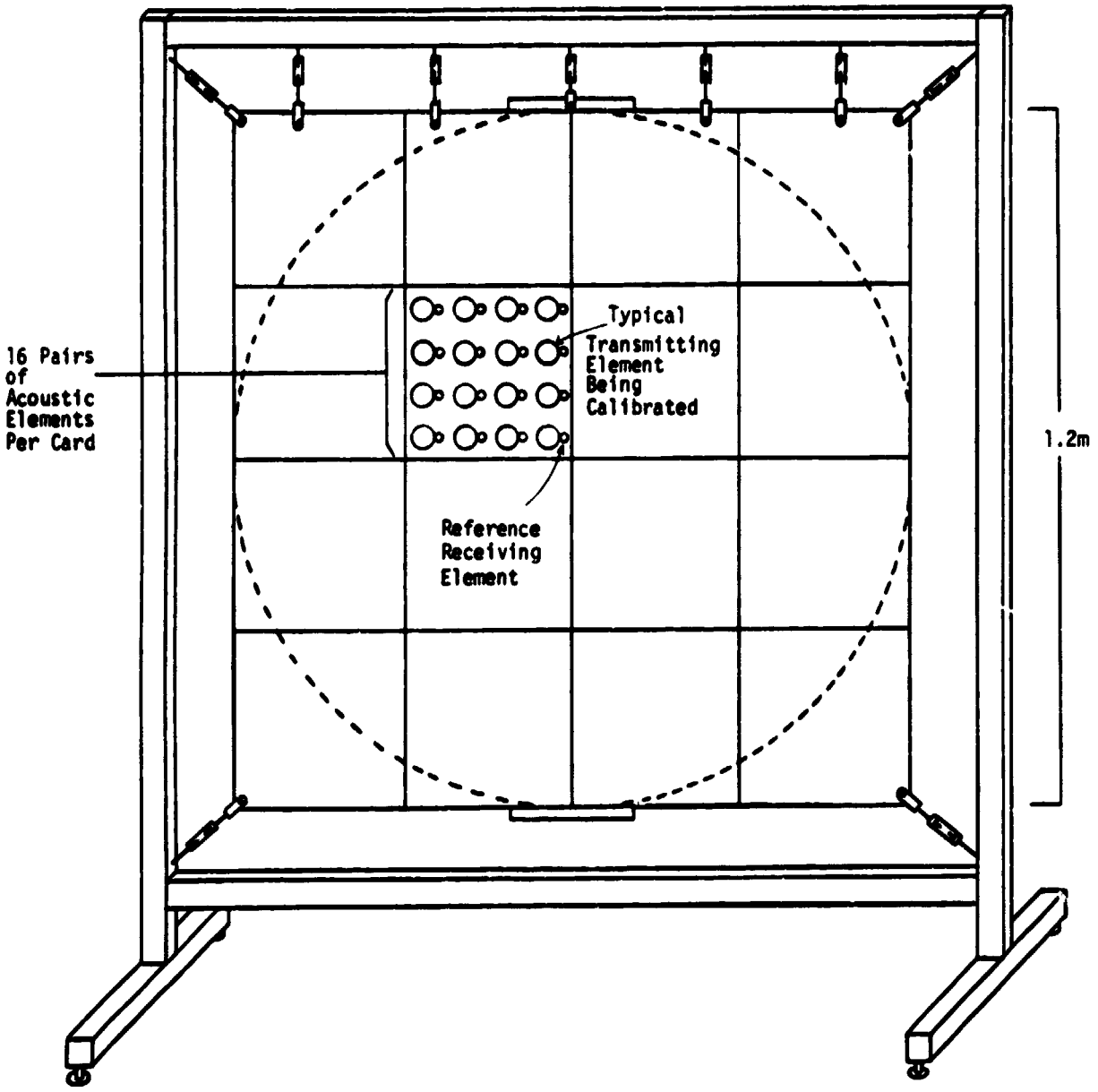

FIGURE 48

RETRODIRECTIVE PHASE CONTROL SONIC ANTENNA

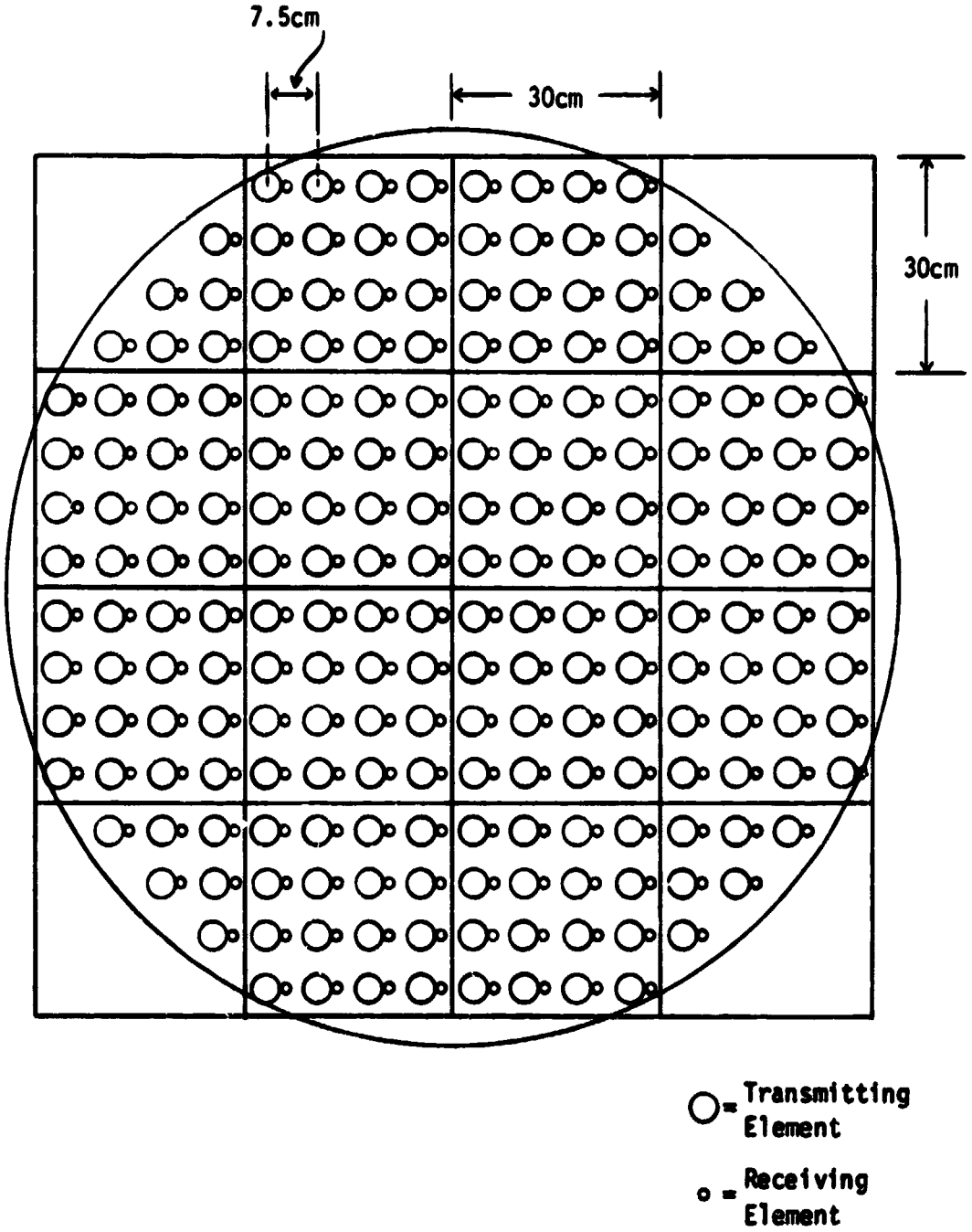

FIGURE 49

RETRODIRECTIVE PHASE CONTROL SONIC ANTENNA TRANSMITTING AND RECEIVING ELEMENTS ARRANGEMENT

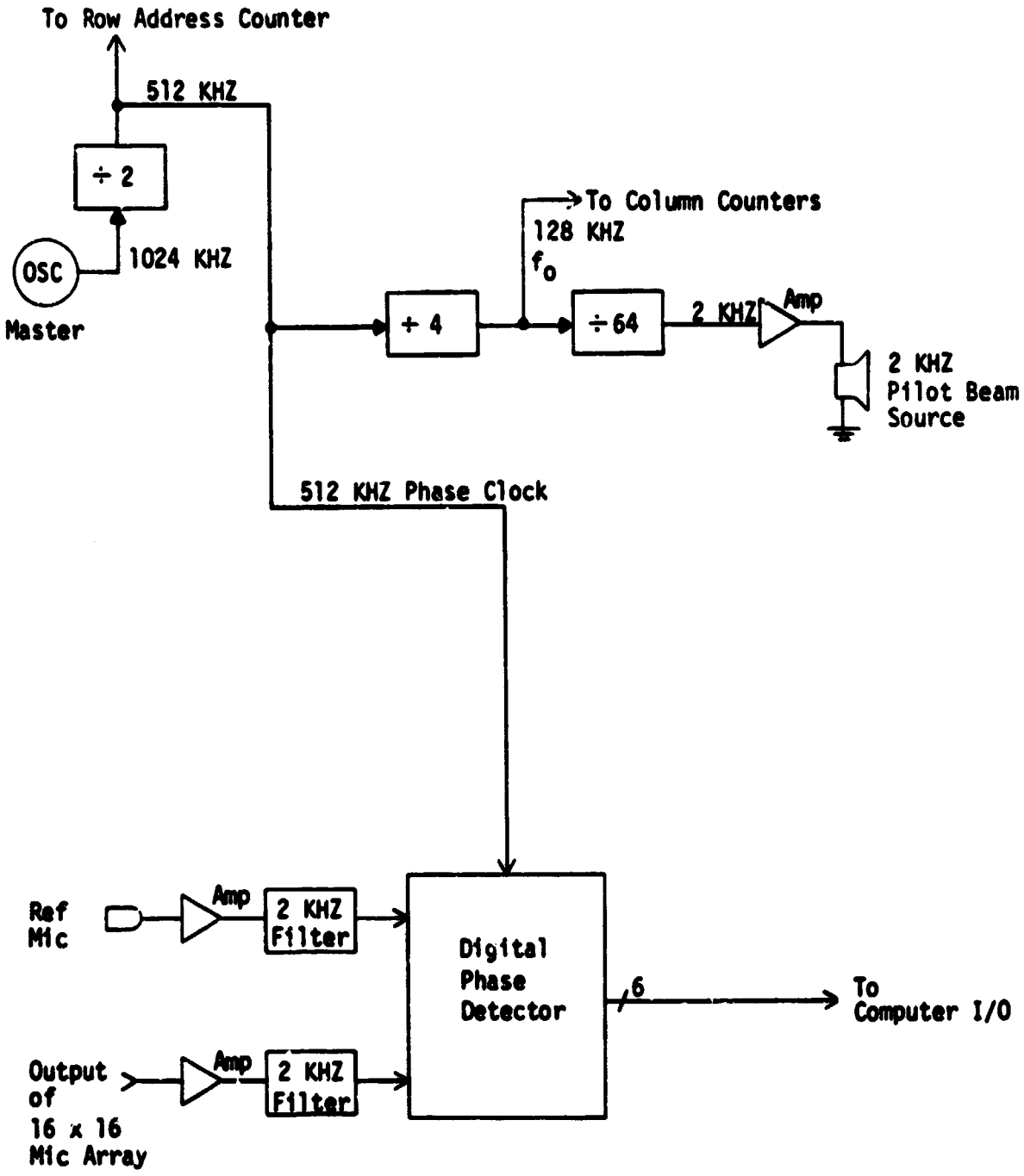

FIGURE 50

MASTER CLOCK AND PHASE DETECTOR
(SONIC RETRODIRECTIVE PHASE CONTROL SYSTEM)

the phase of the pilot beam received at the reference receiving element. The pilot beam source is an acoustic transmitting element with a parabolic reflector that directs the pilot beam onto the sonic array receiving elements to insure a high acoustic signal-to-noise ratio there.

Computer access to each receiving element is via an analog multiplexing scheme (Figure 51).

The computer sends the column and row address coordinates and phase data for each transmitting element to the appropriate Column Driver/Memory Board (Figures 52 and 53). Stored in the ROM on the Column Driver/Memory Board (Figure 53) are 15 different amplitude sinewaves plus one zero amplitude one. The 15 sinewaves range in 2 dB amplitude steps from 0 dB, which corresponds to maximum amplitude, down to 28 dB below maximum amplitude. This allows a range of power levels and/or amplitude tapers to be programmed. The particular amplitude level desired for a transmitting element is selected by the amplitude address input to the ROM. Each sinewave consists of a 64 8-bit binary data words. The data words respectively correspond to the values of the instantaneous amplitude of the sinewave as its phase varies from 0° to 360° in increments of $360 \div 64 = 5.625^{\circ}$. Each data word address is a phase address corresponding appropriately to one of the 64 increments in phase of the sinwave. If the amplitude address input to the ROM were constant, then clocking through the 64 phase

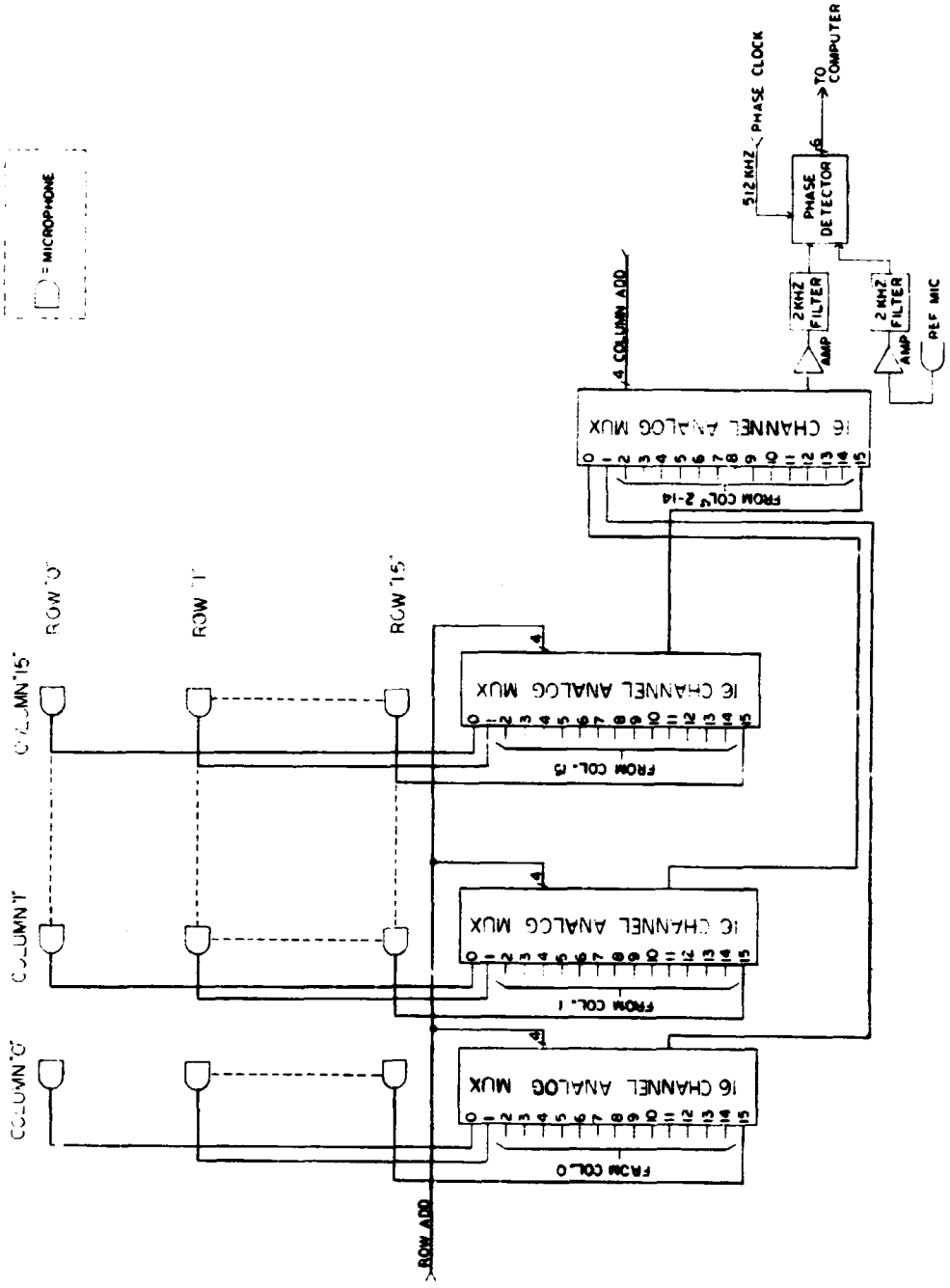

FIGURE 51

RETRODIRECTIVE PHASE CONTROL SONIC ANTENNA
RECEIVING ELEMENTS CIRCUITRY

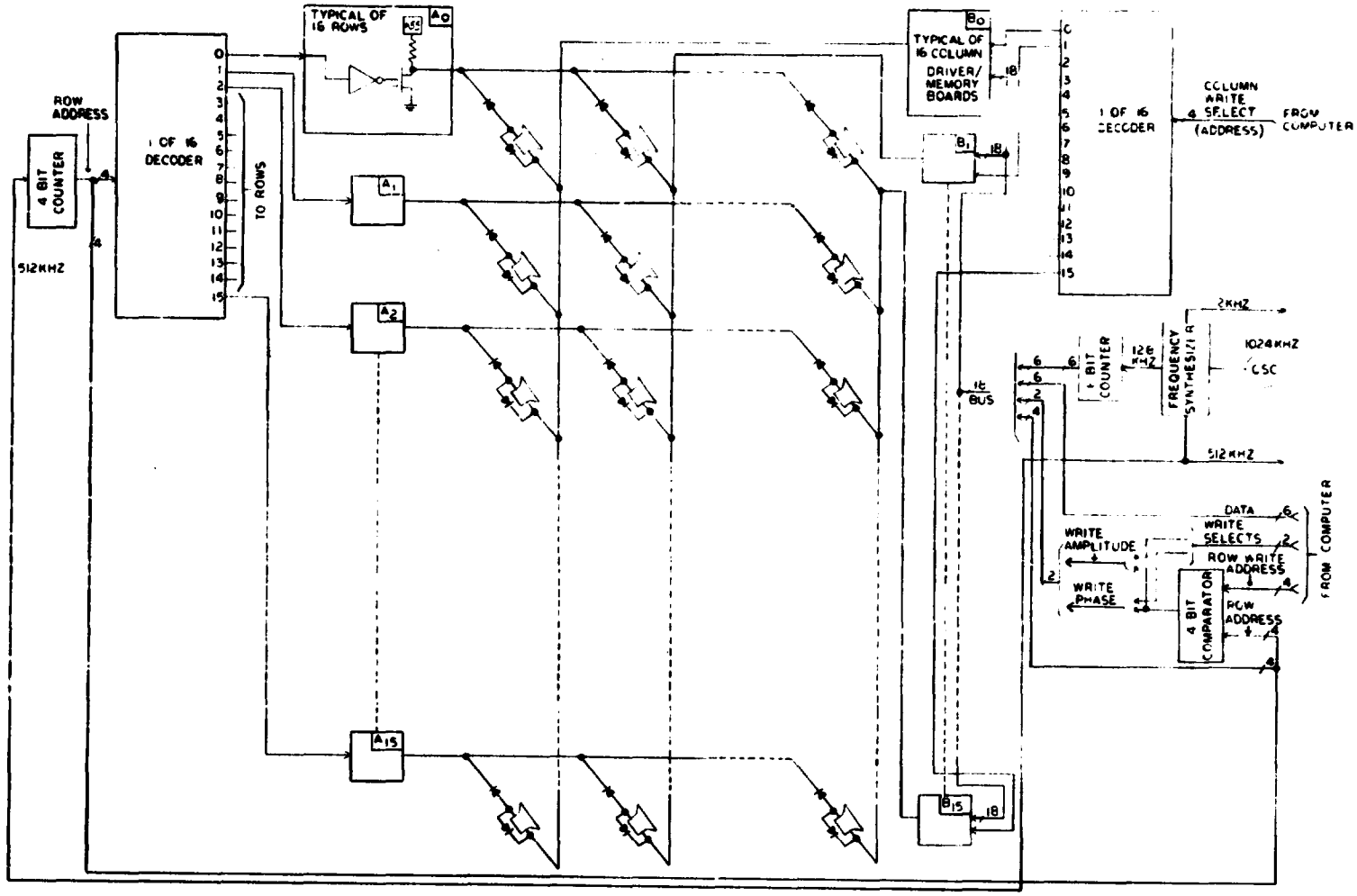

FIGURE 52

RETRODIRECTIVE PHASE CONTROL SONIC ANTENNA
TRANSMITTING ELEMENTS CIRCUITRY

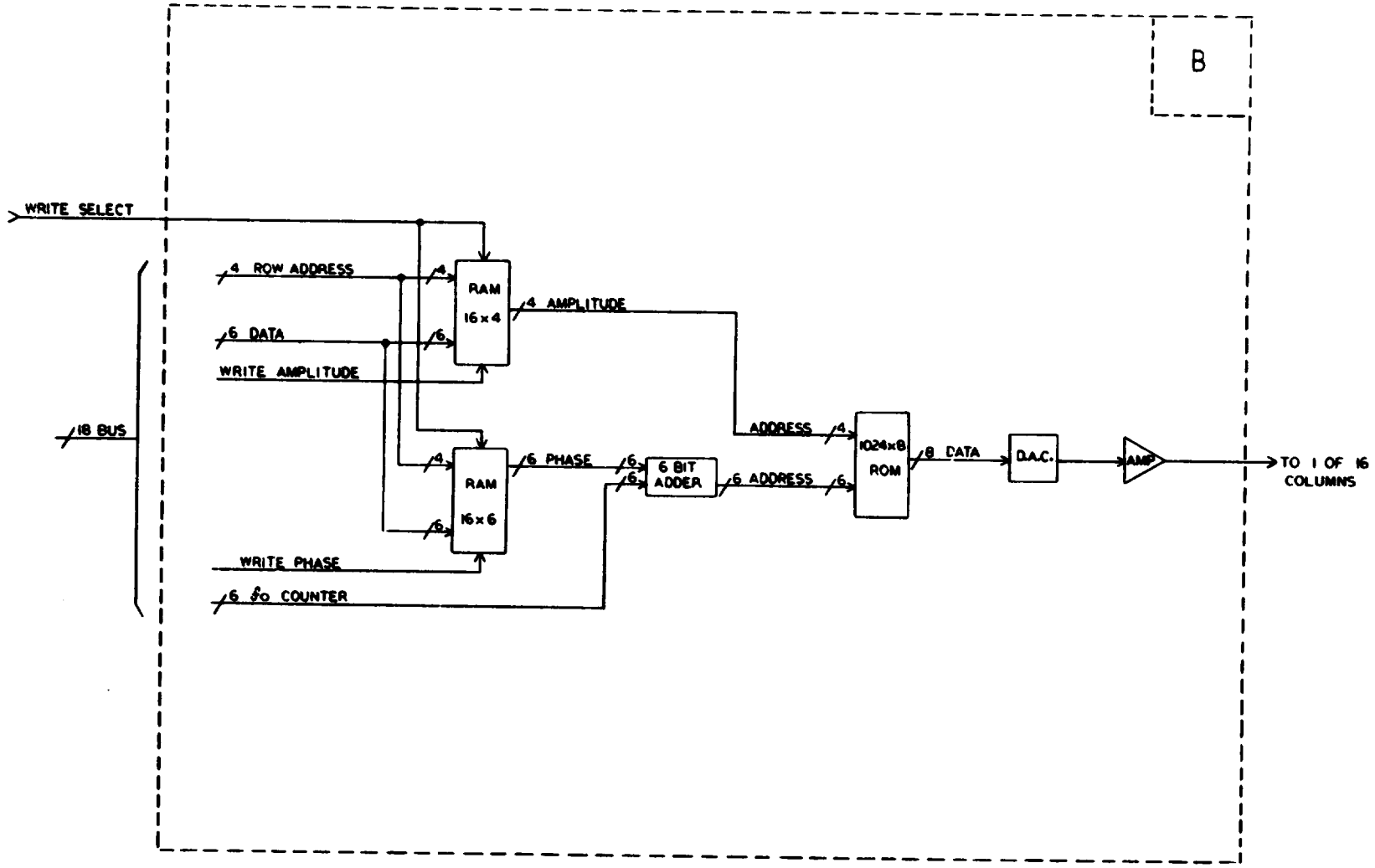

FIGURE 53

TRANSMITTING ELEMENT COLUMN DRIVER/MEMORY
(RETRODIRECTIVE PHASE CONTROL SYSTEM)

addresses at the counter rate of f_o = 128 kHz would generate a step-approximated 2 kHz sinewave out of the DAC. The amplitude and phase addresses actually input to the ROM are those of the sinewaves associated with the 16 transmitting elements in the column being driven by the column driver. Each sinewave is addressed at 1/16th of the 512 kHz row addresses counter rate. This produces multiplexed information for 16 sinewaves which are output from the DAC as a composite signal of 16 uniformly interleaved pulse trains, one per sinewave. After being output in pulse amplitude modulated and multiplexed form by the Column Driver/Memory Board, each sinewave is extracted by demultiplexing and by the intrinsic analog filtering that takes place at its respective row transmitting element to beomce the drive signal for that element.

The relative phase of each of the sinewaves output by the column driver is determined by adding counters from 0 to 63 by means of the 6 bit adder (Figure 53) to the phase address being clocked into the ROM at the time that the amplitude and phase addresses for an individual sinewave are being input to the ROM. The counts from 0 to 63 correspond to phase shifts from 0° to 354.375°. Therefore any phase shift in that range, in 5.625° increments, can be obtained.

Demultiplexing of the row signals input to the 16 columns of transmitting elements from the 16 column drivers is accomplished in the Transmitting Elements Circuitry (Figure 52) by sequentially strobing each row of transmitting elements in

the 16 column by 16 row matrix. The strobes are generated at a 32,000 times/sec. rate by the row address decoder and are input to the matrix from 16 row drivers which operate in synchronism with the row pulses being output for a particular row by the column drivers. Therefore 16 transmitting elements in a row are simultaneously driven by the column and row drives at one time.

Analog filtering of the demultiplexed pulses at the transmitting elements is accomplished by the elements' natural low-pass filter characteristic which filters out frequencies above the audio range in the pulse amplitude modulated pulse train.

REFERENCES

1. J. H. Ott and J. S. Rice, "An Interferometer-Based Phase Control System", Solar Power Satellite Microwave Power Transmission and Reception, NASA Conference Publication 2141, pp. 139-140 (Proceedings of a workshop, Lyndon B. Johnson Space Center, Houston, Texas, January, 15 - 18, 1980.)

2. J. H. Ott and J. S. Rice, "Digital SPS Phase Control Using Traveling Wave Interferometry", Novar Electronics Corporation Technical Report, October, 1978.

3. B. D. Steinberg, Principles of Aperture and Array System Design, Wiley, 1976, pp. 305 - 308.

4. W. E. Kock and F. K. Harvey, "A Photographic Method for Displaying Sound Waves and Microwave Space Patterns" Bell System Technical Journal, Vol. 30, July 1951, pp. 564 - 587.

5. R. K. Moore, "Acoustic Simulation of Radar Returns", Microwaves, December, 1962.

APPENDIX A

SONIC SIMULATION OF ELECTROMAGNETIC WAVES

APPENDIX A

SONIC SIMULATION OF ELECTROMAGNETIC WAVES

Electromagnetic and acoustic waves obey many of the same equations and thus are analogous for the conditions described by those equations. As pointed out by Moore[5], this analogy can be appreciated by examination of the equations describing acoustic and electromagnetic plane waves. The sometimes called "Telegrapher's" Equations below describe these plane waves traveling in the positive z direction in a x,y,z rectangular coordinate system:

"Telegrapher's" Equations

Acoustic		Electromagnetic	
$\frac{\partial p}{\partial z} = - \rho_v \frac{\partial u_z}{\partial t}$	(1a)	$\frac{\partial E_x}{\partial z} = - \frac{\partial H_y}{\partial t}$	(1b)
$\frac{\partial u_z}{\partial z} = - k \frac{\partial p}{\partial t}$	(2a)	$\frac{\partial H_y}{\partial z} = - \epsilon \frac{\partial E_x}{\partial t}$	(2b)

where

p = acoustic pressure

u_z = particle velocity in the +z direction

ρ_v = mass density of the acoustic medium

k = compressibility of the acoustic medium

E_x = electric field in the +x direction

H_y = magnetic field in the +y direction

μ = permeability

ϵ = permittivity

Equation 1b is Faraday's Law and 2b is Ampere's Law. By taking partial derivatives of the expressions in Equations 1 and 2 with respect to z and t and equating like terms, one obtains the wave equations:

Wave Equations

Acoustic		Electromagnetic	
$\frac{\partial p^2}{\partial z^2} = \frac{1}{c_a^2} \frac{\partial p^2}{\partial t^2}$	(3a)	$\frac{\partial^2 E_x}{\partial x^2} = \frac{1}{c_e^2} \frac{\partial^2 E_x}{\partial t^2}$	(3b)
$\frac{\partial^2 u_z}{\partial z^2} = \frac{1}{c_a^2} \frac{\partial^2 u_z}{\partial t^2}$	(4a)	$\frac{\partial^2 H_y}{\partial z^2} = \frac{1}{c_e^2} \frac{\partial^2 H_y}{\partial t^2}$	(4b)

where $c_a = 1/\sqrt{k\rho_v}$ is the velocity of propagation of an acoustic wave and $c_e = 1/\sqrt{\mu\varepsilon}$ is the velocity of propagation of an electromagnetic wave (speed of light).

Since an acoustic plane wave is a longitudinal wave whereas an electromagnetic plane wave is a transverse wave, polarization of an electromagnetic wave cannot be simulated acoustically. This difference in the nature of the two types of waves also means that the boundary conditions that must be satisfied are somewhat different. Nevertheless, sonic simulation of the power beam of a Satellite Power System is valid for the study of beam shape, sidelobes, grating lobes and scintillation and fading caused by refraction, and many diffraction and obstruction effects.

The significant sonic simulation scaling factors for the Satellite Power System Microwave Transmission Simulator are given in Table A-1. Two features of sonic simulation of an SPS power beam are that the power beam is audible and that the system response time can be slowed by a factor of 1000. Room air currents did not affect the simulations performed for this report. Room acoustics were easily handled by the appropriate placement of sound absorbant material.

	SPS	SCALE FACTOR	SIMULATOR
Propagation Velocity	3×10^8 m/sec	10^6	3×10^2 m/sec
Range	3.5×10^7 m	3.5×10^6	10 m
Wavelength	12 cm	4	3 cm
Beam Frequency	2.45 GHz	2×10^5	12 kHz
One Way Travel Time	0.1 sec	3	0.03 sec
Filter Settling Time	10^{-3} msec	10^{-3}	1 msec
Transmitter Sources	10^6	31	3300

TABLE A-1

SIGNIFICANT SONIC SIMULATOR SCALING FACTORS

APPENDIX B

INTERFEROMETRIC PHASE CONTROL

APPENDIX B

INTERFEROMETRIC PHASE CONTROL

Precise phase relationships among the transmitted signals of each Space Antenna subarray must be maintained to properly focus and point the microwave power beam. Specifically, the signals transmitted by each power module must arrive at the center of the Rectenna in phase. This results in a power beam focused at the center of the Rectenna. However Space Antenna structural deformations or mechanical pointing errors can, if not compensated for, alter the relative phases of the power module signals received at the Rectenna by altering the lengths of the paths that those signals must travel between the power modules and the Rectenna. In addition, variations within the Space Antenna circuitry can also alter the relative phases of the signals.

Interferometric Phase Control (IPC), an interferometer-based phase control system developed by Novar Electronics Corporation, has three significant characteristics which differentiate it from the Reference System retrodirective approach.

1. Interferometric Phase Control is a ground based closed loop system.

Unlike the retrodirective approach, the phase correction information is obtained on earth by measuring the resultant power transmission of the Space Antenna power modules and comparing them against a reference.

2. The Space Antenna's power modules are calibrated sequentially.

A signal from a reference transmitter near the center of the Space Antenna is sequentially phase compared with a calibration transmission of each of the power modules.

3. During normal power transmission, the frequency of each power module is shifted slightly during phase calibration.

Maintenance of a properly focused and pointed power beam can be accomplished concurrently with the normal transmission of power from the Solar Power Satellite by using frequencies for calibration which are different from the power beam frequency.

System Description

On or near the Rectenna site, an antenna called the Phase Measurement Antenna (PMA) receives the transmission from the Space Antenna Reference Transmitter (SRT) and the particular power module being phased tuned (calibrated). Analysis of these

signals provides sufficient information to generate a phase error correction term which is sent up to the on-board phase control circuitry, shown in Figure B-1, of the power module undergoing calibration.

1. Phase Tuning During Normal Power Transmission

Simultaneous with the transmission of the power beam, coherent signals at three different frequencies are transmitted from the Space Antenna. Two of these signals are transmitted from the SRT, which is located near the center of the Space Antenna, and one is transmitted from the power module being phased tuned, as shown in Figure B-2. The two signals transmitted from the SRT are respectively called s_1 and s_{r1}, and the signal transmitted by the power module being phase tuned is called s_2. The frequency of s_1 is midway between that of s_{r1} and s_2 so that the beat frequency of s_1 and s_2 is the same as that of s_1 and s_{r1}.

At the PMA, simple mixing and filtering circuitry detects two difference frequency signals. One signal is due to s_1 and s_2. The other, which is called a phase reference signal, is that due to s_1 and s_{r1}. These beat frequency signals are then phase compared.

The phase comparison gives the phase difference between the two beat frequency signals which is a function

C-2

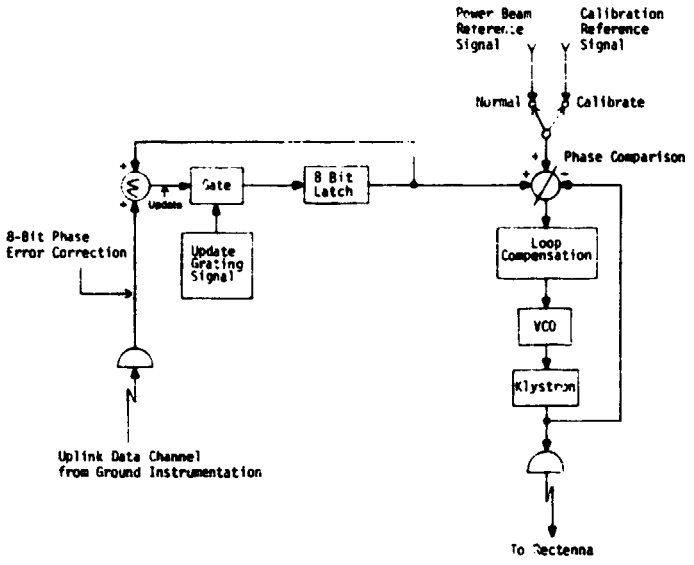

FIGURE B-1

POWER MODULE PHASE CONTROL CIRCUITRY

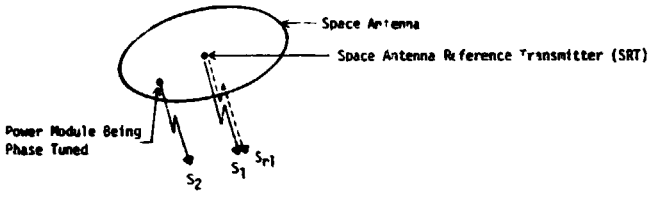

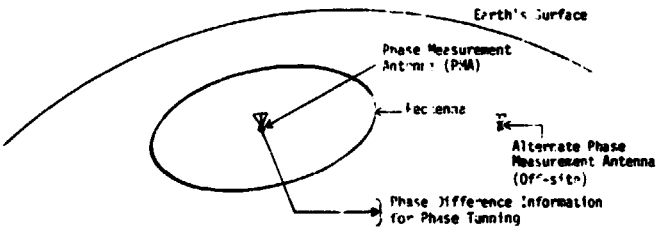

FIGURE B-2

INTERFEROMETRIC PHASE CONTROL

-Pictorial representation of relationship between Space Antenna signals and ground instrumentation.

of z-axis deformations* in the power module being phase tuned plus biases in the phase feed network of the satellite. Certain components of the phase difference change with a change in frequency, others do not. Since the power module being phase tuned is transmitting at a frequency different from the power beam frequency, it is necessary to distinguish between these frequency dependent and frequency independent components in order to determine the phase correction that will be correct at the power beam frequency. This is done by shifting s_{r1} and s_2 to a different set of frequencies, according to a phase ambiguity error avoidance criterion, and making a second phase difference measurement. These two phase difference measurements are numerically adjusted by -2π, 0, or $+2\pi$ according to a second phase ambiguity error avoidance criterion. These two numerically adjusted phase differences provide sufficient information to calculate the phase error correction transmitted back to the SPS power module being phase tuned. This phase error correction can be made with an 8-bit binary word sent to the SPS via a data channel. An 8-bit accuracy produces a phase resolution of $360^\circ \div 2^8 = 1.4^\circ$. This is sufficient to give a power beam pointing resolution better than 140 meters at the Rectenna.

---

*deformations in a direction toward or away from the Rectenna.

A tradeoff exists between satellite bandwidth requirements and the power module updating rate which is limited by filter settling times. It is anticipated that the frequency separation between s_1, s_2, s_{r1} and the power beam will be on the order of 1 MHz. At these frequency separations, the update interval for an entire Space Antenna could be on the order of a few seconds. It is possible that this will be fast enough to correct for any changes that will occur at the Space Antenna due to deformations, thermal effects, etc.

2. Phase Tuning During Initial Startup

With the power beam turned off, it is also possible to use this interferometer technique to phase tune the power modules at the power beam frequency. During initial startup after construction of the satellite system or after major maintenance has been performed, it is necessary to calibrate the phase tuning system used during normal power transmission for any phase vs. frequency nonlinearities. At the power beam frequency, the measured phase difference is the phase error correction. Any difference between the phase error correction determined at the power beam frequency and that determined by the phase tuning system used during normal power transmission is due to a nonlinear phase vs. frequency component in the phase at the power module being phase tuned. This difference must be algebraically

summed with the phase error corrections detected during normal operation.

Ionospheric Effects

With the ground based closed loop interferometer phase control approach, ionospheric effects are limited to phase errors introduced into the space-to-earth transmission path only.

Although, the PMA is shown to be at the center of the Rectenna, it is not necessary that it be located there or even within the Rectenna site. Off-site measurement has the advantage that the signals being phase tuned do not have to pass through an ionosphere that may be subjected to undetermined heating effects by the power beam.

An important advantage of Interferometric Phase Control is its inherent ability to make use of statistical error reduction techniques to minimize any ionospheric effects. This includes time averaging and/or spatial averaging using several on and off-site phase measurement antennas.

Prediction of Deformation Dynamics

Once the space antenna has been initially phase tuned, learning curves or adaptive modeling techniques could be used to predict the dynamics of the space antenna structural deformations. With such predictions, it is felt that the

capability would then exist to phase tune the entire space antenna based on frequency measurements of only a "few" key power modules and occasional measurements of the rest.